Studies on the Affinity Control of T Cell Development

Inauguraldissertation

zur
Erlangung der Würde eines Doktors der Philosophie
vorgelegt der
Philosophisch-Naturwissenschaftlichen Fakultät
der Universität Basel

von
Dieter Naeher
aus Basel (Schweiz)

Basel, 2004

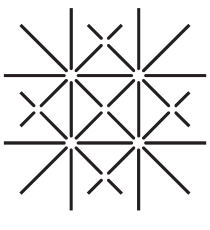

Genehmigt von der Philosophisch-Naturwissenschaftlichen Fakultät auf Antrag der Herren:

Professor Dr. Ed Palmer

Professor Dr. Gennaro de Libero

Basel, den 14. Dezember 2004

Prof. Dr. Hans-Jakob Wirz
Dekan

No law of nature,
however general, has been established
all at once; its recognition has always been preceded
by many presentiments. The establishment of a law,
moreover, does not take place when the first
thought of it takes form, or even when its significance is
recognized, but only when it has been confirmed by
the results of the experiment. The man of science
must consider these results as the only proof of the
correctness of his conjectures
and opinions.

Dmitri Ivanovich Mendeleev
(1834 - 1907)

Acknowledgments

The project which was underlying this thesis emerged from a collaboration between the lab of my supervisor Ed Palmer and the lab of Immanuel Lüscher from the Ludwig Institute in Lausanne, Switzerland. It is mainly due to the help of the people in those two groups that I was able to perform the experiments which are described in this thesis. Besides the lab-mates many other people from the Basel Institute of Immunology and the Department Forschung of the Universitätsspital Basel helped me in many occasions.

In the first line, I want to thank the members of my thesis committee:

I want to thank my supervisor Ed Palmer. He not only accompanied me on my way into the field of Immunology and supported me during the entire time of my thesis with his expertise and enthusiasm but also gave me full scientific freedom to develop my own ideas and experimental approaches in a protected surrounding. From discussions with other students and own observations, it became clear to me that there are not too many group leaders or supervisors which support the development of PhD students to become independently thinking and working scientists. With Ed, I had the great luck and pleasure to have such a supervisor.

I want to thank Immanuel Lüscher who let me perform many of my experiments with the photoaffinity labeling technique. The measurements of TCR-ligand affinities on developing thymocytes would not have been possible without this technique. He also provided me with radioactively labeled pMHC monomers which allowed to study the impact of the α-CPM in TCR ligand binding.

I want to thank Gennaro de Libero, for being a member of my thesis committee and for helpful discussions concerning the projects.

Ton Rolink I want to thank for being 'Prüfungsvorsitzender' of my oral PhD defense exam.

Furthermore I want to thank all the people who provided me with technical help:

First of all, I want to thank Barbara Hausmann, who taught me most of what I know concerning the breeding and the experimental work with mice. She always offered a third or even a forth hand, in times when I had to do too many things at once. In particular she was doing most of the fetal thymic organ culture experiments presented in this thesis. During the entire time of my thesis she provided me with the most reliable technical assistance a PhD student can hope for.

I want to thank Philippe Guillaume for teaching me how to produce soluble pMHC ligands and providing me with fluorescently labeled pMHC monomers and tetramers.

Marek Cebecaver I want to thank for providing me with photo-reactive peptides, technical advise and good company during my stays in Lausanne. I want to thank Sebastiano Sansano for assisting me with the purification of photo-reactive peptides.

I want to thank Ernst Wagner, for taking care of the logistics concering the transgenic mouse lines and the bleeding of the mice which was necessary to phenotype them (and for keeping me uptodate about the latest jokes in town). I want to thank Tracy Hayden and Hubertus Kohler for FACS sorting the hybridoma cell lines expressing the various TCR mutants.

Last but not least, I want to thank the people who shared their ideas and thoughts with me, which were the basis of the findings that are described in this thesis:

First of all, the members of the Student Journal Club at the Basel Institute for Immunology. In particular I want to thank Erika Meier, John Gatfield, Thomas Seidl, Nicole Schmitz, Maurus Curti, Jan Kisielow, Piotr Tetlak, Axel Bouchon, Claudia Waskow and Evita Harfst.

In the same line I want to thank Guy Werlen for his concise, frank and incorruptible scientific criticisms which made me think clearly again in moments when scientific vanity was about to veil my thoughts.

I want to thank the people who joined the lab at the Department Forschung of the Universitätsspital Basel. I profited a lot from the experience which was brought to the lab by Diana Gil, Emma Teixeiro, Mark Daniels, Adam Schrum, Michel Mallaun, Dominique Roubaty, Gideon Hönger, Denise Bielmann and Doris Lutz.

Finally I want to thank the people outside of science who supported me a great deal during the time I performed my thesis, in particular my mother and Evita.

Table of Contents

Summary

Defined interactions between thymocytes and thymic antigen presenting cells ensure that each T cell found in an individual is both self-restricted and self-tolerant. By interacting with pMHC ligands, T cell receptors (TCRs) expressed on developing T cells initiate intracellular signaling cascades which lead either to survival and differentiation, referred to as positive selection, or to apoptotic cell death, referred to as negative selection.

This thesis is aimed to a better understanding of how thymocytes distinguish between pMHC ligands inducing positive selection from those inducing negative selection. Transgenic mice and hybridomas expressing TCRs of defined specificity, referred to as T1-TCRs, were produced to study the role of TCR-ligand affinity in thymic selection of developing T cells. Ligand binding studies were performed with the photoaffinity labeling system developed by Immanuel Lüscher (Ludwig Institute; Epalinges, Switzerland).

By defining the selection properties of various T1-TCR ligands and comparing their potency in inducing positive and negative selection with their TCR affinity it is shown, that TCR affinity is a key parameter for thymocyte selection. High affinity ligands induced negative selection, while low affinity ligands induced positive selection. A ligand with a moderate affinity was shown to induce either positive or negative selection, depending on the dose of the peptide. It was further shown, that the reduced sensitivity observed for mature T cells compared to thymocytes is not mediated by developmental changes in the affinity of TCR-ligand interactions. All ligands tested bound the TCR expressed on naive, mature T cells with the same affinity as the TCR expressed on thymocytes. Therefore, the results presented in the first part of this thesis suggest, that positive and negative selection of T cells depends on TCR-ligand affinity and that this affinity is preserved through all stages of T cell development.

In the second part of this thesis studies are presented analyzing the role of the evolutionarily conserved α-chain connecting peptide motif (α-CPM) in TCR-ligand binding and thymocyte development. Experiments performed with hybridomas and transgenic mice showed that α-CPM deficient TCRs are not properly cooperating with the coreceptor molecule, CD8 to elicit responses to low affinity ligands. Interestingly responses to high affinity ligands were less affected. Thymocytes of α-CPM mutant mice were specifically defective in undergoing positive selection but were still able to undergo negative selection. By comparing the TCR-ligand affinities on cells expressing either wildtype or α-CPM mutant T1-TCRs it was shown, that the absence of the α-CPM leads to a slight decrease in CD8 cooperativity

for ligand binding. The data therefore suggest, that the α-CPM plays an important role for successful cooperation of TCR and coreceptor in generating signals to low affinity, positive selecting ligands.

Abbreviations

ABA	Azidobenzoic acid
APC	Allophycocyanine
APS	Ammonium persulfate
ATCC	American Type Culture Collection
β2m	Beta-2 microglobulin
BSA	Bovine serum albumine
BSP	BirA specific peptide
CPM	Counts per minute
CD	Cluster of differentiation antigen
CDR	Complementarity Determining Region
CTL	Cytotoxic T lymphocyte
kD	Kilo Dalton
DOC	Deoxycholic acid
DMEM	Dulbecco's modified eagle medium
DMSO	Dimethylsulfoxid
DTT	Dithiothreitol
ECL	Enhanced chemoluminescence
ER	Endoplasmic Reticulum
FCS	Fetal calf serum
FACS	Fluorescence activated cell sorting
FPLC	Fast performance liquid chromatography
FITC	Fluorescein isothiocyanate
HEPES	N-2-hydroxyethylpoperazine-N-2-ethansulfonic acid
HPLC	High pressure liquid chromatography
HRP	Horse radish peroxidase
IASA	4-iodo azidosalicylic acid
Ig	Immunoglobulin
IP	Immunoprecipitation
IPTG	Isopropyl β-D-1-thiogalactopyranoside
ITAM	Immunoreceptor tyrosine activation motif
LB	Luria-Bertani

MFI	Mean fluorescence intensity
MW	Molecular weight
MES	2-[N-Morpholino]ethansulfonic acid
n.d	Not determined
mAb	Monoclonal antibody
OD	Optical density
PAGE	Polyacrylamid gel electrophoresis
PbCS	Plasmodium circumsporozoite
PCR	Polymerase chain reaction
PE	Phycoerythrin
pMHC	Peptide-majorhistocompatibility complex
PMSF	Phenylmethylsulfonylfluoride
PNA	Peanut agglutinine
PerCP	Peridinine chlorophyll protein
RT	Room temperature
SA	Streptavidin
SDS	Sodium dodecyl sulfate
Si	Sievert (conductivity unit)
TCR	T cell receptor
Temed	N,N,N,N' tetramethyl ethylenediamine
tg	Transgenic
Tris	tris(hydroxymethyl)aminomethane

1. Introduction

The two major functions of the vertebrate immune system are to protect individuals from parasites like bacteria, viruses, fungi, protozoa and worms on one hand and to kill potentially malignant tumor cells on the other hand. Many bacteria, virus and fungus strains expose conserved structural features (i.e. proteins, lipids or carbohydrates) on their cell surface which are recognized by the innate immune system including white blood cells (leucocytes) and soluble factors of the complement system. Organisms which are properly recognized by the innate immune system are either killed or kept under tight control and are therefore non-pathogenic. In contrast, pathogens have developed strategies to escape the survey of the innate immune system by constantly changing the appearance of their cell surface.

To be able to recognize and eliminate such pathogenic organisms, the adaptive immune system has evolved. Cells of the adaptive immune system, including B and T cells, clonotypically express cell surface receptors which are produced by somatic gene recombination. By the stochastic process of VDJ gene-segment recombination, an enormous diversity of B cells and T cells is produced whereby each cell expresses a different B cell receptor (BCR) in the case of B cells or T cell receptor (TCR) in the case of T cells. Because the recombination process produces BCRs and TCRs of random specificities, potentially useless or self-reactive receptors and hence cells are produced during this process. Therefore B and T cells are subjected to selection processes which lead to the withdrawal of those cells which express BCRs or TCRs with unfavorable specificities. These selection processes are of particular importance for T cells, which can not only directly kill tumor cells or virus infected cells of the body, but also control the activation of other immune effector cells like macrophages and B cells.

The thymus has developed as a specialized organ in which the T cell selection processes take place. As soon as the developing T cells in the thymus, referred to as thymocytes, express somatically rearranged TCRs on their cell surface they interact with majorhistocompatibility molecules (MHCs) expressed on thymic stromal cells. If this interaction is too weak, the thymocytes die by 'neglect'. If this interaction is too strong, the thymocytes die by apoptosis, removing potentially 'self-reactive' cells from the T cell repertoire. Only thymocytes which express TCRs that can moderately interact with the MHC ligand molecules receive a survival signal and continue their development leading to mature T cells, which leave the thymus, enter the blood stream and migrate to the peripheral lymphatic organs to protect the individual against infections and tumors. Thus,

TCR ligand binding is a pivotal feature of T cell development, determining the fate of all the thymocytes which have started to express randomly rearranged TCRs. The results shown in this thesis present further insights in the control of T cell development mediated by TCR ligand interactions.

1.1 Molecules Involved in TCR Ligand Binding

1.1.1 The T Cell Receptor (TCR)

Each T cell receptor molecule is a disulfide linked heterodimer composed of polymorphic, membrane-bound polypeptide chains. Two different forms of TCR heterodimers have been identified: TCRα/β and TCRγ/δ. Receptor genes encoding TCRα and δ chains are assembled from separate V, J and C gene segments, while complete TCRβ and γ genes are assembled from separate V, D, J and C gene segments by genetic recombination similar to the biosynthesis of antibody genes (Reviewed in Jung et al., 2004). In the case of TCRα/β receptors, three loops forming complementary determining regions (CDRs) from TCRα pair with three CDRs from TCRβ creating a binding site which interacts with pMHC ligand. While CDR1 and CDR2 are formed by the interaction of germ line encoded in the Vα and Vβ regions, the CDR3 regions are much more diverse, as they are formed by juxtaposition of polymorphic VJ or V(D)J gene segments by an imprecise joining of the coding regions. Regarding the high numbers of Vα gene segments (~70) and the 20 Vβ gene segments found in mice combined with several D (2) and J (12) segments, several thousand different TCRs could be produced. In fact, due to imprecise end-joining the number of successfully, inframe recombined TCRs is estimated to be in the billions (Reviewed in Nikolich-Zugich et al., 2004). Despite this large diversity of the TCR variable regions, all α/βTCRs of a single species express the same constant regions Cα and Cβ. Their extracellular regions consist of an Immunoglobulin (Ig) like domain and a connecting peptide (CP). In the case of Cα, the CP region contains the evolutionarily highly conserved α-chain connecting peptide motif (α-CPM). The transmembrane (TM) regions of Cα and Cβ link the extracellular domains to the very short cytosolic (cyto) regions (See Fig. 1.1A). Importantly, neither of the cytoplasmic tails of the TCRα/β chains contain known signaling domains; therefore, to transduce signals the TCRα/β heterodimer has to be associated with the CD3 complex.

1.1.2 The TCR-CD3 Complex

The CD3 complex consists of four different chains which form two non-covalently linked heterodimers, CD3δ/ε and CD3γ/ε and a disulfide linked ζ homodimer. Proper assembly of

the CD3 complex in the endoplasmic reticulum (ER) together with the TCRα/β heterodimer is essential for TCR expression at the plasma membrane (Fig. 1.1B) (Letourneur et al., 1992; Kearse et al., 1994). The extracellular domains of CD3γ, δ and ε share little homology with Ig domains and the extracellular part of ζ is only 8 amino acids long (Sun et al., 2001). Each intracellular region of CD3γ, δ and ε contains one immunoreceptor tyrosine-based activation motif (ITAM) whereas ζ contains three ITAMs (Reviewed in Garcia et al., 1999). The ITAMs of the CD3 complex couple the TCR to intracellular Src tyrosine kinases Lck and Fyn (Reviewed by Germain, 1999).

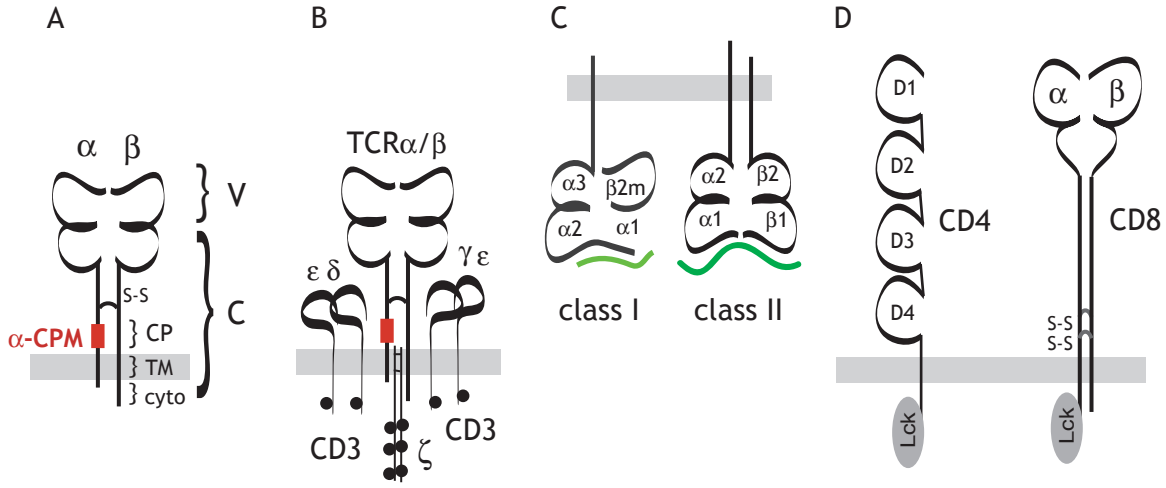

Figure 1.1: Molecules involved in TCR ligand binding. (A) TCRα/β are heterodimeric, disulfide linked transmembrane molecules consisting of variable (V) and constant (C) regions containing a Ig-like domain each. The location of the connecting peptide (CP) the transmembrane region (TM) and the cytosolic (cyto) regions are indicated. The α-CPM is indicated in red. (B) The TCRα/β forms a non-covalent complex with 4 different CD3 chains ($\gamma/\delta/\varepsilon$ and ζ). CD3γ, δ and ε contain each one ITAM (filled circles) while the homodimeric ζ molecule contains 3 ITAMs for each chain. TCR-ligand binding is coupled to the intracellular signaling cascades via the ITAMs found in the CD3 complex. (C) MHC class I and MHC class II molecules. The various Ig-like domains are indicated (α1,α2,α3 for class I MHC and α1,α2,β1,β2 for class II MHC). Class I MHC forms a non-covalent complex with β2m. (D) CD4 coreceptors are comprised of four Ig-like domains (D1-D4) a short stalk region and a transmembrane region followed by a cytosolic regions which can interact with the Src kinase Lck. CD8 coreceptors are either comprised of disulfide linked α/α homodimers or α/β heterodimers. Both CD8α and CD8β contain one Ig-like domain, a long and extended stalk region, transmembrane regions and a cytosolic tail. While CD8α can interact with Lck, CD8β can not, but can instead be palmitoylated (not shown).

1.1.3 pMHC Complexes

TCRs are not able to recognize antigens in their native conformation. Instead, antigens have to be cleaved into relatively short peptides and presented by specialized proteins encoded in the major histocompatibility gene complex (MHC) on mouse chromosome 17. Two major classes of MHC molecules were identified, which are able to present peptides to TCRα/β. MHC class I molecules present peptides which are derived from proteins found in the cytosol. Cytosolic proteins are degraded by the proteasome complex and transported

into the ER via the TAP1/2 proteins. In the ER, the peptides are delivered into the peptide binding groove of the freshly synthesized MHC class I and β-2 microglobulin (β2m) molecules. In contrast, MHC class II molecules present peptides derived from extracellular proteins, which are endocytosed by specialized antigen presenting cells (APCs) and degraded in the early endosomes. The resulting peptides are transported to the Trans-Golgi compartment where they encounter newly synthesized MHC class II molecules bound to an invariant chain. Enzymatic digestion of this invariant chain leads to its release and the extracellularly derived peptides can be placed in the binding groove of the MHC class II molecules. Peptide loaded MHC class I and MHC class II are transported to the plasma membrane and are stably expressed on the surface of APCs (Reviewed by Gascoigne et al., 2001). Despite their different subunit structures, MHC class I and MHC class II molecules show similar three dimensional structures (Fig. 1.1C). The membrane-distal face of the peptide-MHC complex that interacts with the TCR consists of a flat surface made up of two α-helices of the MHC surrounding a central peptide. MHC class I molecules present peptides of 8 to 10 amino acids, while MHC class II molecules are able to bind peptides consisting of 13 to 20 amino acids. In both cases the peptides make tight contacts with polymorphic amino acids lining the peptide binding groove of MHCs via amino acid anchor residues (Reviewed in Rammensee et al., 1995). Besides the TCR interaction site, MHC molecules are able to bind to the CD4 or CD8 coreceptors, which are expressed by T cells. MHC class I molecules interact with their α3 domain with CD8 while MHC class II molecules interact with their α2 domain with CD4.

1.1.4 CD4 and CD8 Coreceptor Molecules

CD4 and CD8 are referred to as coreceptors, because they are able to cooperate with TCR in antigen recognition. Upon induction of the genes encoding CD4 and CD8 during T cell development, both coreceptors are expressed on the cell surface of developing TCRα/β thymocytes. Depending on the type of MHC molecule recognized by the TCR, thymocytes develop into either MHC class II restricted $CD4^+$ T cells or MHC class I restricted $CD8^+$ T cells (Reviewed by Germain, 2002). CD4 is a single chain molecule consisting of four Ig-like domains (D1, D2, D3, D4) a transmembrane region and a cytosolic tail which interacts with the Src kinase Lck. CD8 can either exist as a disulfide linked CD8α/α homodimer or a CD8α/β heterodimer (Fig. 1.1D). Both CD8α and CD8β are glycosylated transmembrane proteins containing a N-terminal Ig domain each, extended hinge and stalk regions and transmembrane as well as cytoplasmic portions. On the other hand CD8β has only about 30% homology to CD8α and has a 13 amino acid longer extracellular domain (Reviewed by Gao et al., 2000). While the cytosolic tail of CD8α interacts with Lck, CD8β does not directly interact with the

kinase but can be palmitoylated and in this way controls the activity of the Lck (Irie et al., 1995; Arcaro et al., 2000). CD8α/α homodimers are found on NK cells and intestinal T cells, while the expression of CD8α/β is necessary for the development of conventional CD8 T cells (Wheeler et al., 1992; Nakayama et al., 1994; Crooks et al., 1994).

1.1.5 Structural Aspects of TCR Ligand Binding

As described in Section 1.1.3 the TCR is not able to bind antigens in their native conformation. Instead peptide fragments of antigens are presented by MHC class I or MHC class II molecules to the TCR. TCR-pMHC interactions are established between the CDR1, CDR2 and CDR3 loops of the TCR and the antigenic peptide bound between two α-helices of the MHC. Several crystal structures of TCR-pMHC interactions have been analyzed, including pMHC

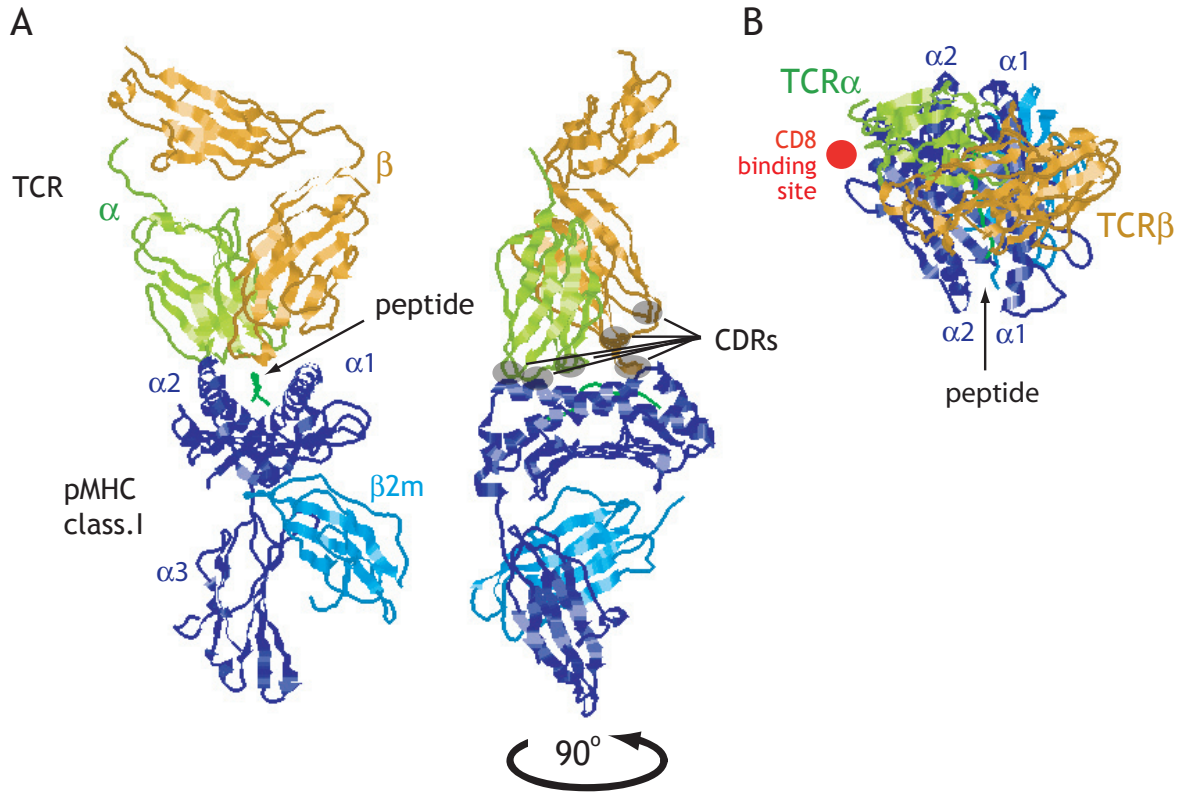

Figure 1.2: Crystal structure of TCR-pMHC class I interactions. (A) Extracellular fragments of TCR interacting with MHC class I ligand. The peptide is bound between the two α-helices of the α1 and α2 domains of class I MHC (blue) and presented to the TCR. The TCR interacts with the CDR2 domains (indicated with gray circles) of TCRα (green) and TCRβ (orange) with the α1 and α2 domains of the MHC molecule, while the CDR3 loops in the center of the binding interface contact the peptide (dark green). A two side views of the same interaction are shown. (B) TCR binds pMHC in a topologically constrained manner with TCRα placed over the N-terminus of the peptide and the α2 domains of MHC and TCRβ placed over the C-terminus of the peptide and the α1 domain of MHC. (Modified Figure from Garboczi et al., 1996).

class I and pMHC class II complexes (Garboczi et al., 1996; Garcia et al., 1996; Garcia et al., 1998; Gao et al., 1997; Hennecke et al., 2000). Detailed analysis of such complexes revealed certain common features of the TCR-pMHC interactions observed with all crystal structures described so far (Fig. 1.2A). TCR binds pMHC in a topologically constrained, diagonal manner with the Vα domain of the TCR positioned over the N-terminal half of the MHC bound peptide and with the TCR Vβ domain over the C-terminal half of the peptide (Fig. 1.2B). In this orientation the CDR1 and CDR2 loops of the TCR are placed over the two α-helices of the peptide binding groove mediating most of the contacts between the TCR and MHC. The CDR3 loop instead is placed directly over the peptide. In this respect it is interesting to consider that the greatest diversity between TCR molecules is observed in the CDR3 loops (due to non-homologous end joining of V (D) and J regions) interacting with the peptide, while the CDR1 and CDR2 loops are less diverse (germline encoded in Vα and Vβ) and generally interact with the MHC. The affinities of a variety of TCR-pMHC interactions have been determined using surface plasmon resonance (SPR; BIACore; see Introduction 1.3.2.2). These measurements revealed very broad affinity range for bimolecular TCR-pMHC interactions from 1μM to 1mM (Reviewed in Davis et al., 1998 and Gascoigne et al., 2001). The fact that all crystallized CDR3 loops showed considerable conformational flexibility suggested that the interaction betweens CDR3s and the peptide utilize an 'induced fit' mechanism, in which proper binding is achieved by small conformational changes at the binding face. Support for this view came from surface plasmon experiments in which the curves gained from association and dissociation kinetics were best fit using induced-fit models (Wu et al., 2002; Gakamsky et al., 2004). This implied that depending on the structure of the CDR3 loop and the peptide, the kinetics of TCR-pMHC interactions can differ considerably due to the varying energy requirements needed to 'induce' an optimal 'fit'. A different binding mechanism is proposed for the interaction of the coreceptors with MHC. Due to the low flexibility at the binding interfaces between CD8 and MHC class I and CD4 and MHC class II, these interactions might resemble the 'rigid-body association' as it is described for many antibody antigen interactions or NK cell receptor-pMHC interactions (Maenaka et al., 1999). Despite this similarity, the interaction between coreceptors and MHCs are much weaker than most antibody antigen interactions. For CD8, K_D values between 50μM and 150μM were described while the interaction between CD4 and MHC class II was described to be even weaker (K_D >200μM). On the other hand, the simultaneous binding of coreceptors and TCR (Fig. 1.3) to the same pMHC complex leads to substantial stabilization of the TCR-pMHC interaction (Lüscher et al., 1995; Denkberg et al., 2001; Holler et al., 2003).

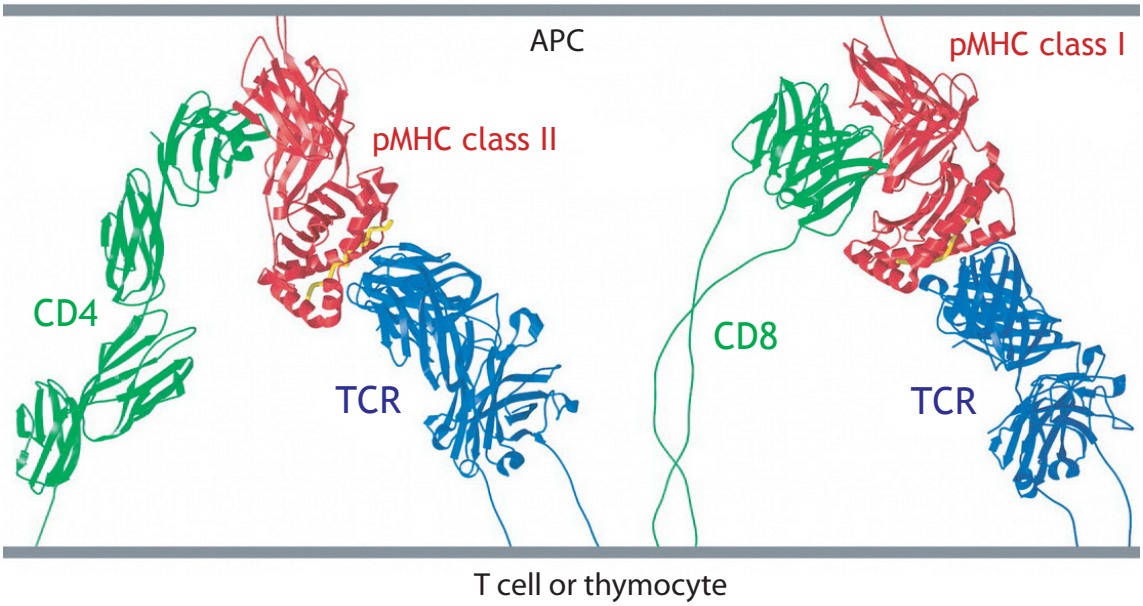

Figure 1.3: Models of TCR/CD4-pMHC class II and TCR/CD8-pMHC class I interactions. Crystallographic models of simultaneous TCR/coreceptor binding to pMHC complexes. The 3-D structures of class I and class II MHC molecules (shown in red) are very similar. While TCR (blue) interacts with MHC (red) and peptide (yellow) in a topologically constraint manner, the coreceptors can bind to membrane proximal domains of the MHC molecules independent of TCR/MHC binding. Coreceptor-MHC interactions do not sterically interfere but stabilize the interaction between TCR and pMHC (Modified Figure from van der Merwe et al., 2003).

1.2 TCR Ligand Binding in T Cell Development

1.2.1 The Role of the Thymus in T Cell Development

Bone marrow derived T cell precursors migrate via the blood stream to the thymus at a very early stage of development, prior to TCR expression. T cell precursors found in the thymus and referred to as thymocytes initiate TCR expression and pass through a tightly controlled series of developmental stages, before they enter the blood stream again as mature, self-restricted and self-tolerant T cells. Several of these developmental stages are non cell-autonomous. Two of these are explained here in more detail.

1.2.2 Positive and Negative Selection of Thymocytes

When T cell precursors enter the thymus, they express neither CD4 nor CD8 coreceptors and are therefore called 'double negative' (DN) thymocytes. DN thymocytes migrate to the subcapsular region of the thymic cortex, where they start to rearrange their TCR genes. Following successful TCRβ gene rearrangement, TCRβ molecules interact with the invariant pre-TCR surrogate chain and the CD3 complex and signal the cell to go through several rounds of division and to upregulate the CD4 and CD8α/β coreceptor molecules.

CD4/CD8 'double positive' (DP) cells then rearrange their TCRα gene locus, which leads to the production of TCRα chains which replace the pre-TCR surrogate chain and form α/βTCR heterodimers. Importantly, due to the processes of allelic exclusion (reviewed by Bassing, 2000), each thymocyte generally expresses TCRs of only one specificity, i.e. TCRs are clonotypically expressed. As soon as TCRα/β is expressed on the surface of DP thymocytes it interacts with pMHC molecules presented by thymic epithelial cells. From this timepoint on, thymocyte survival is critically dependent on TCR signaling. Thymocytes which receive no TCR signal die by neglect within 3 to 4 days. Only those DP thymocytes receiving signals from TCRs engaging positive selecting pMHC will survive and become self-restricted $CD4^+$ or $CD8\alpha^+/\beta^+$ 'single positive' (SP) thymocytes found in the medullary region of the thymus (Reviewed by Germain, 2002). On the other hand if DP or SP thymocytes receive signals from TCR interacting with negative selecting ligands development ceases and the cells undergo apoptosis. Therefore only self-restricted and self-tolerant immature T cells are able to leave the thymus and re-enter the blood stream to seed the peripheral lymphatic organs as either class II MHC restricted CD4 T cells or class I MHC restricted CD8 T cells.

1.2.2.1 Defining Positive and Negative Selecting Ligands

As described above the decision whether a thymocyte gets neglected, positively selected or negatively selected depends on the TCR-pMHC interaction. That means that in the thymus of a wildtype mouse, ~100 million thymocytes, each expressing a TCR of a different specificity undergo the selection processes on a number of different MHC class I and MHC class II molecules expressed in a particular individual. Given the fact that the peptides are unknown and MHC molecules are the most polymorphic proteins found in nature, it is obvious that simplified model systems had to be developed to identify and define positive and negative selecting pMHC ligands. The development of inbred mice expressing a unique combination (haplotype) of MHC molecules together with the development of recombination deficient ($Rag2^{-/-}$) TCR transgenic mice created a system, in which the TCR specificity and the MHC haplotype were well defined. Based on this, several different approaches were developed to study the role of TCR, peptide and MHC in thymic selection. A widely used technique is the so called fetal thymic organ culture (FTOC). In this assay, fetal thymi of TCR transgenic, $Rag2^{-/-}$ mice which are deficient in MHC class I cell surface expression due to the absence of the MHC class I 'light chain', β2m are placed in organ culture. The developmental arrest of MHC class I restricted, DP thymocytes caused by the absence of TCR ligand is restored by exogenous administration of the β2m protein in combination with a well defined (synthetic) peptide (Hogquist et al., 1994). Several variations of this system, including

TAP1 (see Introduction 1.1.3) deficient mice instead of β2m deficient mice (Van Kaer et al., 1992), or mutants of MHC class II peptide presentation (Fukuy et al., 1997) led to the identification of positive and negative selecting peptides in a series of TCR transgenic systems and MHC haplotypes. Interestingly, it was shown, that (agonist) peptides which induced a response in mature T cells, lead to negative selection of thymocytes expressing the same TCR. On the other hand, (antagonistic or weakly agonistic) peptide variants which were unable to fully activate mature T cells induced positive selection in the thymus of the same mice. Thus agonist peptides activate T cells, but induce negative selection of thymocytes. In contrast, antagonist peptides fail to activate mature T cells but induce positive selection in thymocytes. This demonstrates that different TCR signals can be elicited from the same ligand depending on the developmental stage of the cell. To understand this phenomenon in molecular terms, TCR signals involved in thymocyte selection as well as the role of TCR-ligand binding in positive and negative selection has been studied in detail.

1.2.2.2 TCR Signaling Involved in Thymocyte Selection

One approach to understand the differences between weak and strong TCR signals is to study the intracellular signaling cascades that are initiated upon TCR ligand binding during thymic selection. Using knockout animals and various biochemical approaches, profound insights were gained in the signaling cascades coupling TCR triggering to gene activation.

1.2.2.2.1 TCR Signaling Cascades

Figure 1.4A shows a simplified overview of intracellular TCR signaling, emphasizing on membrane proximal signaling (Reviewed by Germain et al., 1999). It is proposed that in unstimulated T cells, membrane proximal tyrosine kinases (Lck, Fyn and ZAP70), are located in specialized membrane compartments (DIGs; detergent insoluble glycolipid complexes), which are spatially separate from their ITAM substrates found in the cytosolic tails of the TCR/CD3 complex. pMHC induced TCR/coreceptor ligation leads to the phosphorylation of the ITAMs from CD3 ζ by Lck or Fyn. Following ITAM phosphorylation ZAP-70 is recruited and phosphorylation of ζ-associated ZAP-70 (by Lck) causes its activation leading to the phosphorylation of the linker of activation of T cells (LAT). LAT is a transmembrane adaptor molecule containing 9 tyrosine residues, which connects events on the plasma membrane to distal signaling cascades. Dependent on which of LAT's tyrosine residues are phosphorylated, distinct sets of cytosolic adaptor proteins (Reviewed by Rudd, 1999) are recruited, contributing to the activation of small GTP-binding proteins (Ras, Rac) or the recruitment of PLCγ1. Small GTP-binding proteins are activators of the Erk, Jnk and MAP kinases, which

control the function of transcription factors (NF-κB, Jun, Fos). On the other hand binding of PLCγ1 to LAT initiates calcium and PKC dependent signaling pathways which can modulate the MAP kinase pathways and NFAT activation (Fig.1.4A).

1.2.2.2.2 Signaling Cascades Involved in Positive and Negative Selection

It is intriguing that TCRs are able to generate signals which result in such opposing cellular responses as differentiation or death. It was proposed that these different MAP kinase pathways account for positive (Erk) and negative (Jnk, p38) selection. A modification of this idea suggests that both positive and negative selection signals use all three MAP kinase pathways but with distinct kinetics (Reviewed in Werlen et al., 2003). According to this model, TCR triggering by negative selection ligands induces a LAT phosphorylation pattern which recruits Grb-2, Gads, SLP-76 and PLCγ, leading to a transient calcium burst and Erk activation which are down-regulated before the Jnk and p38 pathways. This pattern of MAP kinase activation induces negative selection. In contrast, positive selection ligands induce a LAT phosphorylation pattern which recruits only Gads and SLP-76 leading to weak but sustained Erk activation which extends after the down-regulation of Jnk and p38. This configuration induces positive selection. How these different LAT phosphorylation patterns are accomplished is not known. Interestingly, TCRs lacking the α-CPM are completely defective in Erk activation in response to positive selecting ligands while the same α-CPM mutant TCRs

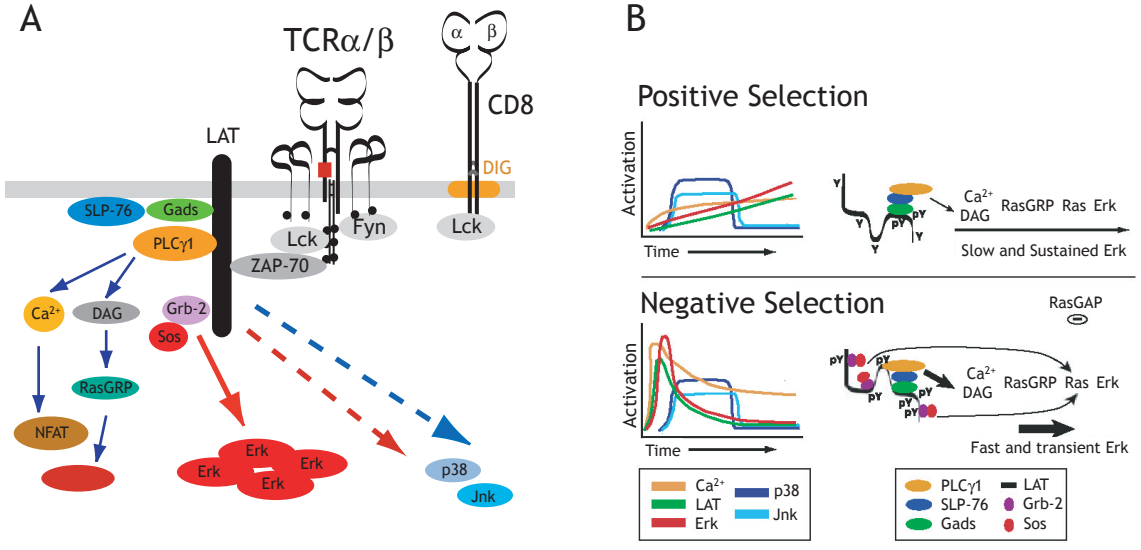

Figure 1.4: Signaling cascades discriminating negative selection from positive selection. (A) Schematic representation of key molecules involved in TCR signaling. Blue arrows schematically represent proposed cascades involved in signals elicited by positive selecting ligands, red arrows represent proposed cascades involved in signaling elicited by negative selecting ligands. Dashed arrows represent phosphorylation of molecules similarly involved in positive and negative selection. (B) Proposed mechanisms underlying signal differentiation between positive and negative selection. Positive selecting ligands lead to slow and sustained phosphorylation of Erk while negative selection ligands lead to fast and transient phosphorylation of Erk.

are fully competent to activate Erk rapidly and transiently and induce apoptosis in response to negative selecting ligands (Werlen et al., 2000). The fact that α-CPM mutant TCRs show defective CD3δ association (Backstrom et al., 1998) leading to defective TCR/coreceptor cooperativity (Naeher et al., 2002; Doucey et al., 2002) could explain the altered coreceptor/Lck recruitment to the TCR/CD3 complex leading to abrogation of positive selection. Along the same line it was shown that CD3δ deficient and CD8β deficient mice show specific defects in positive selection but normal negative selection supporting a model in which the α-CPM links ligand binding to intracellular signaling. In this thesis it has been addressed to what extent the α-CPM plays a role in TCR-ligand binding (See Results 3.2).

1.2.2.3 The α-Chain Connecting Peptide Motif (α-CPM)

The α-chain connecting peptide motif (α-CPM) consists of seven highly conserved amino acids (FETDxNLN) which are found in the membrane proximal connecting peptide (CP) domain of the α-chain from TCRα/β (Fig. 1.1A and Results 3.2.4: Naeher et al., 2002: Fig.1) of all vertebrates. Deletions or point mutations in the α-CPM lead to abrogation of TCR surface expression. Therefore, analysis of the role of the α-CPM in TCR signaling and T cell development was performed using chimeric TCRα chains containing the CP, TM and cytosolic regions from homologous TCRδ regions paired with TCR β chains containing the TM and cytosolic regions from TCRγ which allowed for surface expression of α-CPM mutant TCRs. Such α-CPM mutant TCRs showed defective signaling upon TCR stimulation due to the replacement of the α-CPM (Backstrom et al., 1996).

Thymocytes of transgenic mice either expressing an α-CPM mutant form of the MHC class II restricted 3BBM74 TCR (Backstrom et al., 1998) or an α-CPM mutant form of the MHC class I restricted OT-1 TCR (Werlen et al., 2000) showed a severe block in thymocyte development at the DP stage. Analysis of the TCR/CD3 complex in these mice showed strongly reduced association of the CD3δ chain to the complex and it was shown that the developmental block at the DP stage was caused by a specific signaling defect in response to positive selecting ligands, while signals involved in negative selection were unaffected by the replacement of the α-CPM. Biochemical analysis of the signaling cascades in α-CPM mutant mice revealed defective activation of the MAP kinase, Erk in response to positive selecting ligands, while Erk activation proceeded normally in response to negative selecting ligands. The absence of Erk phosphorylation in α-CPM mutant mice in response to positive selecting ligands was explained by the absence of phosphorylated CD3ζ, Lck and LAT from DIGs (i.e. membrane rafts) upon stimulation with positive selecting ligand. This indicated a defect in the initialization of TCR proximal signaling specifically in response to weak pMHC ligands.

1.3 TCR Ligand Affinity

1.3.1 TCR Ligand Binding in Positive and Negative Selection

It is generally accepted that 'weak' pMHC ligands promote positive selection, while 'strong' pMHC ligands induce negative selection. Nevertheless how a cell 'reads' the 'strength' of pMHC ligands is unresolved. Several models have been proposed on how ligand binding triggers TCR signaling in developing thymocytes. The conformational change model proposes that ligand binding induces qualitatively different responses by inducing different levels of conformational changes which are transduced from the TCR variable regions to the cytosolic regions of the CD3 complex (Janeway et al., 1989; Yoon et al., 1994; Gil et al., 2002). In contrast, the affinity/avidity model (Sprent et al., 1997) proposes, that quantitatively different signals resulting from either differing affinities or avidities of TCR-ligand interactions dictate positive or negative selection. This was supported by the finding, that when the affinity of the bimolecular TCR-pMHC interactions were measured by SPR (see below), the dissociation constants (K_D) correlated in the majority of the cases directly with the biological potency determined on peripheral T cells, i.e. high affinity TCR-pMHC interactions were observed with fully activating ligands (agonists) while low affinity interactions were measured for weak agonists or ligands that did not elicit a response (antagonists) (Garcia et al,. 1997; Alam et al., 1996; Davis et al., 1998; Kersh et al., 1998; Alam et al,, 1998; Ding et al., 1999; Baker et al., 2000; Degano et al., 2000;). When this comparison was performed with thymocytes instead of peripheral T cells less definite results were obtained. In some cases, low affinity ligands were only able to induce positive selection and high affinity ligands were only able to induce negative selection (Hogquist et al., 1994; Hogquist et al., 1995; McKeithan et al., 1995: Alam et al,, 1996). These studies argued that the key determinant of thymic selection is the TCR affinity for a pMHC ligand. However, other reports supported an avidity model of thymic selection, in which TCR occupancy (i.e. ligand avidity) is the key determinant that decides whether a thymocyte gets positively or negatively selected (Ashwell et al., 1986; Sebzda et al, 1994; Ashton-Rickard et al., 1994; Liu et al., 1998; Smith et al., 1998). These conflicting results led to the formulation of two distinct mechanistic models of TCR-ligand binding. While the serial triggering model proposes that ligand avidity is 'read' by a cell by counting the number of TCRs that become serially triggered over a given period of time (Valitutti et al., 1995), the kinetic proof-reading model (McKeithan, 1995) suggests that T cells are able to distinguish the ligand affinities by measuring the time that a single pMHC ligand occupies a single TCR. In both models, the TCR-ligand dissociation kinetics and hence the affinities are a very important parameter concerning the signals initiated by

TCR. TCR affinity measurements have been hampered by the fact, that the TCR as well as its pMHC ligands are integrated into cell surfaces and their affinities could therefore not be directly measured. Instead, soluble forms of TCR and pMHC molecules have been used to study these affinities in various systems.

1.3.2 TCR Ligand Binding Studies: Theoretical and Technical Considerations

1.3.2.1 Affinity and Avidity: Definitions

Considering a ligand (L) binding to a receptor (R) the affinity of the receptor-ligand interaction (RL) is defined as the concentration of free ligand [L] which leads to a condition where 50% of all receptor molecules are bound by ligand. This means that the concentration of free receptor [R] equals the concentration of bound receptor [RL]. Given the fact that these receptor ligand interactions follow the law of mass action, such ligand concentrations represent the reciprocal value of the equilibrium constant and are referred to as dissociation constant K_D (see Fig. 1.5A).

The avidity of a multivalent ligand (L) binding to multiple receptors (R) represents the sum of a single ligand binding to one receptor (RL) and multiple numbers (x) of receptors (R_xL). Because the transition of single binding (RL) to multiple binding (R_xL) can be influenced by parameters, which are independent of the binding forces at the interaction interface (e.g. distance between multiple receptors or 'oversaturation' of ligands such that only one binding site per multivalent ligand interacts with a receptor), the avidity represents a mixture of affinity (K_D) and parameters (K_x) which are not exclusively defined by the physical forces that act between the ligand and receptor molecules (see Fig. 1.5B).

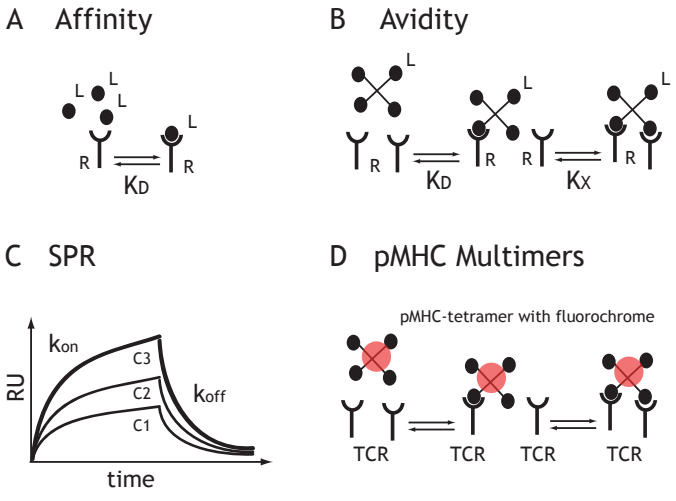

Figure 1.5: Theoretical and technical aspects of TCR-ligand binding. (A) Affinity is defined as the free concentration of monomeric ligand [L], which leads to half-maximal saturation of receptors [R] on a cell, represented by the dissociation constant K_D. (B) Avidity is a mixture of the affinity (K_D) of a monomeric ligand subunit of a ligand multimer and steric factors (K_X) influencing the simultaneous binding of the remaining ligand subunits to receptors. (C) Surface plasmon resonance (SPR) measures binding kinetics (k_{on}) and dissociation kinetics (k_{off}) of ligands applied at different concentrations (C1-C3) expressed by changes in the resonance units (RU). (D) Schematic representation of the binding involved in avidity measurements performed with fluorescently labeled pMHC multimers (tetramers are shown) binding to cell bound receptors.

1.3.2.2 Surface Plasmon Resonance (SPR; BIACore®)

Surface Plasmon Resonance (SPR; BIACore®) (Jonsson et al., 1991) has been widely used to study binding affinities between proteins. In this assay, the changes in surface plasmon resonance is measured by the application of constant flow of a soluble ligand to a polymer coated sensor chip, comprised of gold plated glass, to which soluble receptor molecules have been adsorbed (often the receptor is biotinylated and the sensor is coated with streptavidin). Association kinetics ('on-rates') are measured by injecting ligand at a defined concentration and flow rate. When steady state binding is reached, the ligand is withdrawn from the injected buffer and the dissociation kinetics ('off-rates') can be measured. From the 'on-' and 'off-rates' the K_D values can be calculated (Fig. 1.5C) For the determination of TCR-pMHC interactions both molecules have to be recombinantly produced in a soluble form, lacking the transmembrane and cytosolic regions and in the case of the TCR, lacking the CD3 complex. Using SPR, the affinities as well as the 'on-' and 'off-rates' of several TCR-pMHC and CD4 or CD8 coreceptor-MHC interactions were measured (Reviewed in Gascoigne et al., 2001; König, 2002; van der Merwe et al., 2003).

1.3.2.3 TCR Ligand Binding Studies pMHC Monomers and Multimers

Despite the invaluable advance that has been provided by the development of the SPR technique in the quantification of TCR-pMHC and coreceptor-MHC interactions, it did not allow the study of the cooperative binding of TCR and coreceptor to the same pMHC as it occurs on living T cells. The development of soluble pMHC multimers carrying fluorochromes allowed to study TCR-pMHC binding on live cells using flow-cytometry. Fluorochrome labeled pMHC dimers, tetramers and octamers have been widely used to study TCR ligand binding avidities under various binding conditions on mature T cells and thymocytes and shed light on the role of coreceptors in cognate TCR-pMHC as well as non-cognate coreceptor-MHC binding (Altman et al., 1996; O'Herrin et al., 1997; Guillaume et al., 2003).

In order to be able to study TCR ligand binding affinities, pMHC monomers have to be used (see Introduction 1.3.2.1 and Fig. 1.5). Initial experiments using pMHC monomers were hampered by the fast dissociation kinetics of most TCR-pMHC interactions which interfered with the detection of TCR bound pMHC monomers by lysis and PAGE analysis or flow cytometry. This drawback was overcome by the development of photo-reactive pMHC monomers (Lüscher et al., 1994), which allowed specific covalent crosslinking of pMHC bound to TCR expressed on live T cells. Using this technique, quantitative aspects of TCR ligand binding to pMHC monomers on thymocytes and T cells were analyzed in this thesis.

1.3.3 Measuring TCR Ligand Affinities on Living T Cells

1.3.3.1 The Principle of the Photoaffinity Labeling System

Ligand binding studies in this thesis were performed using the photoaffinity labeling system developed by Immanuel Lüscher. This system is based on the *Plasmodium berghei Circumsporozoite* (PbCS) peptide derivative $_{252}$SYIPSAEK(ABA)I$_{260}$ containing a photo-reactive azido-benzoic acid (ABA) group (Fig.1.6A), which is selectively activated by UV light at ~312 nm. This photo-reactive peptide derivative is bound by H-2K^d MHC class I molecules to form defined pMHC complexes. After binding of such pMHC complexes to specific TCRs, photo-activation of the ABA group allows covalent cross-linking of the pMHC ligand to the TCR. Several TCRα/βs specific for this peptide were obtained from different CTL clones (e.g. S1, S4, S14, S15, S17, S18, T1) (Lüscher et al., 1992) isolated from mice injected with a derivative of this peptide containing photo-reactive iodo-4-azidoslicylic acid (IASA) in place of PbCS Serine$_{252}$ (Fig.1.6B). The N-terminal IASA group can be photo-activated selectively by UV light at ≥ 350 nm and allows covalent crosslinking of the peptide derivative to H-2K^d molecules (Lüscher et al., 1991). In this thesis, TCR ligand binding was studied using the T1-TCR which specifically binds soluble, monomeric H-2K^d complexes either loaded with $_{252}$SYIPSAEK(ABA)I$_{260}$ or (IASA)-$_{253}$YIPSAEK(ABA)I$_{260}$ peptide derivatives (Fig.1.6C). Dependent on the assay, ligand binding was either detected by autoradiography or fluoresence based flow-cytometry.

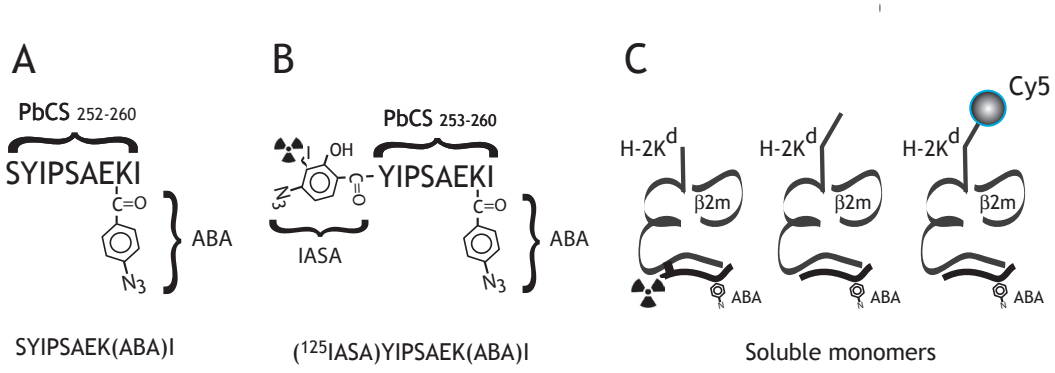

Figure 1.6: Peptide derivatives used for photoaffinity labeling. (A) The PbCS$_{252\text{-}260}$ SYIPSAEK(ABA)I peptide derivative contains a photo-reactive ABA group (activated by UV light ~312 nm) coupled to lysine$_{259}$. (B) The PbCS$_{253\text{-}260}$ (^{125}IASA)YIPSAEK(ABA)I peptide derivative contains two photo-reactive groups, ^{125}IASA and ABA. The ^{125}IASA group is activated by UV light of >350 nm; the ABA group is activated by UV light of ~ 312 nm. (C) The peptides can be bound to soluble H-2K^d complexes to form ligands of the T1-TCR. Detection of TCR bound H-2K^d monomers was performed either by autoradiography (^{125}I signal) or fluorescence intensity (Cy5 fluorochrome signals).

1.3.3.2 Photoaffinity Labeling Using Fluorescently Labeled pMHC Ligands

To detect TCR bound ligand by flow-cytometry, fluorescently labeled pMHC monomers were produced. After refolding of soluble H-2K^d molecules in the presence of β2m and photo-reactive peptide, monomeric pMHC complexes were purified and coupled to Cy5 fluorochrome molecules by alkylation via a cystein residue at the C-terminal end of the soluble H-2K^d chain. Like this, defined Cy5 labeled pMHC monomers were produced with a 1:1 ratio of Cy5:pMHC monomer (Fig.1.7A). These monomeric Cy5 labeled pMHC complexes were then applied to thymoyctes or lymph node T cells at various concentrations for defined times leading to steady state ligand binding. Subsequent UV irradiation at ~312 nm led to covalent crosslinking of bound pMHC ligand to TCR. After washing the amount of bound ligand was determined by flow-cytometry (Fig.1.7B).

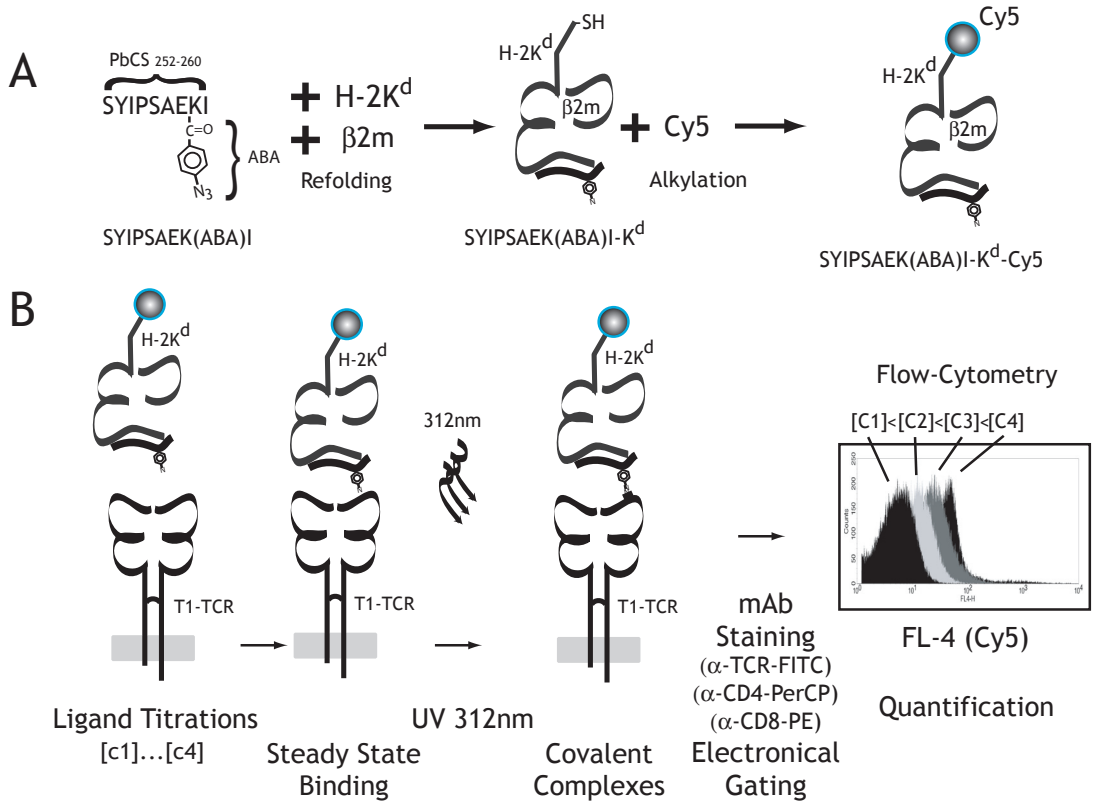

Figure 1.7: Direct Photoaffinity Labeling with Cy5 labeled pMHC monomers. (A) Production of soluble, Cy5 labeled pMHC monomers. The PbCS$_{252-260}$ SYIPSAEK(ABA)I peptide derivative is refolded together with pMHC class I heavy chain (H-2K^d) and β2m. Purified SYIPSAEK(ABA)I-K^d complexes are specifically linked to the Cy5 fluorochrome by alkylation of a free cysteine at the C-terminus of the H-2K^d heavy chain. (B) Photo-reactive, Cy5 labeled pMHC monomers are applied to cells expressing T1-TCR at defined concentrations (C1-C4) and incubated for a defined period of time allowing steady state ligand binding. UV irradiation at ~312 nm leads to the formation of covalent bonds between peptide and TCR. The amount of bound ligand is determined by FACS analysis of the fluorescence signal emitted by Cy5.

1.3.3.3 Photoaffinity Labeling Using Radioactive pMHC Ligands

To compare TCR ligand binding to various mutants of the T1-TCR expressed on hybridomas, radioactively labeled pMHC monomers were produced by Immanuel Lüscher. This was achieved using iodinated (I^{125}) (IASA)-$_{253}$YIPSAEK(ABA)I_{260} peptide derivatives (either (IASA)-$_{253}$YIPSAEK(ABA)I_{260} referred to as ^{125}I-Ag11.3 or (IASA)-$_{253}$YIASAEK(ABA)I_{260} peptide derivatives referred to as ^{125}I-P255A) (Fig. 1.8A). After refolding of soluble H-2K^d molecules in the presence of β2m and radioactive, bi-reactive peptide, monomeric pMHC complexes were purified and the peptide was covalently crosslinked to the H2-K^d heavy chain by UV irradiation at 360 nm. These covalent peptide-MHC complexes were applied to T1 hybridoma cells to study ligand binding, following their photo cross-linking to the TCR by UV irradiation at 312 nm. After washing and lysis, T1-TCR variants were immunoprecipitated and analyzed by PAGE. The radioactive signals obtained from covalent TCR-peptide-MHC complexes were quantified by autoradiography (Fig.1.8B).

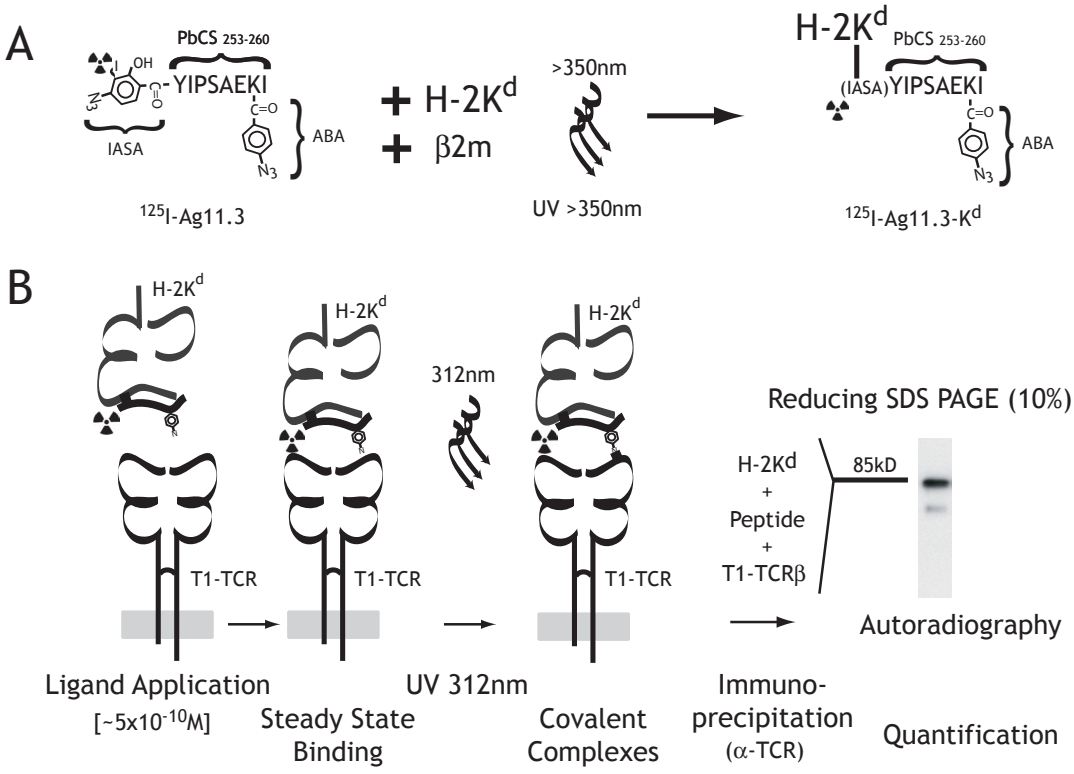

Figure 1.8: Direct Photoaffinity Labeling using ^{125}I labeled pMHC monomers. (A) Production of soluble, covalently linked pMHC monomers, labeled with ^{125}Iodine. The bifunctional PbCS$_{253-260}$ (^{125}IASA)YIPSAEK(ABA)I peptide derivative was refolded together with pMHC class I heavy chain (H-2K^d) and β2m and subsequently covalently crosslinked to the H-2K^d heavy chain by UV irradiation >350 nm.
Purified, monomeric PbCS$_{253-260}$(^{125}IASA)YIPSAEK(ABA)I-K^d complexes were referred to as ^{125}I-Ag11.3-K^d. (B) Photo-reactive, ^{125}I labeled pMHC monomers were applied to cells expressing T1-TCR at non-saturating concentrations (~5x10^{-10} M) and incubated for a defined period of time allowing steady state ligand binding. UV irradiation at ~312 nm led to the formation of covalent bonds between H2-K^d-peptide and bound TCR. The amount of bound ligand was determined by immunoprecipitation, SDS-PAGE and autoradiography.

2. Materials and Methods

2.1. Reagents and Solutions

Materials and reagents used for cellular techniques:

alamar blue oxidation red.	Alamar
β-mercaptoethanol	Gibco BRL
β-2 microglobulin	Calbiochem
DMEM	Gibco BRL
fetal calf serum (regular)	Gibco BRL
fetal calf serum (FTOC)	Roche
IL-2, mouse, recombinant	Genzyme
non-essential a.a. (100x)	Gibco BRL
polybrene	Sigma
sodium pyruvate (100x)	Gibco BRL

Materials and reagents used for biochemical techniques:

Reagents which are not listed were all purchased from Sigma or Fluka

Bottle top, 0.45µm (cellulose acetate) filters	Corning
Kodak Biomax films	Kodak
protein A sepharose	Pharmacia
L-Arginine HCl	Merck
Ultrafree-CL 2ml centrifugal filter devices	Millipore
Ultrafiltration membranes polyethersulfone (10kD)	Millipore
Stirred ultrafiltration cell 350ml	Millipore

Antibiotics used for cellular and biochemical techniques:

ampicillin	Sigma
carbenicillin	Sigma
gentamycin	Gibco
hygromycin B	Roche
l-histidinol	Roche
neomycin	Gibco BRL
penicillin-streptomycin	Gibco BRL
puromycin	Sigma

Enzymes:

lysozyme	Sigma
restriction enzymes/ligases	New England Biolabs

Kits used for molecular techniques:

QuickChange mutagenesis	Stratagene
DNA MaxiPrep	Qiagen
QiaEx gel extraction	Qiagen

Solutions and Media:

Solutions used for molecular techniques:

TAE	40mM	Tris-acetate pH 8.0
	1mM	EDTA
TBE	45mM	Tris-borate
	1mM	EDTA
TE	10mM	Tris pH 8.0
	1mM	EDTA
10x universal buffer	1M	K-glutamate
	250mM	Tris-acetate, pH 7.5
	100mM	Mg-acetate
	500µg/ml	BSA
	5mM	β-mercaptoethanol
5x ligation buffer	500mM	Tris pH 8.0
	100mM	DTT
	100Mm	$MgCl_2$
	10mM	ATP

Solutions used for biochemical techniques:

Lysis buffer	1%	TritonX-100
	1%	Nonidet P-40
	150mM	NaCl
	0.2mM	EDTA
	50mM	HEPES pH 8.0
	1mM	PMSF
	10µg/ml	leupeptin
	10µg/ml	aprotinin
	10µg/ml	iodoacetamide
IP wash buffer	0.5%	TritonX-100
	150mM	NaCl
	0.2mM	EDTA
	50mM	HEPES pH 8.0
Tris freezing buffer	50mM	Tris pH 8.0
	25%	sucrose
	1mM	EDTA
	1mM	DTT
	1mM	PMSF

DOC detergent buffer	50mM	Tris pH 8.0
	2%	Triton X-100
	1%	NaDOC
	100mM	NaCl (5M)
	0.1%	NaN_3
	1mM	DTT
Detergent buffer	50mM	Tris pH 8.0
	1%	Triton X-100
	100mM	NaCl
	0.1%	NaN_3
	1mM	DTT
Inclusionbody wash buffer	100mM	Tris pH 8.0
	150mM	NaCl
	1mM	EDTA (0.5M)
Upscaled urea buffer	10M	Urea
	62.5mM	MES pH 6.5
	0.125mM	EDTA
	0.25mM	DTT
Urea buffer	8M	Urea
	50mM	MES pH 6.5
	0.1mM	EDTA
	0.1mM	DTT
Refolding buffer	400mM	L-Arginine-HCl
	100mM	Tris pH 8.0
	2mM	EDTA
	0.4mM	PMSF
	5mM	Glutathione reduced
	0.5mM	Glutathione oxidized

Solutions used for SDS-PAGE and blotting techniques:

Stacking gel solution		H_20
	30%	acrylamide solution
	1.0M	Tris pH 6.8
	10%	SDS
	10%	APS
	0.25%	TEMED
Separating gel solution		H_20
	30%	acrylamide solution
	1.5M	Tris pH 8.8
	10%	SDS
	10%	APS
	0.25%	TEMED

SDS running buffer		H_20
	25mM	Tris pH 8.3
	250mM	glycine pH 8.3
	0.1%	SDS
SDS gel loading buffer	50mM	Tris pH 6.8
	100mM	DTT
	2%	SDS
	10%	glycerol
	0.1%	bromphenol blue
Coomassie stain. solution	10%	Acetic acid
	45%	MeOH
	0.25%(w/w)	Coomassie brillant blue
Coomassie destain	10%	Acetic acid
	10%	MeOH
Transfer buffer	38mM	glycine
	48mM	Tris pH 8.3
	0.04%	SDS
	20%	methanol
Blocking solution	5%	TopBlock (Juro, Switzerland)
	0.01%	antifoam A
	0.02%	NaN_3

Solutions used for cellular techniques:

PBS	137mM	NaCl
	2.7mM	KCl
	8.0mM	Na_2HPO_4
	1.5mM	KH_2PO_4
FACS buffer	2%	FCS
	10mM	NaN_3 in PBS
LB-media	1%	Peptone
	0.5%	yeast extract
	90mM	NaCl
LB freezing media		LB media
	30%	glycerol
2x HEPES buffer	50mM	HEPES, pH 7.05
	10mM	KCl
	12mM	Dextrose
	280mM	NaCl
	1.5mM	Na_2HPO_4

Media used for cell cultures:

Basic media		DMEM (Gibco)
	100U/ml	penicillin
	100µg/ml	streptomycin
	2mM	L-glutamine
	1mg/ml	gentamycin
	50µM	β-mercaptoethanol
58 Hybridoma media		Basic media
	2%	FCS
		addition of the respective selecting antibiotics
T cell media		Basic media
	10%	FCS
	1x	non-essential amino acids
	1mM	sodium pyruvate
FTOC media		T cell media
	10%	FCS (from Roche)
	5µg/ml	β-2-microglobulin

Devices:

ÄKTA FPLC, Amersham Biosciences, Umea, Sweden
Avanti J25, Beckman Coulter, Palo Alto, CA, USA
DNA sequencer, Applied Biosystems Inc.
JLA-10.500, JA-25.15, JA-25.50 rotors, Beckman Coulter, Palo Alto, CA, USA
Biometra Thermocycler T3, Chatel-St.Denis, Switzerland
Coulter ChannalyzerR, Instrumentengesellsschaft, Zürich, Switzerland
CentrifugeStar 5417R, Eppendorf, Germany
FACSCalibur, Becton Dickinson, Mountainview, CA, USA
FACSVantage, Becton Dickinson, Mountainview, CA, USA
JASCO PU 1580 HPLC System, Omnilab, Mettmenstetten, Switzerland
JASCO UV 2075 Spectrometer, Omnilab Mettmenstetten, Switzerland
Multifuge3 S-R, Heraeus, Kendro, Osterode, Germany
BioRad molecular imager FX pro, BioRad Inc., Reinach, Switzerland
SpectraMax 250 plate reader, Molecular Devices, Palo Alto, CA, USA
Stirred Ultrafiltration Cell, Millipore Corporation, Bedford, MA, USA
UV lamp (VL-215 L), Fisher Bioblock Scientific, Illkirch, France

Columns used for FPLC:

Desalting:	Hi Prep 26/10	Amersham Biosciences
Anion Exchange:	Resorce Q (6ml)	Amersham Biosciences
Gel Filtration:	Superdex 75	Amersham Biosciences

Columns used for HPLC:

Reverse Phase:	C18 (218TP510)	Grace Vidac, Hesperia, CA, USA

Software:

Program	Application	Provider
CellQuest Pro	FACS	Becton Dickinson
Unicorn	FPLC	Amersham Biosciences
SoftMax Pro	Spectraphotometry	GraphPad Software Inc.
ImageQuant	Phosphorimaging	Molecular Dynamic
Prism	Curve fitting	GraphPad Software Inc.
Adobe Illustrator	Graphics	Adobe Inc.
Adobe Indesign	Layout	Adobe Inc.
Microsoft Word	Time wasting	Microsoft Inc.
Microsoft Excel	Data storage	Microsoft Inc.

Antibodies:

Commercial antibodies were titrated and applied at saturating concentrations for FACS staining. Antibodies produced in the laboratory had been individually titrated beforehand.

Antigen	Clone	Ref.
α-mouse CD3ε	(142-2C11)	(Leo et al. 1987)
α-mouse CD3δ	(polyclonal)	(Backstrom et al. 1996)
α-mouse TCR-Cβ	(H57-597)	(Kubo et al. 1989)
α-mouse CD8β(Ly-3.2)	(H35-17)	(Golstein et al. 1982)
α-mouse H-2K^d(α3)	(SF1-1.1)	(Abasto et al. 1993)
α-mouse H-2K^d(α1)	(20-8-4S)	(ATTC, Rockville, MD)

Antibodies used for FACS analysis:

Antigen	Clone	Fluorochrome	Provider
α-mouse CD3ε	(142-2C11)	PE or APC	PharMingen
α-mouse CD4 (L3T4)	(RM4-5)	FITC or PerCP	PharMingen
α-mouse CD8α (Ly-2)	(53-6.7)	PE or FITC	PharMingen
α-mouse CD8β (Ly-3.2)	(53-5.8)	PE	PharMingen
α-mouse CD69	(H1.2F3)	biotinylated	PharMingen
α-mouse TCR-Cβ	(H57-597)	FITC or PE	PharMingen
α-mouse TCR Vb8.1/2	(MR5-2)	FITC or PE	PharMingen
α-mouse H-2K^b	(AF6-88.5)	FITC or PE	PharMingen
α-mouse H-2K^d(α3)	(SF1-1.1)	FITC or PE	PharMingen

Secondary FACS reagents and fluorescently labeled pMHC complexes:

Streptavidin-PerCP		PharMingen
4P-H-2K^d-tetramers*	PE	provided by I. Lüscher
4P-H-2K^d-tetramers*	Cy5	provided by I. Lüscher
4A-H-2K^d-tetramers**	Cy5	provided by I. Lüscher
4P-H-2K^d-monomers*	Cy5	provided by I. Lüscher

* 4P represents the $PbCS_{252-260}$ SYIPSAEK(ABA)I peptide derivative; ** 4A represents the $PbCS_{252-260}$ SYIASAEK(ABA)I peptide derivative

Peptides:

The peptide sequence was derived from the *Plasmodium berghei circumsporozoite* $(PbCS)_{252-260}$ SYIPSAEKI peptide to which photochemical crosslinking groups were covalently linked (IASA and/or ABA) (Lüscher et al., 1994).

Sequence	Abbreviation	Provided by
(IASA)YIASAEK(ABA)I	I-P255A	I. Lüscher, Lausanne, CH
(IASA)YIPSAEK(ABA)I	I-Ag11.3	I. Lüscher, Lausanne, CH
(IASA)YISSAEK(ABA)I	I-S255A	I. Lüscher, Lausanne, CH
SYIASAEK(ABA)I	4A	I. Lüscher, Lausanne, CH
SYILSAEK(ABA)I	4L	I. Lüscher, Lausanne, CH
SYINSAEK(ABA)I	4N	I. Lüscher, Lausanne, CH
SYIPSAEK(ABA)I	4P	I. Lüscher, Lausanne, CH
SYISSAEK(ABA)I	4S	I. Lüscher, Lausanne, CH

Expression vectors:

LXSN	Retroviral Vector	Miller, 1989
LXSP	Retroviral Vector	Backstrom, 1996
pET3α	Proc. Expr. Vector	Novagen Inc.
pHSE3'	Transgenic Vector	Pircher,1989

2.2 cDNA Sequences

T1-TCR Sequences:

The T1 TCR is derived from the H-2K^d restricted, PbCS derivative $_{253-260}$(IASA)-YIPSAEK(ABA)I (Ag11.3)–specific CTL clone, T1 (Lüscher et al., 1992). Sequences were determined using the ABI sequencing kit (ABI Prism).

T1-TCRα (wildtype):

5'ATGAACACTTCTCCAGCTTTAGTGACTGTGATGCTGCTGTTCATGCTTGAGAGGACACATGGAAATTCAG
TGACCCAGATGCAAGGTCAAGTGACCCTTTCAGAAGAGGAGTTTCTATTTATAAACTGTACCTATTCAACCA
CAGGGTACCCGACTCTTTTCTGGTATGTCCAATATCCTGGAGAAGGTCCACAGCTCCTTTTGAAAGTCACAA
CAGCCAACAATAAGGGAAGCAGCAGAGGTTTTGAAGCTACATATGATAAAGGGACCACGTCCTTCCACTTG
CAGAAAGCCTCAGTGCAGGAATCAGACTCGGCTGTGTACTACTGTGTTCTGGGTGATCGGGGTAACAATAA
CAGAATCTTCTTTGGTGATGGGACGCAGCTGGTGGTGAAGCCCAACATCCAGAACCCAGAACCCGCGGTG
TACCAGTTAAAAGATCCTAGATCTCAGGACAGCACCCTCTGCCTGTTCACCGACTTTGACTCCCAAATCAAT
GTGCCGAAAACCATGGAATCTGGAACGTTCATCACTGACAAAACTGTGCTGGACATGAAAGCTATGGATTCC
AAGAGCAATGGGGCCATTGCCTGGAGCAACCAGACTAGTTTCACCTGCCAAGATATCTTCAAAGAGACCAAC

GCCACCTACCCCAGTTCAGACGTTCCCTGTGATGCCACGTTGACTGAGAAAAGCTTCGAAACAGATATGAAC
CTAAACTTTCAAAACCTGTCAGTTATGGGACTCCGAATCCTCCTGCTGAAAGTAGCCGGATTTAACCTGCTCA
TGACGCTGAGGCTGTGGTCCAGTTGA3'

T1-TCR α-δ chimera αIV:

Nucleotides 1-672 identical to T1-TCR-α (wildtype):

5'...673:TATGGCCCAAGAGTCACAGTTCACACTGAGAAGGTAAACATGATGTCCCTCACGGTGCTGGGCCT
ACGACTGCTGTTTGCCAAGACCATTGCCATCAATTTTCTCTTGACTGTTAAGTTATTCTTTTAA3'

T1-TCR α-δ chimera αIV:

Nucleotides 1-726 identical to T1-TCR-α (wildtype):

5'...727:TCCCTCACGGTGCTGGGCCTACGACTGCTGTTTGCCAAGACCATTGCCATCAATTTTCTCTTGAC
TGTTAAGTTATTCTTTTAA3'

T1-TCR-β (wildtype):

5'ATGGGCTCCAGGCTCTTCTTCGTGCTCTCCAGTCTCCTGTGTTCAAAACACATGGAGGCTGCAGTCACC
CAAAGCCCAAGAAACAAGGTGGCAGTAACAGGAGGAAAGGTGACATTGAGCTGTAATCAGACTAATAACCAC
AACAACATGTACTGGTATCGGCAGGACACGGGGCATGGGCTGAGGCTGATCCATTATTCATATGGTGCTGGC
AGCACTGAGAAAGGAGATATCCCTGATGGATACAAGGCCTCCAGACCAAGCCAAGAGAACTTCTCCCTCATT
CTGGAGTTGGCTACCCCCTCTCAGACATCAGTGTACTTCTGTGCCAGCGGTGAGGGACAGTCCTATGAACA
GTACTTCGGTCCCGGCACCAGGCTCACGGTTTTAGAGGATCTGAGAAATGTGACTCCACCCAAGGTCTCCT
TGTTTGAGCCATCAAAAGCAGAGATTGCAAACAAACAAAAGGCTACCCTCGTGTGCTTGGCCAGGGGCTTC
TTCCCTGACCACGTGGAGCTGAGCTGGTGGGTGAATGGCAAGGAGGTCCACAGTGGGGTCAGCACGGACC
CTCAGGCCTACAAGGAGAGCAATTATAGCTACTGCCTGAGCTCTAGACTGAGGGTCTCTGCTACCTTCTGGC
ACAATCCTCGAAACCACTTCCGCTGCCAAGTGCAGTTCCATGGGCTTTCAGAGGAGGACAAGTGGCCAGAG
GGCTCACCCAAACCTGTCACACAGAACATCAGTGCAGAGGCCTGGGGCCGAGCAGACTGTGGGATTACTAG
TGCATCCTATCAACAAGGGGTCTTGTCTGCCACCATCCTCTATGAGATCCTGCTAGGGAAAGCCACCCTGTAT
GCTGTGCTTGTCAGTACACTGGTGGTGATGGCTATGGTCAAAAGAAAAAACTCATGA3'

T1-TCR β-γ chimera βIII:

Nucleotide 1-825 identical to T1-TCR-β (wildtype):

5'...826:CTCCTCCTGCTCCTCAAGAGTGTGATCTACTTGGCCATCATCAGCTTCTCTCTGCTTAGAAGAACA
TCTGTCTGTGGCAATGAGAAGAAGTCCTAA3'

H-2K^{d}-BSP Sequence:

The cDNA encoding for the BSP (BirA specific peptide) tail is shown in bold:

5'ATGGCACCCTGCACGCTGCTCCTGCTGTTGGCGGCCGCCCTGGCCCCCACTCAGACCCGCGCGGGCCCA
CATTCGCTGAGGTATTTCGTCACCGCCGTGTCCCGGCCCGGCCTCGGGGAGCCCCGGTTCATCGCTGTCGG
CTACGTGGACGACACGCAGTTCGTGCGCTTCGACAGCGACGCGGATAATCCGAGATTTGAGCCGCGGGCGC

CGTGGATGGAGCAGGAGGGGCCGGAGTATTGGGAGGAGCAGACACAGAGAGCCAAGAGCGATGAGCAGT
GGTTCCGAGTGAGCCTGAGGACCGCACAGAGATACTACAACCAGAGCAAGGGCGGCTCTCACACGTTCCAG
CGGATGTTCGGCTGTGACGTGGGGTCGGACTGGCGCCTCCTCCGCGGGTACCAGCAGTTCGCCTACGACG
GCCGCGATTACATCGCCCTGAACGAAGACCTGAAAACGTGGACGGCGGCGGACACGGCGGCGCTGATCAC
CAGACGCAAGTGGGAGCAGGCTGGTGATGCAGAGTATTACAGGGCCTACCTAGAGGGCGAGTGCGTGGAG
TGGCTCCGCAGATACCTGGAGCTCGGGAATGAGACGCTGCTGCGCACAGATTCCCCAAAGGCCCATGTGAC
CTATCACCCCAGATCTCAAGTTGATGTCACCCTGAGGTGCTGGGCCCTGGGCTTCTACCCTGCTGATATCAC
CCTGACCTGGCAGTTGAATGGGGAGGACCTGACCCAGGACATGGAGCTTGTAGAGACCAGGCCTGCAGGG
GATGGAACCTTCCAGAAGTGGGCAGCTGTGGTGGTGCCTCTTGGGAAGGAGCAGAATTACACATGCCATGT
GCACCATAAGGGGCTGCCTGAGCCTCTCACC**GGATCCCTGCATCATATTCTGGATGCACAGAAAATGGTGT**
GGAATCATCGTTAAAAGCTT3'

2.3 DNA Constructs

The cDNA encoding the TCR-α chain was cloned into the G418 resistant retroviral vector, LXSN. Similarly, the T1 TCR-β chain was cloned into the puromycin resistant retroviral vector, LXSP. The cDNAs encoding the T1 TCR α-δ chimeras were constructed using the previously described αII and αIV chimeric cDNAs (Backstrom et al., 1996) specific for the 3BBM74 TCR (Di Giusto et al., 1994) by replacing the VJC containing, EcoRI–SpeI fragment byT1 TCR VJCα chain sequences. Similarly theT1 TCRβ-γ chimera βIII was constructed by replacing the VDJC containing EcoRI-XbaI fragment of the 3BBM74 chimeric β chains by T1 TCR VDJCβ chain containing sequences.
For the production of T1-TCR transgenic mice the cDNAs either encoding the T1-TCRα chains or the αII and αIV T1-TCRα-δ chimerias or the T1-TCRβ chains or the T1 TCRβ-γ chimera βIII were excised with EcoRI and BamHI and individually cloned into the SalI and BamHI sites of the expression vector pHSE3'. The pHSE3' vectors encoding the various T1-TCR cDNAs were enzymatically cleaved with the XhoI endonuclease and purifed using agarose gel electrophoresis and the QiaEx gel extraction kit (Qiagen) before injection into zygotes.

The pET3a Vectors containing either the cDNA encoding the H-2K^d–BSP protein or containing the cDNA encoding human β2m used for the production of inclusion bodies were provided by Immanuel Lüscher (Guillaume et al., 2003). The H-2K$^d_{\Delta 223/227}$ constructs were produced by site directed mutagenesis of H-2K^d-BSP cDNA. The cDNA encoding the H-2K^d-BSP protein cloned in the pET3α vector was used as a template to perform site directed mutagenesis by PCR amplification using the QuickChange mutagenesis kit (Stratagene). For PCR amplification the following primers were used:

-5'-TTGAATGGGGAGAAGCTGACCCAGGACATG-3' (forward primer)
-5'-CATGTCCTGGGTCAGCTTCTCCCCATTCAA-3' (reverse primer)
-5'-AGCTGACCCAGAAGATGGAGCTTGTAG-3' (forward primer)
-5'-CTACAAGCTCCATCTTCTGGGTCAGCT-3' (reverse primer)

2.4 Cell Lines

BOSC	fibroblast cell line	Pear, 1993
HT-2	T cell line	Watson, 1970
RMA-SK^d	H-2K^d tranfected RMA-S	provided by T. Potter
T2K^d	H-2K^d transfected T2 cell line	Cerundolo, 1990
58	thymoma	Letourneur, 1989
58CD8$\alpha\beta$	CD8α/β tranfected 58 cell line	Stotz, 1999

2.5 Inbred Mouse Strains

Zygotes used for injection of the pHSE3' vectors containing the cDNA encoding the various T1-TCR chains were obtained from BDF1xBDF1 mice. T1-TCR transgenic mice were backcrossed either on Balb/c;$Rag^{-/-}$ or B10.D2;$Rag^{-/-}$;$\beta 2m^{-/-}$mice. T1-TCR transgenic mice, OT-1-TCR;$Rag^{-/-}$ and TCRβ^{+} ;$Rag^{-/-}$ tg mice were bred in the mouse facilities of the Basel Institute for Immunology or the mouse facilities of the Department Research of the Universitätsspital Basel.

2.6 Molecular Techniques

Transformation of Competent Bacteria

Plasmid DNA or ligation mix was added to 50µl of XL-1blue competent bacteria (Stratagene) and incubated on ice for 20 to 30 min., followed by 90 sec. incubation at 42°C. Subsequently, the bacteria were plated on LB agar plates containing 50µg/ml ampicillin and incubated overnight at 37°C.

Plasmid Preparation

150ml of LB broth containing 50µg/ml ampicillin were inoculated with transformed bacteria and incubated over night at 37°C while shaking (250 rpm). The bacteria were harvested by centrifugation (3500xg, 15min. at 4°C). Subsequently the plasmids were isolated using Qiagen (500) columns following the manufacturers protocol. Purified plasmids were dissolved in H_20 to a final concentration of 0.5mg/ml.

Restriction Enzyme Digestion of Plasmid DNA

Enzymatic digestion of plasmid DNA was performed in 50µl using the appropriate restriction enzyme and the recommended concentration of 10x universal buffer for 1 hour at 37°C. Digested plasmids were loaded onto 2% agarose gels and the appropriate DNA fragments were isolated using the QiaEx gel extracting kit following the manufacturers protocol.

DNA Ligation

DNA ligation was carried out in a 20µl volume using 100ng vector DNA and 50ng insert DNA mixed with appropriately diluted 10x ligation buffer and 1 unit of T4 DNA ligase for 30 min. at RT. 5µl of the DNA ligation mixture were used to transform XL-1 Blue competent bacteria.

DNA Sequencing

DNA sequencing was performed using the ABI prism sequencing reaction kit and following the manufacturers protocol. For each reaction 300ng of template DNA and 3.2pmol final concentration of each primer was used. 30 cycles of PCR reactions were performed using the following cycle steps: I: 96°C, 30 sec.; II: 50°C, 30 sec., III: 60°C, 4 min. Subsequently, amplified DNA fragments were precipitated, washed in 70% ethanol and dried before resuspending in 4µl ABI prism loading buffer and heating for 2 min. at 90°C. Samples were loaded on a 8.5% polyacrylamide gel containing 15M urea and analyzed on a ABI prism sequencer.

2.7 Cellular Techniques

Production of Retroviral Supernatant

The retroviral packaging cell line BOSC was used to transfect 58 and 58CD8αβ hybridomas. BOSC cells were plated in 6-well plates at subconfluent density to allow cell growth up to 48 hrs. post transfection to obtain high titer viral supernatant. The cells were tranfected using the Calciumphosphate precipitation method. 10µg vector DNA in 450µl H_2O were sterile filtered using 0.2µm Acrodisc syringe filters prior to mixing with 125µl 2M $CaCl_2$. The mixture was added dropwise to 0.5ml cold 2X HEPES buffer and subsequently added to subconfluently plated BOSC cells. After 12 hrs. incubation at 37°C the supernatant was exchanged with fresh basic DMEM containing 5% FCS. 24 hrs. post-transfection, medium was exchanged again and replaced by 3ml fresh medium. 36 hrs. post-transfection the virus containing supernatant was harvested and instantly used for infection of 58 or 58CD8αβ hybridomas.

Infection of 58 and 58CD8α/β Hybridomas

The supernatant containing retroviral particles was used to infect the 58 and the 58CD8αβ hybridomas. $5x10^5$ 58 or 58CD8αβ hybridomas were resuspended in 500µl DMEM containing 4µg/ml Polybrene. After 24 hrs., 5ml of fresh basic DMEM medium containing 5% FCS and the appropriate selective drugs were added (1mg/ml G418, 3µg/ml puromycin, 2mM histidinol or 0.5mg/ml hygromycin B). Surviving cells were analyzed after 4 days and sorted for high TCR surface expression by FACS®. Transfected cells were continuously maintained in medium containing selective drugs.

Stimulation of T1-TCR Transfected Hybridomas

80µl 58 hybridoma medium containing $6x10^4$ T2-K^d cells were plated in flat bottomed 96-

well plates and incubated with various amounts of peptide for 2 hrs. at 37°C. T hybridoma cells (6 x 10^4 in 100µl medium) were subsequently added. After a further 24 hrs. of incubation at 37°C, the supernatant was transferred into 96-well round bottom plates and frozen at -20°C for storage and to kill any transferred cells.

IL-2 Assays

The IL-2 content of supernatants obtained from stimulation of T1-TCR transfected 58 and 58CD8$\alpha\beta$ hybridomas was determined by incubating 2x10^3 HT-2 cells per well in round-bottom 96-well plates with serial dilutions of culture supernatant for 24 hrs. Alamar Blue substrate was then added over night and IL-2 titers were spectraphotometrically determined by comparison to a standard curve generated using recombinant murine IL-2 and the SOFTMax Pro version 3.1 software.

K^d-Stabilization on RMA-S-K^d Cells

The affinity of the SYIPSAEK(ABA)I peptides for the H-2K^d molecules was indirectly measured by peptide induced stabilization of K^d molecules on the cell surface of RMA-S-K^d cells. At RT due to a defective TAP-2 transporter gene only 'empty' MHC molecules are expressed on the cell surface of these cells. Therefore, the RMA-S-K^d cells were kept for 36 hrs. at RT to allow the expression of 'empty' MHC molecules on the cell surface. Subsequently, graded concentrations of peptides were added. Afer 30 min. the samples were transferred to 37°C to allow the degradation of MHC molecules which had not been successfully loaded and stabilized by peptide binding. After 3 hrs. incubation at 37°C, cells were washed and stained with the PE labeled K^d-specific antibody SF1-1.1 (20µg/ml) in FACS buffer for 1 hour on ice. Mean channel fluorescence was determined using a FACSCalibur flow-cytometer and CellQuest 3.0 software.

CD69 Upregulation Assays

150µl T cell medium containing 7.5x10^5 T2-K^d cells were plated in flat bottomed 96-well plates and incubated with various concentrations of peptide for 2 hrs. at 37°C. Thymocytes or lymphocytes (5x10^5 cells in 100µl CD69 assay medium) from T1 transgenic mice were subsequently added. After a further 18 hrs. of incubation at 37°C, cells were transferred to 96-well round bottom plates, washed and transfered to FACS buffer containing a mix of fluorescently labeled mAbs specific for TCR-Cβ, CD4, CD8 and CD69. Subsequently cells were analyzed by FACS.

Neuraminidase Treatment of Cells

$2x10^6$ cells were incubated in 0.016 units of neuraminidase from Vibrio cholerae for 60 min. at 37°C in DMEM (without additives). Cells were subsequently washed three times in DMEM and incubated in 0.1µg/ml PNA for 30 min. on ice. Cells were transferred to 96-well round bottom plates, washed and transferred to FACS buffer containing a mix of fluorescently labeled mAbs specific for TCR-Cβ, CD4 and CD8. Subsequently cells were analyzed by FACS.

Fetal Thymic Organ Culture (FTOC)

FTOCs were performed using thymi of E15 feti from $Rag^{-/-}$;$\beta2m^{-/-}$; T1-TCR transgenic mice. Thymic lobes were placed on 13mm diameter, 0.8µm polycarbonate filter discs in 24-well tissue culture plates on top of 1ml of DMEM supplemented with 10% FCS (tested for FTOC suitability), 5µg/ml human β2m and various concentrations of peptide. 24-well plates were incubated for 7 days in a cell culture incubator with 7.5% CO_2 at 37°C and supplemented DMEM with peptide was exchanged once after 3 days of culture. After 7 days thymocytes were harvested from the lobes, stained and analyzed by FACS for TCR, CD4 and CD8α/β expression.

FACS Analysis

FACS analysis was performed on a FACSCalibur flow-cytometer using the CellQuest Pro software. Cells were stained with fluorescently labeled mAbs or pMHC tetramers for 1 hour on ice in 96-well round bottom plates and FACS buffer and subsequently washed twice with 200µl FACS buffer before analysis. In the case of biotinylated primary antibodies, a secondary staining step was necessary and the cells were incubated with fluorescently labeled SA for 10 min. on ice before washing and analysis.

Quantitation of TCR Surface Expression on Hybridoma Cell Lines

The levels of TCR expression were measured using the FITC labeled anti-TCR-Cβ mAb, H57-597 and flow-cytometrical analysis on a FACSCalibur using CellQuest Pro version 3.0. Due to the different T1-TCR expression levels observed on the various 58 and 58CD8αβ hybridomas the ligand binding signals obtained from the binding analysis by autoradiography had to be normalized for the different T1-TCR expression levels to be able to compare the signal per TCR and hence the binding capacity of the different T1-TCR variants tested. To calculate the relative amounts of the three different TCRs expressed on $CD8^+$ and $CD8^-$ hybridomas, the expression of the TCR, measured with the anti-TCR-Cβ mAb, H57-597 was

normalized to the expression of the wild type TCR measured on $CD8^+$ hybridomas. The following equation was used:

relative TCR expression = MFI of TCR staining expressing variant TCR/MFI of TCR staining on $CD8^+$ hybridomas expressing wildtype T1-TCR.

2.8 Biochemical Techniques

Photoaffinity Labeling Using ^{125}I-Ag11.3-K^d and ^{125}I-P255A-K^d pMHC Monomers

Soluble H-2K^d molecules loaded with the ^{125}IASA-YIPSAEK(ABA)I peptide or the P255A derivative were generously provided by Immanuel Lüscher. TCR photoaffinity labelings were performed by incubation of 10^7 T hybridoma cells (10^9 cells/ml in 58 hybridoma medium) either at 0°C for 1.5 hrs. or at 37°C for 10 min., with 5 x 10^6 cpm of H-2K^d-^{125}IASA-YIPSAEK(ABA)I or P255A pMHC monomers followed by UV irradiation at 312 ± 40 nm. After UV irradiation, cells were washed three times in ice cold PBS before lysis and immunoprecipitation.

Lysis and Immunoprecipitation

Cells were washed three times in ice cold PBS and incubated in lysis buffer (2 x 10^7 cells/ml) containing a protein inhibitor cocktail (1mM PMSF, 10µg/ml leupeptin, 10µg/ml aprotinin and 10µg/ml iodoacetamide) for 30 min. at 4°C. Lysed cells were centrifuged at 12000 rpm for 15 min. at 4°C and the supernatants were transferred to fresh 1.5ml Eppendorf tubes containing saturation amounts of the antibodies used for immunoprecipitation. In the case of the T1-TCR transfected 58 and 58CD8$\alpha\beta$ hybridoma cells the α-TCR-Cβ mAb (H57-597) was used at 20µg/ml final concentration. In the case of the thymocytes from T1;Rag$^{-/-}$ mice immunoprecipitation was either performed with the α-TCR-Cβ mAb (H57-597) used at 20µg/ml or the α-CD3-ε mAb (142-2C11) used at 20µg/ml. Following 2 hrs. of incubation at 4°C, the immune complexes were isolated using BSA-blocked protein A sepharose beads. After further incubation at 4°C for 30 min., the beads were washed three times in IP wash buffer and twice in PBS.

Polyacrylamide Gel Electrophoresis

The immunoprecipitated material on protein A sepharose beads was boiled immediately in 5X SDS sample buffer and analyzed on 10% reducing SDS PAGE gels. In the case of the samples obtained from photoaffinity labeling assays on hybridoma cells, the gels were fixed (45% MeOH, 10% acetic acid, 45% H_2O), dried and exposed to Kodak Biomax films at -80°C. In the case of the thymocytes from T1-TCR mice, SDS-PAGE gels were further processed by Western Blotting.

Coomassie Blue Staining of Gels

Gels were incubated for 3 min. in Coomassie blue staining solution and washed 3 times 30 min. with Coomassie wash at RT.

Western Blotting

SDS PAGE gels were electroblotted for 1 hour at 0.7A in ice-cold transfer buffer onto PVDF membranes. After blotting, the membranes were blocked using blocking solution for 30 min. at RT followed by incubations with 1:2000 dilutions of primary antibodies for 1 hour at RT. After 3 washes in blocking solution 1:8000 diluted secondary HRP-coupled antibodies were added for 30 min. at RT. The membranes were washed twice for 5 min. in blocking solution and finally washed once in PBS containing 0.1% Tween-20 before being dried. Proteins were detected using the ECL detection kit from Amersham and Kodak Biomax films. In the case of reprobing with a different antibody, membranes were boiled in PBS + 0.1% Tween-20 for 2 min. at 80°C before addition of the reprobing primary antibody and being processed the same way as described above.

Quantification of Radioactive Signals from SDS-PAGE Gels

Signals obtained on Kodak BioMax films were quantified using a PhosphorImager and ImageQuant software. To compare the photoaffinity labeling of the various receptors, the values were normalized for TCR expression and compared to the labeling value obtained on $CD8^+$ hybridomas expressing the wild type T1 TCR.

The following equation was used: relative binding = (CPM bound by variant TCR/CPM bound by CD8+ hybridoma expressing wildtype TCR)/ relative TCR expression).

2.9 Production of Soluble Monomeric pMHC Complexes

Production of Inclusion Bodies

BL21(DE3)pLys bacteria transformed either with the pET3α vector containing the cDNA encoding human β2m or containing the cDNA encoding H-$2K^d$-BSP were kindly provided by Immanuel Lüscher. Bacteria were grown at 37°C in LB medium containing 50µg/ml carbenicillin. Inclusion body production was induced by addition of 0.5mM IPTG at an OD_{600} of 0.9 of the bacterial culture. Cultures were incubated at 30°C and 250 rpm for 5 hrs. before isolation and purification of the inclusion bodies.

Isolation and Purification of Inclusion Bodies

IPTG induced bacterial cultures were centrifuged and resuspended in 'Tris freezing buffer' (50ml/1L of bacterial culture) before shock-freezing in liquid nitrogen. After thawing in a 37°C water bath lysozyme (1mg/ml) was added for 10 min. on ice before addition of 2% Triton X-100 and DNAse I (30µg/ml) to lyse the cells and degrade bacterial DNA and RNA. After sonification and centrifugation at 8500xg for 12 min., the pellet containing the inclusion bodies was further lysed in 'DOC detergent buffer', followed by sonification, centrifugation and resuspending in 'Detergent buffer' until a clean white pellet was obtained. The inclusion bodies were washed in 'Inclusion body wash buffer' to remove the detergent, solubilized in 'Upscaled urea buffer' and frozen in liquid nitrogen. The purity of the protein was assessed by SDS-PAGE and Coomassie blue staining.

Refolding of pMHC Complexes

pMHC complexes were produced by refolding of H-2K^d heavy chain in the presence of the peptide derivative PbCS$_{252\text{-}260}$ SYIPSAEK(ABA)I or variants. 18mg of H-2K^d heavy chain and 9mg of β2m in upscaled urea buffer were mixed and the volume of the solution was adjusted to 5ml with urea buffer. This mixture was added dropwise to 500ml ice cold refolding buffer containing 10mg of peptide under continuous stirring in the cold room. After stirring for 4 days at 4°C in the dark, insoluble components were removed by filtration over a 0.45 µm membrane filter and the solution was concentrated 50-fold by ultrafiltration in a stirred ultrafiltration cell and polyethersulfone membranes (molecular cut-off: 10kD).

Purification of Soluble pMHC Complexes

The refolded pMHC complex concentrates were loaded onto a 10ml superloop and run over a HiPrep 26/10 desalting column equilibrated with 20mM Tris pH 8.0 using an Äkta FPLC. The protein fraction was collected and applied on a 6ml ResorceQ anion exchange column. Proteins were eluted using an isocratic gradient of 1M NaCl in 20mM Tris pH 8.0. The monomeric pMHC complexes were eluted at a conductivity of 18mSi and concentrated to a final concentration of 3mg/ml using 4ml spinning concentrators (cut-off: 10kD) and stored at 4°C in the dark.

Photoaffinity Labeling Using Fluorescently Labeled pMHC Monomers and Tetramers

50µl of CD69 assay medium containing 2.5x10^5 freshly isolated thymocytes or T-lymphocytes from T1 transgenic mice were plated in 96-well flat bottom plates and 50µl of diluted Cy5 labeled monomeric or tetrameric pMHC complexes (provided by Immanuel Lüscher)

were applied either on ice, at 24°C or at 37°C. After various incubation times depending on the temperature (90 min. on ice, 15 min. at 24°C or 2 min. at 37°C) the samples were irradiated for 30 sec. with UV light of 312 ± 40 nm (60 Watt) to induce covalent UV-crosslinking of T1-TCR associated ligand. Irradiated cells were transferred to 96-well round bottom plates and 3 times washed with 200µl ice-cold T cell medium and once washed with 200µl FACS buffer before FACS analysis.

Two Step TCR Photoaffinity Labeling

The first step of the two step TCR photoaffinity labeling was performed with unlabeled peptide-H-2K^d monomers as described for the direct photoaffinity labeling using Cy5-labeled pMHC complexes. Instead of the last washing step using FACS buffer, the cells were incubated for 90 min. on ice in 100µl T cell medium containing 5x10^{-7} molar of fresh 4P-K^d-Cy5 monomers before the second irradiation with UV light of 312 ± 40 nm (60 Watt) to induce covalent UV-crosslinking of the freshly applied fluorescently labeled pMHC monomers. Cells were then washed 3 times with 200µl ice-cold T cell medium and once washed with 200µl FACS buffer before FACS analysis.

Ligand Dissociation Kinetic Measurements

10^5 cells were incubated in 50µl of DMEM containing 5% FCS for a defined period of time (90 min. at 0°C, 15 min. at 24°C or 2 min. at 37°C). Samples were 200-fold diluted with medium containing 40µg/ml α-H2-K^d(α1) mAb (20-8-4S) and samples were UV (~312 nm) irradiated at defined intervals. Cells were washed three times with medium and subsequently incubated for 90 min. on ice in 50µl cell culture medium containing 5x10^{-6} M 4P-K^d-Cy5. After UV irradiation (~312 nm), cells were washed and analyzed by flow cytometry.

Determination of Dissociation Constants

Affinities of T1-TCR-ligand interactions were measured by determining the concentration of free ligand leading to half-maximal fluorescence signals on single cells (represented by the K_D values). Values were determined using either Scatchard analysis or non-linear regression using the Prism4 software. K_D values shown in Tables III, IV and VIII represent the means determined from at least two independent experiments. The differences between the determined K_D values from multiple repetitions of experiments were less than 2-fold at 0°C and less than 3-fold at 24°C and 37°C.

3. Results

3.1 Functional Responses and TCR-Ligand Affinities in T1 Mice

3.1.1 Production and Characterization of T1-TCR Transgenic Mice

To study TCR-pMHC ligand affinities and functional responses of T cells at different developmental stages, T1-TCR transgenic mice were produced by co-injection of T1-TCRα and T1-TCRβ cDNAs into zygotes of BDF2 mice (see Materials and Methods). To eliminate cells which expressed endogenously rearranged TCRs, these mice were backcrossed onto Balb/c; $Rag2^{-/-}$ mice, preventing endogenous TCR gene rearrangements. Consequently, these Balb/c T1-TCR; $Rg^{-/-}$ mice (referred to as T1 mice) gave only rise to T-cells expressing the $H\text{-}2K^{d}$ restricted T1-TCR. As illustrated in Figure 3.1A, flow-cytometrical analysis of T1 thymocytes

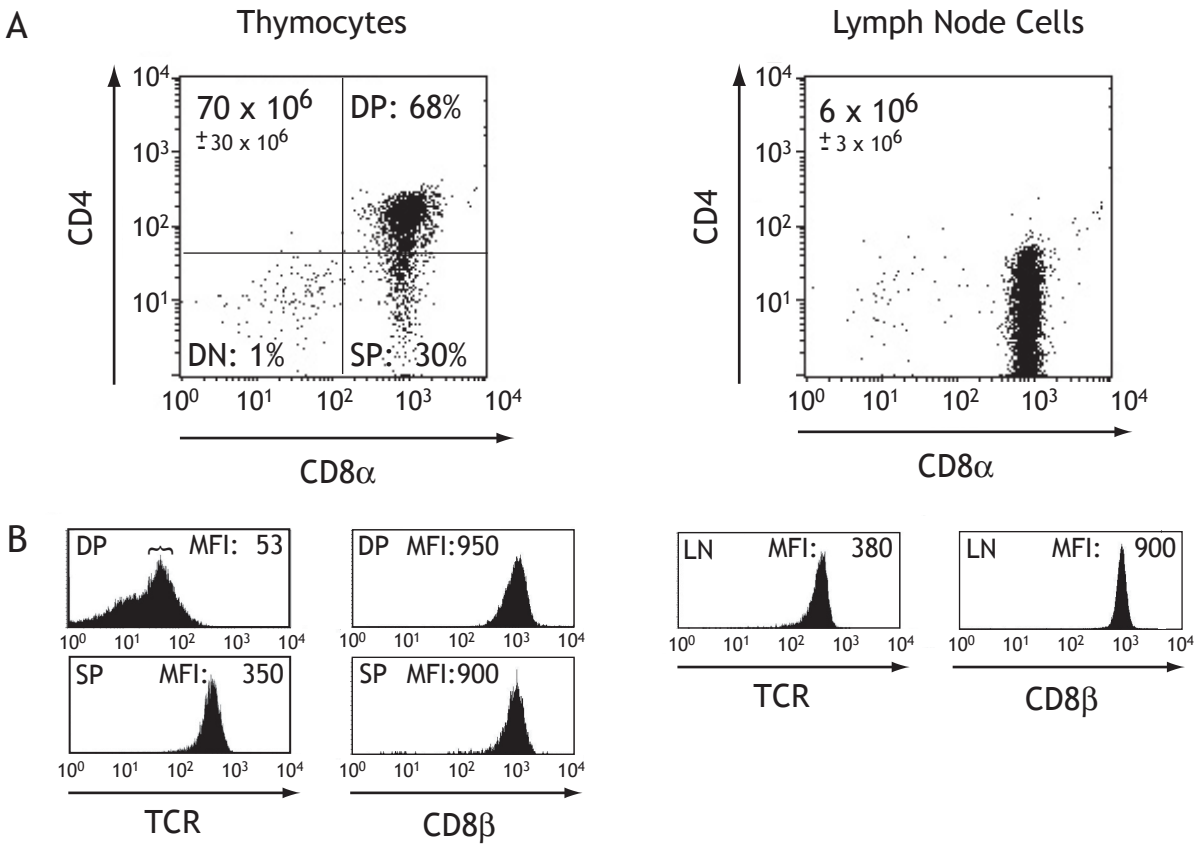

Figure 3.1: Flow cytometric analysis of thymocytes and lymph node cells from T1 mice. Thymocytes and lymph node cells from 6 to 8 week old T1; $Rag^{-/-}$ mice were isolated and stained with fluorescently labeled α-CD4(RM4-5), α-CD8α(53-6.7), α-CD8β(53-5.8), α-TCRβ(H57-597) mAb. (A) CD4 and CD8α cell surface expression measured on thymocytes or lymph node cells. Numbers in the upper left corner of each panel indicate total cell number of thymocytes or lymph node cells per animal (SED indicated; n=3). Cells were electronically gated and the percentages of double negative (DN), single positive (SP) and double positive (DP) determined. (B) Mean fluorescence intensities of TCRβ and CD8β were determined on electronically gated DPs, SPs and lymph node cells. MFI of TCR levels on DP thymocytes was determined for $TCR^{intermediate}$ cells (bracket).

revealed that 68% ($50x10^6 \pm 20x10^6$ cells) of all cells co-expressed the CD4 and CD8α/β coreceptor molecules representing the double positive (DP) population. Following T1-TCR dependent and H-2K^d restricted positive selection, DP cells further developed into CD8$^+$ single positive (SP) cells, which represented 30% of all T1 thymocytes ($20x10^6 \pm 9x10^6$ cells). Only 1% of thymocytes expressed neither CD4 nor CD8 and account for the double negative (DN) population. In T1 mice CD8$^+$ T-cells populated the spleen and the lymph nodes. These animals showed similar numbers of splenic T cells ($6x10^6 \pm 3x10^6$ cells, data not shown) and lymph node T cells ($6x10^6 \pm 3x10^6$ cells). The histograms in Fig. 3.1B show TCR and CD8β coreceptor expression on thymocytes and lymphnode T cells. While TCR expression levels were low on DP thymocytes (MFI: 53) the levels increased upon positive selection and were higher in SP cells (MFI: 350). Approximately 20% of DP thymocytes expressed no or only very low levels of TCR on their surface. TCR on peripheral T cells was comparable to SP thymocytes. CD8α and CD8β expression levels were similar throughout all developmental stages (DP, SP and LN; MFIs: 900-1000, see Fig. 3.1A and B). As these mice displayed the expected subpopulations of thymocytes and peripheral T cells, they were used to study TCR ligand binding and cellular responses at various developmental stages.

3.1.2 Characterization of Photo-reactive T1-TCR Peptide Ligands

Five variants of the photo-reactive, *Plasmodium berghei circumsporozoite* derived peptide SYIPSAEK(ABA)I, were used to probe cellular responses and TCR binding properties of thymocytes and lymphocytes from T1 mice. The five photo-reactive peptide variants are shown in Figure 3.2A. All of them carried an azidobenzoic acid (ABA) group linked to the lysine at position eight of the peptide. The variants differed in one amino acid at position four of the peptide. Position four of the peptide either consisted of a leucine (4L), a proline (4P), an alanine (4A), a serine (4S) or an asparagine (4N) residue. To determine the capacity of the variant peptides to bind to H-2K^d molecules presented by antigen presenting cells (APCs), their efficiencies in binding to H-2K^d expressed on RMA-S cells were tested (see Material and Methods). As indicated in Figure 3.2B, all peptides tested were capable of binding to H-2K^d molecules and stabilizing cell surface expression of the H-2K^d complexes. The strongest H-2K^d binding was observed for the 4P peptide (EC_{50}: $1.5x10^{-8}$ M, relative binding capacity: 1.0) followed by the 4N (0.7), the 4A (0.5), the 4S (0.3) and the 4L (0.2). The biggest difference in binding to H-2K^d molecules was the 5-fold difference observed between the 4P and the 4L peptides.

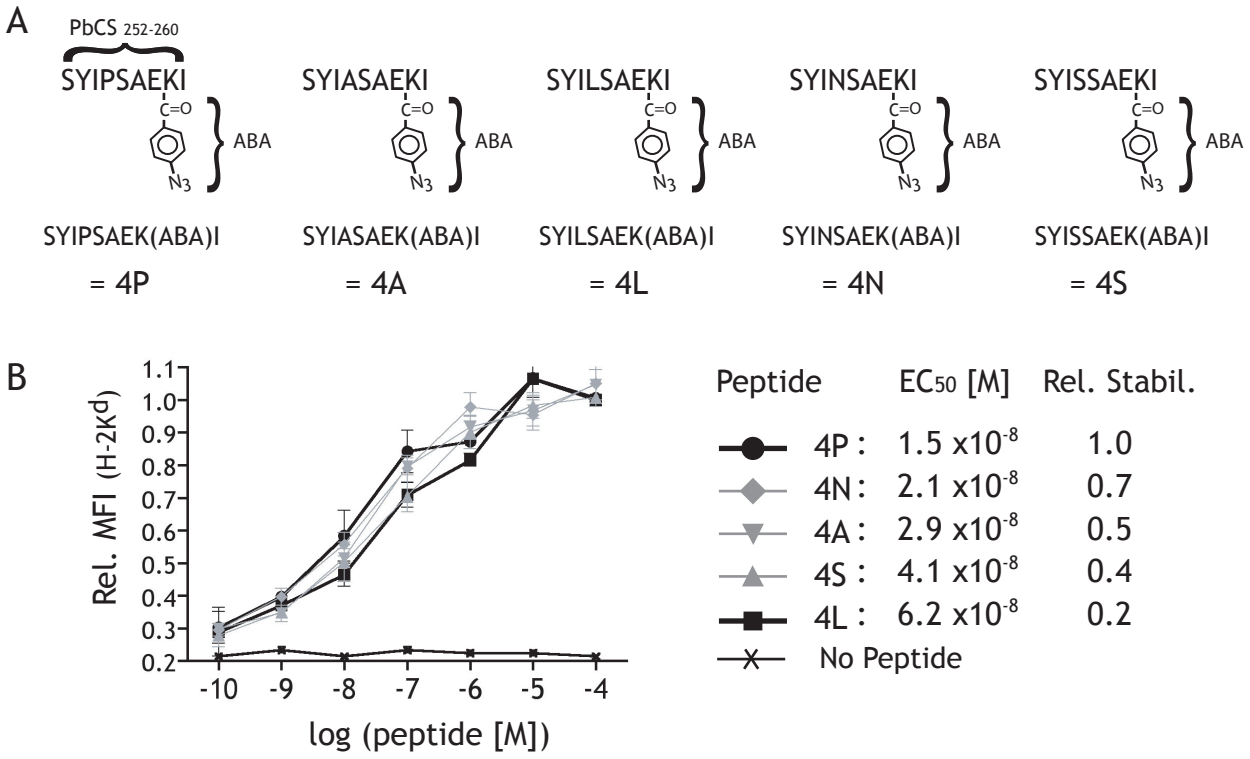

Figure 3.2: Stabilization of H-2K^d cell surface expression by binding of PbCS$_{252-260}$ SYIPSAEK(ABA)I peptide variants. (A) Variants of the photo-reactive PbCS$_{252-260}$ SYIPSAEK(ABA)I peptide derivative. For PbCS$_{252-260}$ SYIPSAEK(ABA)I variants, proline$_{255}$ at position 4 of the peptide (4P) was replaced either by alanine (4A), leucine (4L), asparagine (4N) or serine (4S) residues. Photo-reactivity (~312 nm) was mediated by the azido-benzoic acid (ABA) moiety linked to lysine$_{259}$. (B) Peptide induced stabilization of cell surface pMHC class I molecules expressed on RMA-S H-2K^d cells determined by fluorescence labeled α-H-2K^d(α3) SF1-1.1 mAb staining and measured by flow cytometry. Doses of the peptides shown in (A) required for half-maximal H-2K^d stabilization are indicated by the EC$_{50}$ values. Relative stabilization of H-2K^d was determined by comparison of the EC$_{50}$ values for each peptide with the EC$_{50}$ value obtained with 4P (Relative stabilization = EC$_{50}$ (peptide X) / EC$_{50}$ (4P)).

3.1.3 T1-TCR Ligands: Analysis of Biological Potency and CD8 Dependency

The potency of the five photo-reactive PbCS peptide variants to stimulate T1-TCR expressing T cells was analyzed. Thymocytes or peripheral T cells of T1 animals were incubated overnight in the presence of peptide loaded T2-K^d antigen presenting cells and subsequently analyzed by flow-cytometry for the percentage of T1 cells which had upregulated the CD69 activation marker. Figure 3.3A shows the percentage of cells undergoing CD69 up-regulation upon stimulation with peptide loaded APCs as a function of peptide dose. When thymocytes were analyzed, DP and SP thymocytes were gated separately. DP cells were most sensitive for the 4L peptide and the 4P peptide, followed by the 4A, the 4S and the 4N peptides. SP cells were similarly sensitive for the 4L, the 4P and the 4A peptide, while their sensitivity for the 4S and 4N peptides was reduced as indicated by a shift in the dose response curves of these peptides towards higher concentrations compared to DP cells.

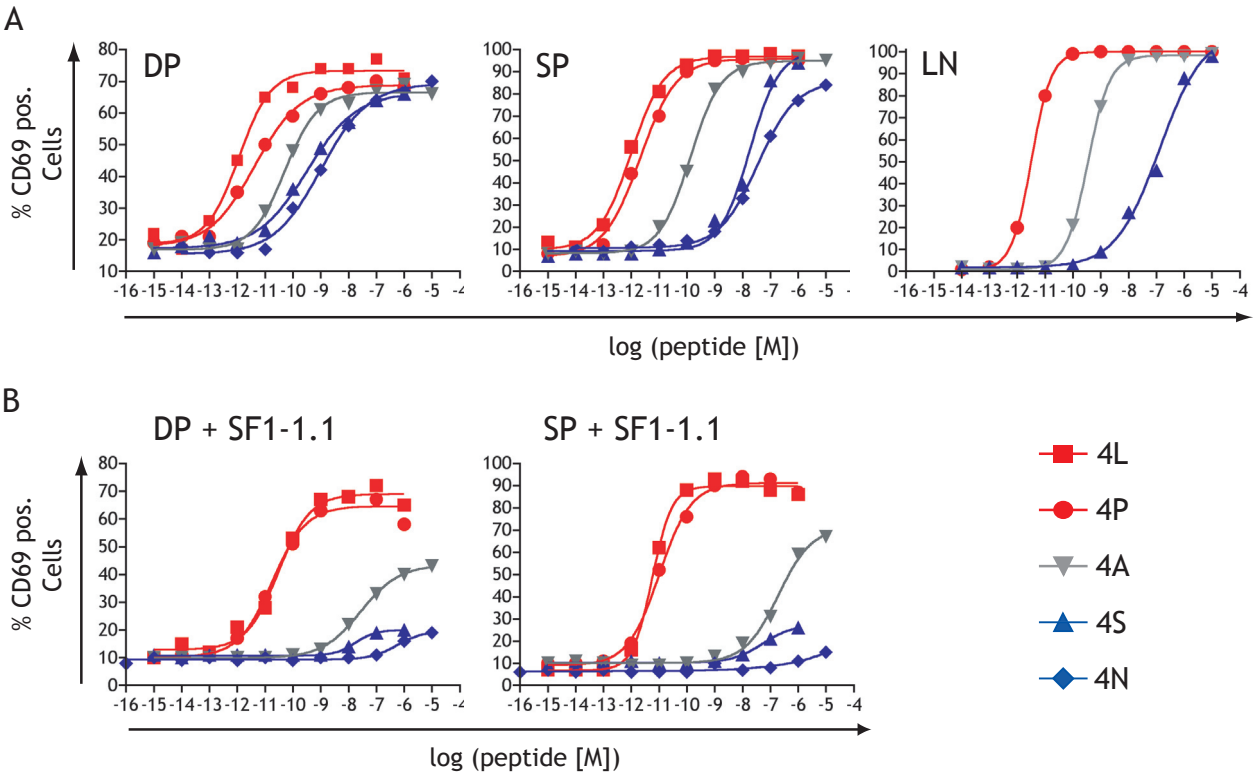

Figure 3.3: Peptide dose dependent CD69 upregulation on T1 thymocytes and lymph node T cells. Thymocytes and lymph node cells from T1 mice were stimulated for 18 hrs. with various doses of 4L(■), 4P(●), 4A(▼), 4S(▲) or 4N(◆) peptides presented on T2-K^d cells in the presence or absence of α-H-$2K^d$(SF1-1.1) (20μg/ml). Cultures were subsequently stained with fluorescently labeled α-CD4(RM4-5), α-CD8α(53-6.7), α-CD69 (H1.2F3) mAb. CD69 expression on DP and SP thymocytes was discriminated by electronic gating. (A) Percentages of DP thymocytes, SP thymocytes and lymph node T cells expressing surface CD69, in the absence of α-H-$2K^d$(SF1-1.1) mAb. (B) Percentages of DP thymocytes and SP thymocytes expressing surface CD69, stimulated in the presence of α-H-$2K^d$(SF1-1.1) mAb. A representative experiment from a total of at least two independent experiments is shown.

Dose response curves obtained from peripheral T cells on the other hand were comparable to response curves obtained on SP thymocytes. In case of DP thymocytes, only 80% of the cells upregulated CD69, due to the fact that about 20% of the DP thymocytes of T1 mice did not express TCRs (Fig. 3.1B) and were therefore unresponsive to pMHC ligands.

When these same experiments were performed in the presence of the α-H-$2K^d$(α3) mAb SF1-1.1, which blocks the CD8 binding site on H-$2K^d$, a substantial increase of the EC_{50} of both DP and SP thymocytes was observed for the 4S and the 4A peptide while the EC_{50} values of 4L and 4P peptides were only slightly increased (Fig. 3.3B). This indicated that the cellular responses to the 4L and 4P peptide were slightly CD8 dependent while the responses to the 4A and 4S peptide were highly CD8 dependent. These results were consistent with a previous report claiming that the CD8 dependence in functional responses was inversely correlated with the strength of the peptides tested, i.e. weak peptides were highly CD8

Table I: EC_{50} values [M] determined for T1 thymocytes.

	Peptides				
Cell type; mAb	4L	4P	4A	4S	4N
DPs; no mAb	1.0×10^{-12}	3.1×10^{-12}	5.2×10^{-11}	3.3×10^{-10}	1.1×10^{-9}
DPs; + SF1-1.1 mAb	3.0×10^{-11}	1.0×10^{-11}	$1.7 \times 10^{-8*}$	$2.8 \times 10^{-8*}$	$5.5 \times 10^{-7*}$
∆EC50 (+/- SF1-1.1)	**26 x**	**3 x**	**> 335 x**	**>> 83 x**	**>515 x**
SPs; no mAb	1.2×10^{-12}	4.3×10^{-12}	1.3×10^{-10}	1.8×10^{-8}	3.6×10^{-8}
SPs; + SF1-1.1 mAb	4.5×10^{-12}	1.8×10^{-11}	$2.0 \times 10^{-7*}$	$5.3 \times 10^{-8*}$	$1.0 \times 10^{-5*}$
∆EC50 (+/- SF1-1.1)	**4 x**	**4 x**	**> 1468 x**	**>> 3 x**	**>280 x**
LNs; no mAb	not done	3.2×10^{-12}	3.5×10^{-10}	1.3×10^{-7}	not done

Mean values of at least two experiments are shown. (*) less than 50% of all cells responded

dependent while strong peptides were only moderately CD8 dependent (Kerry et al., 2003). Based on the sensitivity and the CD8 dependence of the cells for the different peptide variants the 4L and 4P were considered strong peptides, (indicated in red), while the 4S and the 4N peptides were considered weak peptides (indicated in blue). The 4A peptide on the other hand elicited CD69 upregulation responses which could not be characterized as either weak or strong and was therefore considered a peptide of moderate potency (indicated in grey). Table I lists the EC_{50} values representing peptide concentrations leading to CD69 upregulation in 50% of the cells analyzed.

3.1.4 Sensitivity Differences Between DP and SP Thymocytes

The difference in responsiveness between DP and SP thymocytes depended on the potency of the tested peptides. This is illustrated in Figure 3.4. The CD69 upregulation curves from DP and SP thymocytes were normalized for their maximal values and overlaid to allow comparison of the CD69 responses obtained with either strong (e.g. 4P), moderate (e.g. 4A) or weak (e.g. 4S) peptides. In the case of the strong 4P peptide, the two curves were very similar and the EC_{50} values for DP and SP thymocytes specified in Table II were almost equivalent (1.4-fold difference). Similarly with the moderate 4A peptide, the EC_{50} value for SP thymocytes was 2.6-fold higher than the EC_{50} value obtained for DP thymocytes. In terms of the weak 4S ligand the EC_{50} value observed with DP thymocytes was 54.3-times

higher than that observed with DP thymocytes. A similar observation was made for the 4N peptide where the EC_{50} difference between SP and DP thymocytes was 33.6-fold (Table II). Therefore, in terms of sensitivity differences between SP and DP thymocytes the moderate potency 4A peptide showed characteristics reminiscent of strong peptides.

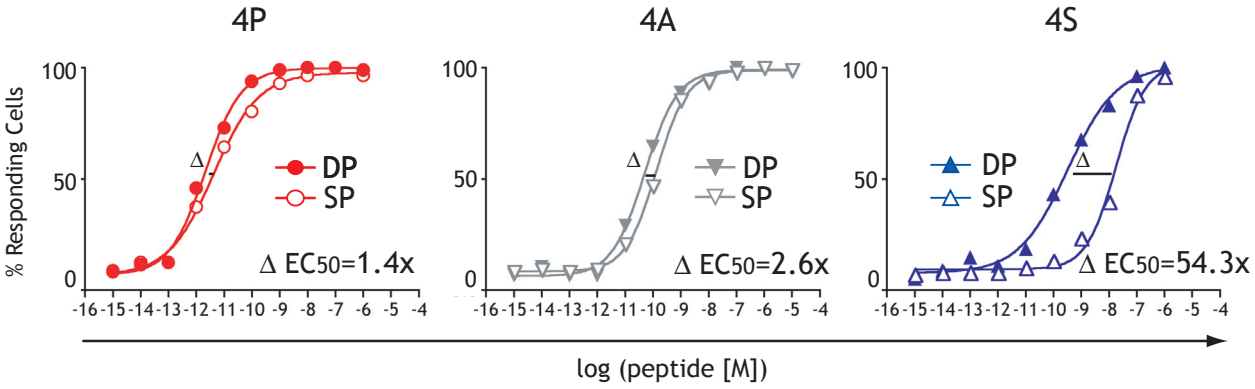

Figure 3.4: Sensitivity differences between DP and SP T1 thymocytes. Dose response curves obtained from DP or SP T1 thymocytes shown in Figure 3.3 were normalized for the fraction of the cells undergoing CD69 upregulation (% responding cells). Overlays of these normalized CD69 response curves of DP and SP thymocytes stimulated with either 4P (red curves), 4A (gray curves) or 4S (blue curves) are shown. The fold difference between the EC_{50} values determined from DP and SP thymocytes is indicated in the lower right of each panel.

Table II: EC_{50} values [M] determined for T1 thymocytes and LN T Cells.

	Peptides				
Cell type	4L	4P	4A	4S	4N
DPs	1.0×10^{-12}	3.1×10^{-12}	5.2×10^{-11}	3.3×10^{-10}	1.1×10^{-9}
SPs	1.2×10^{-12}	4.3×10^{-12}	1.3×10^{-10}	1.8×10^{-8}	3.6×10^{-8}
LNs	not done	3.2×10^{-12}	3.5×10^{-10}	1.3×10^{-7}	not done
ΔEC50 (SP/DP)	**1.2 x**	**1.4 x**	**2.6 x**	**54.3 x**	**33.6 x**

Mean values of at least two experiments are shown. (*) less than 50% of all cells responded

3.1.5 Determination of TCR-Ligand Affinities Using Fluorescent pMHC Monomers

To study the correlation between the affinity of a specific TCR ligand interaction and the cellular response, affinities of T1-TCR for its various peptide-MHC ligands were determined. The TCR affinity labeling system developed by Immanuel Lüscher was ideal for this purpose (see Introduction 1.3.3). To examine the differences in ligand binding between DP and SP thymocytes, flow-cytometry was an optimal detection method allowing single cell analysis. By electronic gating for thymocytes which either expressed CD4 and CD8 or CD8 alone, DP thymocytes could be distinguished from SP thymocytes. Three requirements had to be fulfilled to allow affinity measurements on thymocytes and lymphocytes by flow-cytometry. First, the TCR bound, monomeric pMHC complexes had to be stably fixed to the cell to allow flow-cytometric analysis, as preliminary studies (data not shown) showed that interactions of TCRs with pMHC monomers that were not covalently crosslinked to the cells were too unstable to be quantified by flow-cytometry. Stable association of TCR bound pMHC monomers was achieved by photochemical crosslinking of the ligands to bound TCR (see Introduction 1.3.3.2). Second, the ligand derived fluorescence signal had to be high enough to be detected on a single cell and third, the highest concentration of pMHC monomers had to be high enough to lead to TCR saturation.

In a first set of experiments it was tested whether the photo-reactive, Cy5 labeled 4P-K^d monomers were suitable to determine the affinities of TCR ligand interactions on thymocytes and lymphocytes. Figure 3.5A shows a schematic representation of a photo-reactive

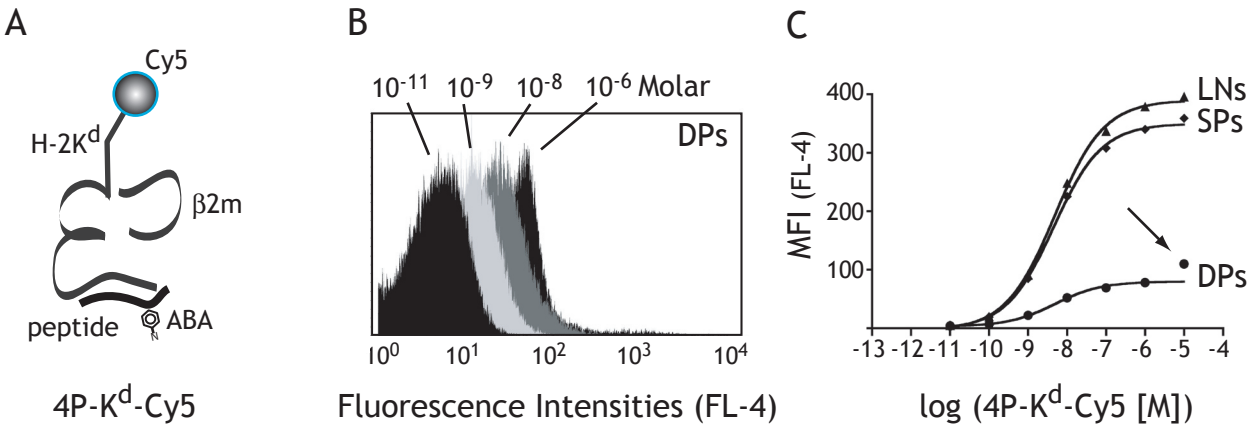

Figure 3.5: TCR ligand binding measurements using fluorescence labeled, photo-reactive 4P-K^d monomers. (A) Schematic representation of a Cy5 labeled complex of photo-reactive peptide (4P) bound to a soluble, monomeric H-2K^d MHC class I molecule. (B) Overlay of histograms obtained from electronically gated DP thymocytes, which were subjected to photoaffinity labeling using the indicated doses of 4P-K^d-Cy5. (C) Graphical representation of fluorescence signals obtained as described in (B) for DP thymocytes (DP), SP thymocytes (SP) or lymph node T cells (LN) from T1 mice. Curves were obtained by curve fitting of the measured fluoresence intensities using non-linear regression. The arrow indicates a signal which was higher than the fitted TCR saturation curve.

4P-K^d-Cy5 monomer. When thymocytes were incubated with various concentrations of the 4P-K^d-Cy5 monomers for 90 minutes on ice, photochemical crosslinking led to concentration dependent fluorescent signals on these cells. As illustrated in Figure 3.5B, the fluorescent signals obtained from DP thymocytes that were incubated with various concentrations of 4P-K^d-Cy5 monomers and photo-crosslinked could easily be distinguished. When the fluorescent signals obtained from DP and SP thymocytes and from lymphocytes were plotted against the 4P-K^d-Cy5 concentration, TCR-ligand saturation curves were obtained (Fig. 3.5C). As discussed above and shown in Figure 3.1B the TCR expression levels were substantially higher on SP thymocytes and lymph node cells (LNs) compared to DP thymocytes. Therefore the same concentration of ligand resulted in higher fluorescence signals on SP thymocytes compared to DP thymocytes. These experiments demonstrated that the signal intensities were strong enough to allow single cell flow-cytometric analysis of TCR ligand binding on cells from all stages of T cell development. It is noteworthy that at 4P-K^d-Cy5 concentrations higher than 10^{-6} M an enhanced increase in the Cy5 signal was measured that could not be explained by TCR saturation and that was most prominent on DP thymocytes (see arrow in Figure 3.5C). Although this was not hampering these measurements, it would have been detrimental for studying saturation curves of TCR ligand interactions with affinities that were more than 10-fold lower than the one shown in Figure 3.5C because then the TCR mediated signal would be distorted by this enhanced signal of unknown origin. This non-TCR-mediated binding of the 4P-K^d-Cy5 ligand observed at high ligand doses (>10^{-6}M) was studied in more detail.

3.1.6 Non-Cognate, CD8 Mediated Ligand Binding

The enhanced signals obtained with ligand concentrations higher than 10^{-6} M were studied in more detail. It was evident that these signals were mainly observed on DP and to a lesser extent on SP thymocytes of T1 mice. When $TCR^{-/-}$, $CD4^-$, $CD8\alpha/\beta^{-/-}$ double negative (DN) thymocytes were analyzed, these signals were not observed (Fig. 3.6A), excluding nonspecific monomer binding to thymocytes. When DP thymocytes were pretreated with antibodies which either enhanced or reduced the binding of $CD8\alpha/\beta$ to pMHC monomers, more distinct results were obtained (Fig. 3.6B). When the α-$CD8\alpha$ mAb 53.6-7 was applied prior to ligand binding TCR specific, pMHC binding was slightly enhanced at saturating concentrations of pMHC complexes. Binding of the 53.6-7 mAb also enhanced pMHC labeling at 10^{-5} M 4P-K^d-Cy5 (red curve Fig. 3.6B). This has been implicated in several other studies to alter cognate as well as non-cognate pMHC interactions on T cells (Bosselut et al., 2000; Daniels et al., 2001; Moody et al., 2001). Due to the results obtained with this enhancing

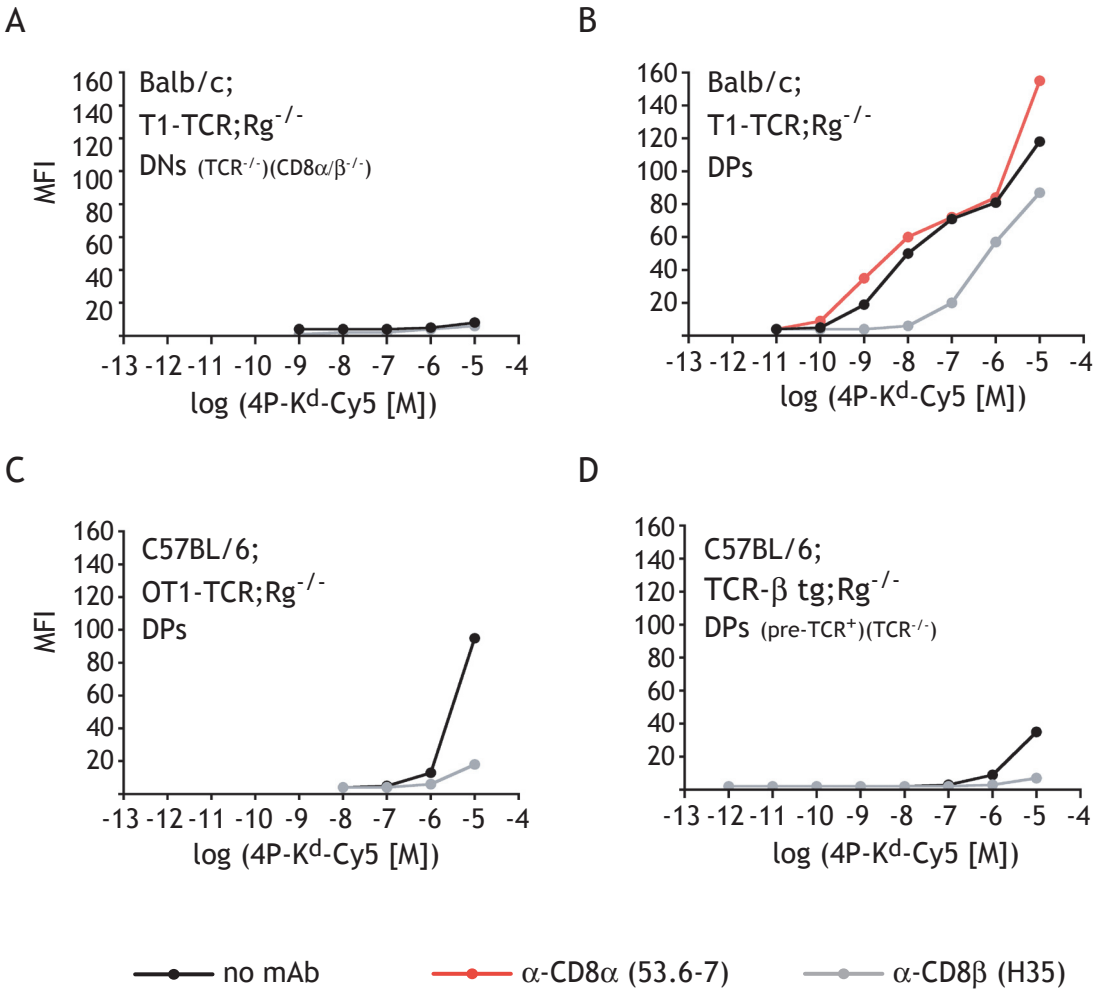

Figure 3.6: CD8 mediated non-cognate photo-crosslinking to DP thymocytes at high ligand doses. Thymocytes of either T1-TCR; $Rag^{-/-}$ (A and B), (OVA)H2-K^b specific OT-1-TCR; $Rag^{-/-}$(C) or $TCR\beta^+$; $Rag^{-/-}$ (D) mice were incubated with indicated doses of 4P-K^d-Cy5 either in the absence (black curves) or in the presence (red curve) of α-CD8α(53-6.7) or α-CD8β(H35) mAbs (gray curves). Following UV crosslinking (~312nm), cells were stained with α-CD4(RM4-5), α-CD8α(53-6.7), α-TCRβ(H57-597) mAb and analyzed by flow cytometry. MFIs of Cy5 fluorescence signals obtained from (TCR-negative) DN T1 thymocytes (A), (TCR-positive) DP T1 thymocytes (B), (OT-1 TCR-positive) DP thymocytes from OT-1 transgenic (C) or TCRα/β-negative DP thymocytes from TCRβ transgenic mice (D) are shown.

α-CD8 antibody the studies were repeated in the presence of the α-CD8β mAb H35 which was previously reported to block the CD8 contribution to pMHC ligand binding (Lüscher et al., 1995). This was confirmed with the T1-TCR when this antibody was included in ligand binding assays using DP T1 thymocytes (gray curve in Figure 3.6B). Cognate binding was clearly reduced and importantly the signal obtained with 10^{-5} M 4P-K^d-Cy5 was also reduced when the H35 mAb was included. Thus, CD8 was responsible for the enhanced fluorescence signals observed with high ligand concentrations. This was confirmed when thymocytes were included in these studies which either expressed a TCR of different specificity, i.e. the OT-1 TCR (specific for SIINFEKL-K^b) or which only expressed a pre-TCR and no mature

TCRα/β. The data in Figure 3.6C show that DP thymocytes from C57BL/6 OT-1;$Rg^{-/-}$ mice can be labeled with 10^{-5} M 4P-K^d-Cy5 complexes even though they only express a non-cognate TCR (Fig. 3.6C, black curve). This labeling was almost completely blocked in the presence of the α-CD8β mAb H35 (gray curve), arguing that the non-cognate labeling observed at high pMHC concentrations was mediated by CD8. A similar observation was made when DP thymocytes of C57BL/6 β^+/β^+; $Rag^{-/-}$ mice were analyzed (Fig. 3.6D). Due to their expression of a transgenic TCRβ chain in the absence of endogenous TCR gene recombination ($Rag^{-/-}$) these thymocytes proceed to the DP stage expressing only a pre-TCR. Again, the enhanced signal (black curve) was strongly reduced in the presence of the α-CD8β mAb H35 (gray curve). Taken together, these experiments revealed that at ligand concentrations higher than 10^{-6} M, the photo-reactive pMHC monomers were covalently crosslinked to the cells in a CD8 dependent and TCR independent manner. This was possible because the TCR and the CD8 (or CD4) coreceptor bind to independent binding sites on MHC molecules (see Fig. 1.3).

This observation led to two important consequences. First, when used at ligand concentrations greater than 10^{-6} M, ligand binding reflected a combination of cognate (TCR/CD8) and non-cognate (CD8 only) components. Second, for low affinity TCR/CD8-pMHC interactions the shape of the binding curves would no longer represent a hyperbolic receptor saturation curve and thus no dissociation constants could be determined. Therefore an alternative method to determine the affinities of TCR ligand interactions was developed.

3.1.7 Development of a Two Step TCR Labeling Assay

To avoid non-cognate pMHC binding signals at high ligand concentrations and to be able to determine dissociation constants for high, medium and low TCR/CD8-pMHC ligand affinities an assay was developed in which the effect of the non-cognate (CD8-MHC only) interaction was excluded. This assay was based on a first round of photoaffinity labeling with pMHC monomer ligands of interest followed by the measurement of the free TCR molecules remaining. Given a constant number of TCR molecules on the cell surface during the course of an experiment, the number of free TCR molecules on a cell reflected the total number of TCRs minus the number of TCRs engaging pMHC ligand. At half maximal saturation of all TCR molecules the numbers of bound and free TCR molecules are identical. The affinity of a receptor-ligand interaction is defined by the dissociation constant (K_D), which equals the concentration of free ligand that leads to half-maximal receptor saturation on a single cell. Therefore the dissociation constants determined by the measurement of either the fraction of engaged TCRs or the fraction of free TCR are theoretically identical. Figure 3.7 illustrates

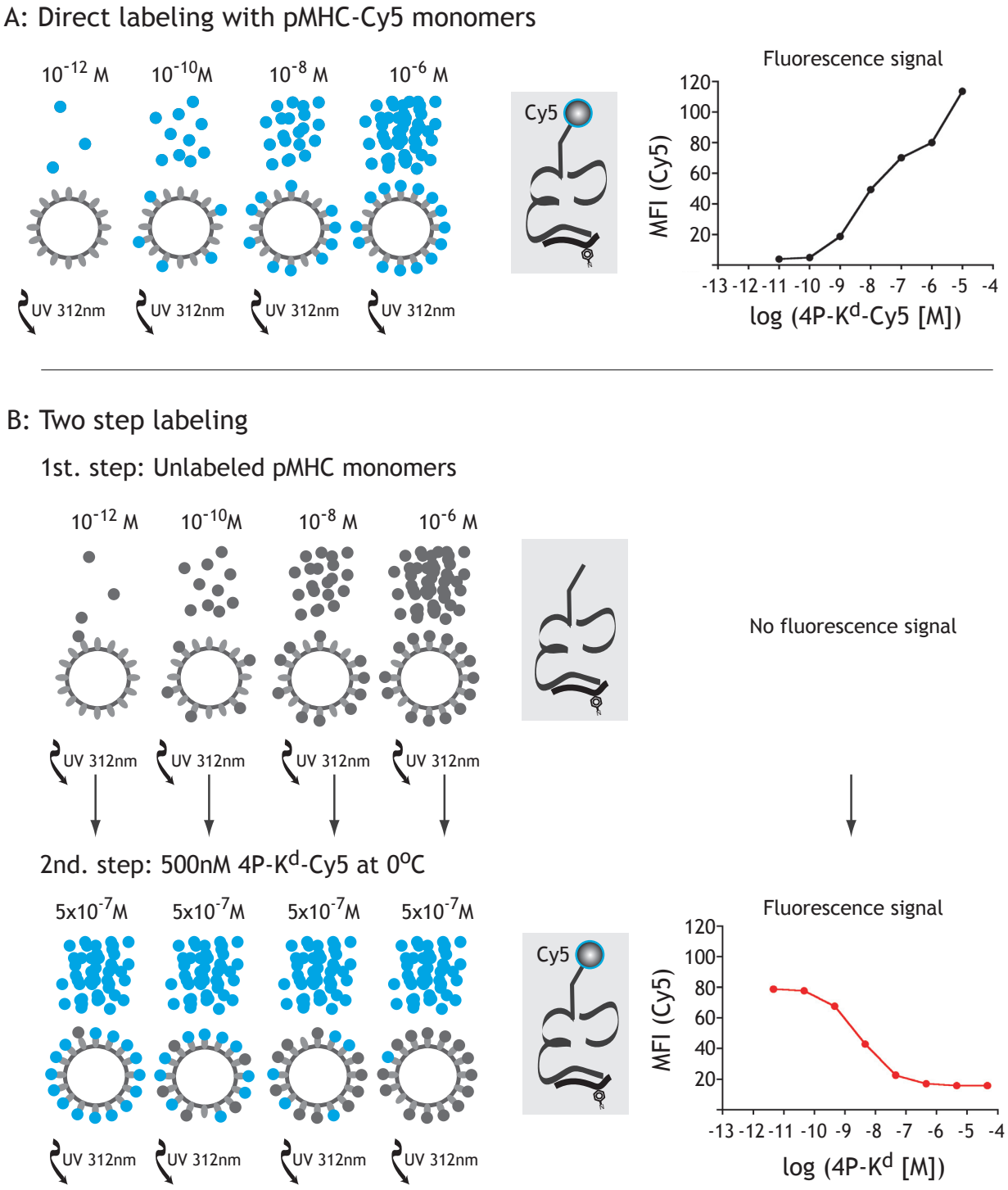

Figure 3.7: Principle of the two step labeling assay. (A) Direct photoaffinity labeling was assessed by incubation of thymocytes or lymph node T cells with various doses of 4P-K^d-Cy5 monomers followed by UV crosslinking (~312nm). Cell were subsequently stained with fluorescently labeled α-CD4(RM4-5), α-CD8α(53-6.7), α-TCRβ(H57-597) mAb and the Cy5 fluorescence signals obtained from DP thymocytes, SP thymocytes or lymph node T cells were analyzed by flow-cytometry. (B) In the two step labeling assay, a first round of photoaffinity labeling was performed with unlabeled, photo-reactive pMHC monomers as described in (A). TCRs remaining unoccupied in the first round were detected in a second step by incubating the cells with fluorescently labeled 4P-K^d-Cy5 (500nM) followed by a second round of UV crosslinking (~312nm). Cells were subsequently stained with fluorescently labeled α-CD4(RM4-5), α-CD8α(53-6.7), α-TCRβ(H57-597) mAbs and the Cy5 fluorescence signals were analyzed by flow-cytometry.

the principle of the two step TCR labeling assay. As described above, direct photoaffinity labeling with the 4P-H-2K^d-Cy5 monomers resulted in fluorescent signals proportional to the portion of ligand bound to cells expressing T1-TCR molecules (Fig. 3.7A). In the two step assay unlabeled, monomeric pMHC ligands were applied at different concentrations to the T1-TCR expressing cells. After steady state binding was achieved, TCR-bound pMHC monomers were covalently crosslinked to the TCR by photochemical crosslinking and unbound monomers were washed off (Fig. 3.7B). Depending on the concentration and affinity of the crosslinked pMHC monomers the fraction of covalently crosslinked TCR-pMHC complexes varied and hence the fraction of free, unbound TCR varied in the different samples. The fraction of free, unbound TCR was then determined in a second step by incubation of these various samples with $5x10^{-7}$ M Cy5 labeled 4P-K^d at 0°C and subsequent photocrosslinking which labeled the remaining, unbound TCRs. Therefore the Cy5 signals observed by flow-cytometry (Fig. 3.7B) were proportional to the portion of unbound, free TCRs remaining after the first round of photoaffinity labeling with the pMHC ligands of interest. The two step assay is not a classical ligand competition assay. Due to the photochemical crosslinking after the first step and the removal of unbound ligand by washing, the labeled 4P-K^d-Cy5 monomers used in the second step were not competing for TCR binding with the first step ligands. This was important to ensure that the 4P-K^d-Cy5 monomers used in the second step exclusively labeled unbound TCR. Importantly, the 4P-K^d-Cy5 monomers were applied at a concentration ($5x10^{-7}$ M) which only reflected cognate TCR binding; this avoided additional signals from non-cognate binding. It should be noted that the pMHC monomers applied in the first step were used at concentrations as high as $5x10^{-5}$ M. At these concentrations, non-cognate interactions between the unlabeled first step monomers and CD8 were also taking place, but they did not reduce the number of free TCRs and were therefore excluded from signals obtained with the two step TCR labeling assay. A series of experiments was performed to ensure the practical accuracy of this assay to determine TCR ligand binding affinities.

3.1.8 Comparison of Direct and Two Step TCR Photoaffinity Labeling Assays

Several properties of the two step assay were characterized to ensure that the dissociation constants determined by this assay were accurate. First, the concentration of the 4P-K^d-Cy5 probe used in the second step ($5x10^{-7}$ M) was sufficient to saturate only 90 to 95% of the TCRs on a cell. The fact that this probe was therefore not able to bind every free TCR could potentially have influenced the determination of the dissociation constant (K_D). Therefore the dependence of the K_D value on the concentration of the second step 4P-K^d-Cy5 was tested. As shown in Figure 3.8A, the fluorescence signal was decreased with

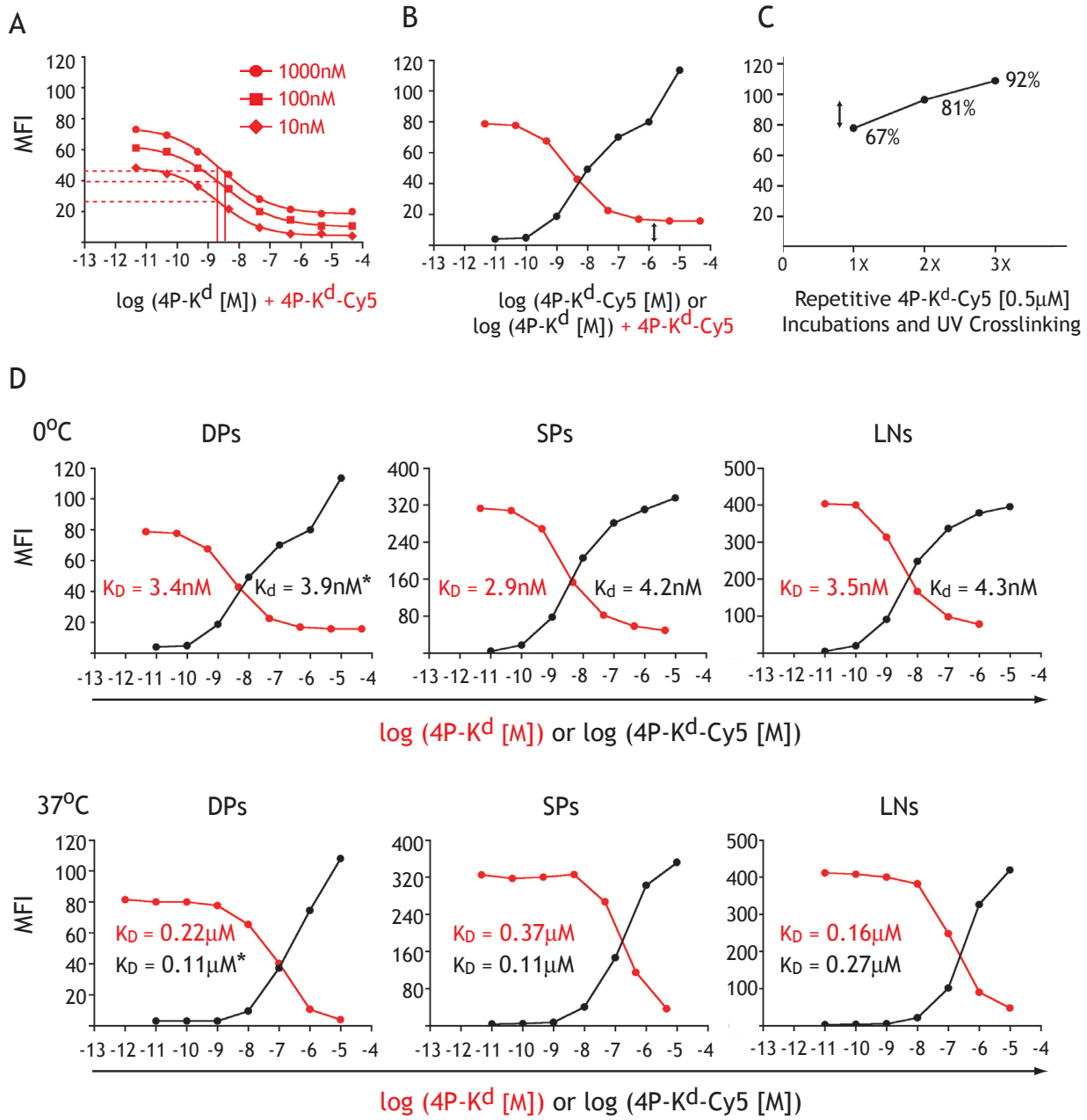

Figure 3.8: Comparison of K_D determinations using direct photoaffinity labeling or two step labeling. The accuracy of affinity determinations using the two step labeling assay was tested by comparison to the K_D values determined by direct photoaffinity labeling. K_D values were in both cases measured by determining the concentration of ligand leading to half-maximal fluorescence signals using non-linear regression and the Prism4® software. (A) Relative independence of the K_D determination on concentration of the second step reagent (4P-K^d-Cy5). All three concentrations of 4P-K^d-Cy5 tested (10 nM (◆), 100 nM(■) or 1000 nM(●)) led to a calculation of very similar K_D values. (B) At high primary ligand concentrations, specific fluorescence signals were observed with the two step labeling assay (indicated by arrow). (C) Performing three rounds of direct photoaffinity labeling (at ~312nm) with 500nM 4P-K^d-Cy5 led to incrementally increasing fluorescence signals, consistent with a UV-crosslinking efficiency of ~70%. (D) Comparison of K_D values determined by direct photoaffinity labeling or two step labeling for the binding of 4P-K^d to either T1 thymocytes or lymph node T (LN) cells at 0°C or 37°C. K_D values, which were determined from direct photoaffinity labeling curves that represented a mixture of cognate TCR-pMHC and non-cognate CD8-MHC binding are marked with an asterisk (*).

decreasing concentration of 4P-K^d-Cy5 monomers. Nevertheless, the determined K_D of the first step ligand 4P-K^d was 3nM for the two highest concentrations ($1x10^{-6}$ M, $1x10^{-7}$ M) of second step probe and 4nM for the lowest concentration (10^{-8} M) of the second step reagent (4P-K^d-Cy5) tested, demonstrating that the determination of K_D values in the two step assay was very robust over a broad range of second step reagent concentrations. A concentration of $5x10^{-7}$ M was therefore considered an optimal concentration for the second step reagent. At this concentration the fluorescence signals were high enough to allow flow-cytometric analysis while being 20-fold lower than the concentration at which the non-cognate cross-linking was observed. Second, as indicated in Figure 3.8B even at concentrations where the first step ligand (4P-K^d) should saturate all TCRs on a cell ($5x10^{-5}$ M) the signals observed in the two step labeling assay (red curve), were not zero (indicated by the arrow). This is due to the fact, that the treatment of TCR-bound ligands in the first step did not lead to covalent crosslinking of all pMHC molecules bound by TCR. As shown in the right panel of Figure 3.8C, when UV crosslinking of the 4P-K^d-Cy5 ligand used at high concentrations was performed repeatedly, the signal increased with every round of ligand binding and UV cross-linking, approaching a maximum. Considering the increase of labeling with each cycle, the efficiency of UV-crosslinking was estimated ~70%. Thus, despite using a ligand concentration that should lead to TCR saturation, only 70% of the bound pMHC monomers were actually covalently crosslinked by the UV crosslinking reaction. pMHC monomers, which were bound to TCRs, but failed to be covalently crosslinked were washed off between the first and the second step of the two step TCR labeling assay. Therefore even at concentrations of the first step pMHC monomers which led to saturation of all TCRs on a cell with non-covalently bound ligand, the second step 4P-K^d-Cy5 monomers were crosslinked to some TCRs which had failed to be crosslinked to TCR bound pMHC monomers from the first step binding. As a result of this inefficiency in establishing a cross-link there was a background fluorescent signal even when the unlabeled ligand was used at high concentrations in the first step.

In Figure 3.8D, K_D values of the TCR/CD8-4P-K^d interaction were determined either by direct labeling (black curves; 4P-K^d-Cy5 monomer) or the two step labeling protocol (red curves). The measurements were carried out for T1-TCRs expressed on DP and SP thymocytes and lymph node T cells (LN) from T1 animals and were performed at 0°C or 37°C. Importantly the indicated temperatures and concentrations, only refer to the 4P-K^d-Cy5 ligand from the direct labeling or the unlabeled 4P-K^d ligand of the first step from the two step assay. The 2^{nd} step 4P-K^d-Cy5 monomer was applied at 0°C and at a constant concentration ($5x10^{-7}$ M) for all measurements described in this thesis. The curves obtained from these comparisons between direct labeling with the 4P-K^d-Cy5 monomers and the two step TCR

labeling measuring the level of TCR occupancy mediated by the first step 4P-K^d monomer were compared as illustrated in Figure 3.8C. At 0°C the differences between the K_D values of the two different labeling assays were within 2-fold. At 37°C the differences between the two methods were maximally 3-fold. In conclusion, the two step TCR labeling assay was considered to be reliable for determining the K_Ds of the T1-TCR for its various pMHC ligands, with a 2-fold deviation of K_Ds at 0°C and a three fold deviation at 37°C.

Furthermore the experiments described in Figure 3.8D led to two observations: First, the affinity of the interaction between the T1-TCR, CD8 and 4P-K^d appeared to be substantially temperature dependent. The T1-TCR affinity for 4P has a K_D of $3.4x10^{-9}$ M at 0°C and a K_D of $2.2x10^{-7}$ M at 37°C. Second, no significant differences in the affinities of the T1-TCR/CD8-pMHC interaction were observed, when DP thymocytes were compared to SP thymocytes and lymph node T cells (LN). These observations were studied in further detail by including all ligands available, representing pMHC complexes which lead to different cellular responses.

3.1.9 CD8 Mediated Temperature Dependence of TCR-Ligand Binding

The affinities of the 4L, 4P, 4A, 4S and 4N pMHC ligands for T1-TCRs expressed on DP thymocytes were determined. As described above, the affinities measured were dependent on the temperature at which ligand binding was performed. Figure 3.9A shows the curves obtained with the two step TCR labeling assay where the first labeling step was either performed at 0°C, 24°C or 37°C. When these ligand binding curves were compared with the CD69 response curves in Figure 3.3A it was evident that the biological potency of a given peptide was proportional to its affinity for the T1 receptor, i.e. strong ligands showed high affinities for the T1-TCR (red curves in Fig. 3.3A and Fig. 3.9A) while weak ligands bound the T1-TCR with lower affinities (blue curves in Fig. 3.3A and Fig 3.9A). These measurements further showed that the affinity of a given TCR/CD8-pMHC interaction was considerably temperature dependent. All binding curves were shifted to the right with increasing temperatures, demonstrating a decrease in TCR/CD8 ligand affinities with increasing temperatures. This is illustrated by the K_D values shown in Table III: For all ligands tested the K_D values of the trimolecular TCR/CD8-pMHC interactions increased from 0°C to 24°C and even further from 24°C to 37°C.

To test, whether this temperature dependent change in affinity was due to changes in the bimolecular TCR-pMHC interaction or rather due to a change in the binding contribution of the CD8 coreceptor, the affinity measurements were repeated with pMHC ligands that allowed TCR binding but were defective in binding to CD8. These peptide- $K^d_{\Delta 223/227}$ mono-

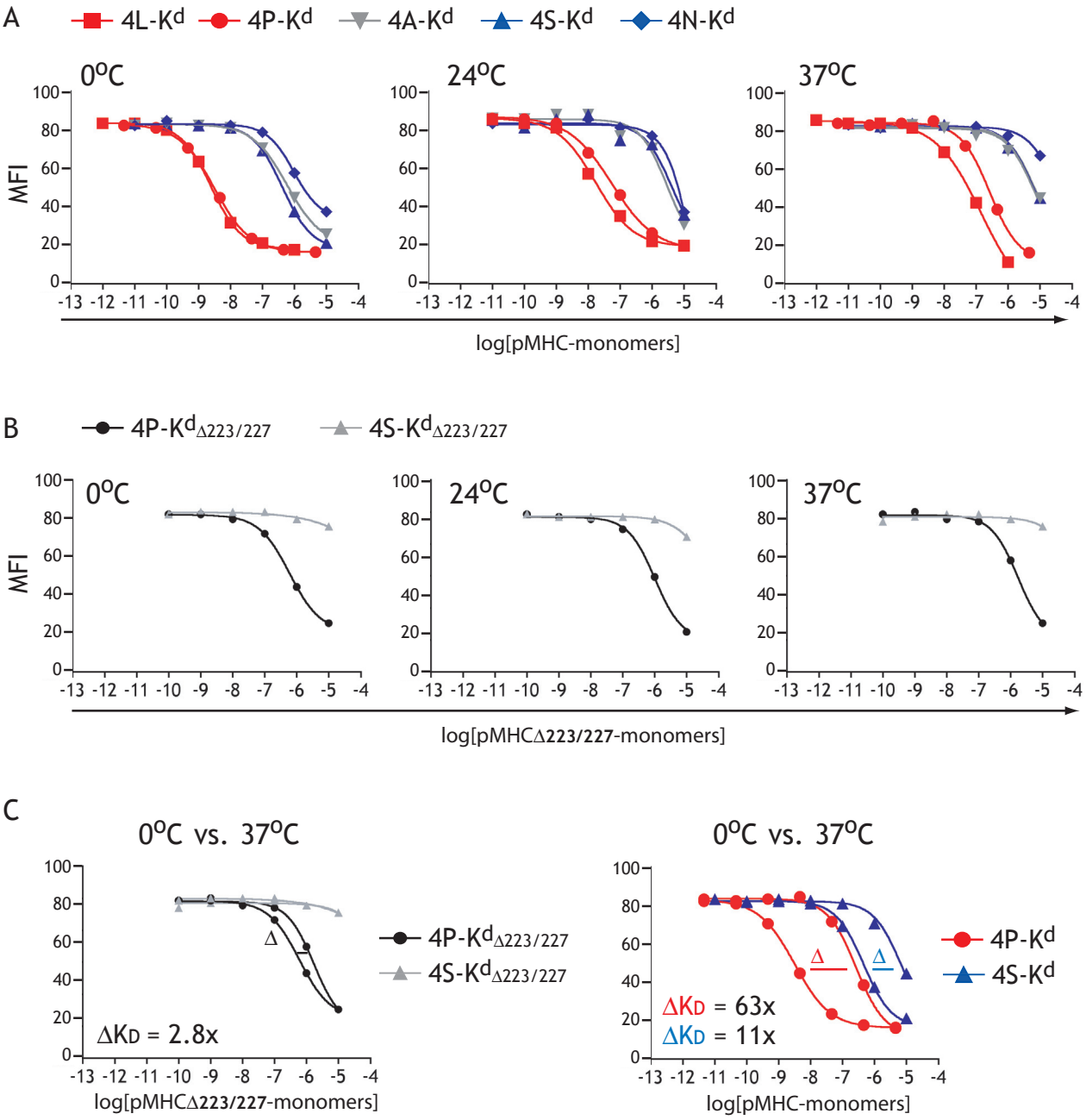

Figure 3.9: Temperature dependence of TCR-ligand binding. T1 thymocytes were incubated with various doses of photo-reactive, unlabeled monomers at 0°C, 24°C or 37°C and subsequent photo-crosslinking (~312nm); this was followed by incubation with 500nM 4P-K^d-Cy5 and a second round of photo-crosslinking (~312nm) according to the two step TCR labeling protocol. Cells were stained with fluorescently labeled α-CD4(RM4-5), α-CD8α(53-6.7), α-TCRβ(H57-597) mAbs. MFIs of Cy5 fluorescence signals obtained from DP thymocytes are plotted as a function of primary ligand dose. (A) Fluorescent signals obtained with the two step labeling assay for various doses of 4L-K^d(■), 4P-K^d (●), 4A-K^d (▼), 4S-K^d (▲) or 4N-K^d (◆) at 0°C, 24°C and 37°C are shown. (B) Fluorescent signals obtained with the two step labeling assay for various doses of 4P-K$^d_{\Delta 223/227}$ (●) or 4S-K$^d_{\Delta 223/227}$ (▲) at 0°C, 24°C and 37°C. (C) Comparison of the signals obtained for 4P-K$^d_{\Delta 223/227}$ (●) or 4S-K$^d_{\Delta 223/227}$ (▲) and 4P-K^d (●) or 4S-K^d (▲) at 0°C and 37°C. The differences of the affinities determined for TCR binding at 0°C or 37°C are indicated by ΔK_D. A representative experiment from a total of at least two independent experiments is shown.

Table III: K_D values [M] determined for pMHC monomers bound to DP T1 thymocytes at 0°C, 24°C and 37°C

Temperature	Ligands					
	4L-K^d	4P-K^d	4A-K^d	4S-K^d	4N-K^d	4L-$K^d_{\Delta 223/227}$
0°C	2.0×10^{-9}	3.4×10^{-9}	4.7×10^{-7}	5.7×10^{-7}	1.5×10^{-6}	5.7×10^{-7}
24°C	1.6×10^{-8}	5.3×10^{-8}	3.3×10^{-6}	3.8×10^{-6}	$>1.0 \times 10^{-5}$*	1.4×10^{-6}
37°C	6.5×10^{-8}	2.2×10^{-7}	4.5×10^{-6}	5.4×10^{-6}	$>1.0 \times 10^{-5}$*	1.6×10^{-6}

Mean values of at least two experiments are shown. (*) half-maximal TCR saturation was not reached.

mers carried two charge inversions (D223K and D227K) which abolished binding of the pMHC molecule to the CD8 coreceptor. As previously described, the affinities of the bimolecular TCR-pMHC interactions are much lower than the affinities resulting from the trimolecular TCR/CD8-pMHC interactions. In the case of the T1-TCR the affinities of the weak peptide ligands loaded on the mutant $K^d_{\Delta 223/227}$ monomers were too low to be determined (Fig. 3.9B; gray curve and Table III), therefore only the affinity of the strong 4P peptide on the $K^d_{\Delta 223/227}$ monomers could be determined (Fig. 3.9B; black curve). In contrast to the binding data obtained with the 4P-K^d monomers that were able to bind CD8 (see Fig. 3.9C) the decrease in affinity from 0°C to 37°C was only 2.8-fold in case of the 4P-$K^d_{\Delta 223/227}$ monomers representing the bimolecular TCR-pMHC interaction. In contrast, when the affinity differences between 0°C and 37°C were compared for the TCR-ligand binding including CD8, a 10-fold difference in the affinity of the 4S-K^d monomer and a 63-fold difference for the 4P-K^d monomers was measured.

Surprisingly, the CD8 impact on pMHC binding was higher at low temperatures than at high temperatures, resulting in higher affinity interactions at 0°C than at physiological temperatures. One reason could be that the reduced membrane fluidity at 0°C might stabilize the trimeric TCR/CD8-pMHC binding complexes by reducing the lateral mobility of the coreceptor in the membrane at 0°C. This hypothesis was supported by the fact that the steady state binding equilibrium of the TCR/CD8-4P-K^d complexes was only reached after 90 minutes at 0°C while it was reached in less than 30 seconds at 37°C (data not shown). This may be due to the faster co-recruitment of the TCR and CD8 at 37°C than 0°C. In any event the differences in TCR/CD8-ligand affinities at different temperatures were shown to be mediated by CD8 and seemed to affect high affinity ligands more than low affinity ligands. On the other hand the rank order of the K_D values for high affinity, intermediate affinity and low affinity ligands was preserved at all three temperatures tested and reflected the potency hierarchy determined in CD69 assays.

3.1.10 Similar TCR-Ligand Binding on Thymocytes and Peripheral T Cells

Several previous studies using multimeric pMHC ligands have shown that the avidities of non-cognate CD8-pMHC interactions were increased on DP thymocytes compared to SP thymocytes and peripheral T-cells (Bosselut et al., 2000; Daniels et al., 2001; Moody et al., 2001). To test whether these differences could be detected with the cognate TCR/CD8 pMHC monomers, two step labeling studies performed on DP thymocytes (Fig.3.9) were carried out with SP thymocytes and lymph node T cells as well. Thymocytes and lymph node T cells of T1 mice were analyzed for their ability to bind monomeric pMHC ligands of various potencies. Figure 3.10 shows the fluorescence signals observed with the two step TCR labeling assay derived either from DP thymocytes, SP thymocytes or lymphocytes (LN) incubated with the 4L-K^d, 4P-K^d, 4A-K^d, 4S-K^d and 4N-K^d monomers at 0°C. As expected, due to the different TCR expression levels, the signal maxima were different when DP thymocytes (MFI_{max}: 90) were compared to SP thymocytes (MFI_{max}: 350) and lymphocytes (MFI_{max}: 420). Despite these different signal intensities, the hierarchy of the dose dependence on ligand binding was not changed when DP, SP and LN cells were compared. Even more importantly the curves were not shifted when the three developmental stages were compared, indicating that the affinities measured on DP thymocytes, SP thymocytes and lymphocytes were very similar (see below).

3.1.11 TCR-Ligand Affinity Does not Change During T Cell Development

To compare TCR saturation at the three different stages of T-cell development, the fluorescence signals shown in Figure 3.10 were normalized for the different TCR expression levels observserved on thymocytes and lymphocytes. The normalized values represent the binding ratio (r = occupied TCRs / total TCR) for TCR saturation and in the case of the two step TCR labeling assay the ratio of free TCRs (1-r). Direct comparison of fluorescence signals obtained with the 4P-K^d, the 4A-K^d and the 4S-K^d monomers bound to DP, SP and LN cells at 0°C were made by overlaying binding curves representing the ratio of free TCRs (1-r) (Fig. 3.11A). For each ligand tested the affinity labeling curves obtained from DP, SP and LN cells of T1-TCR;$Rg^{-/-}$ mice were equivalent. For a given ligand, the affinity of the T1-TCR was constant irrespective whether the TCR was expressed on DP thymocytes, SP thymocytes or peripheral lymph node T cells. The experiments were also repeated at 37°C (Fig. 3.11B and Table V). Again no differences in the affinities of the TCR/CD8-pMHC interaction were evident between DP thymocytes and SP thymocytes. The K_D values determined from these measurements are shown in Table IV. In the case of the 4P-K^d and the 4A-K^d monomers the

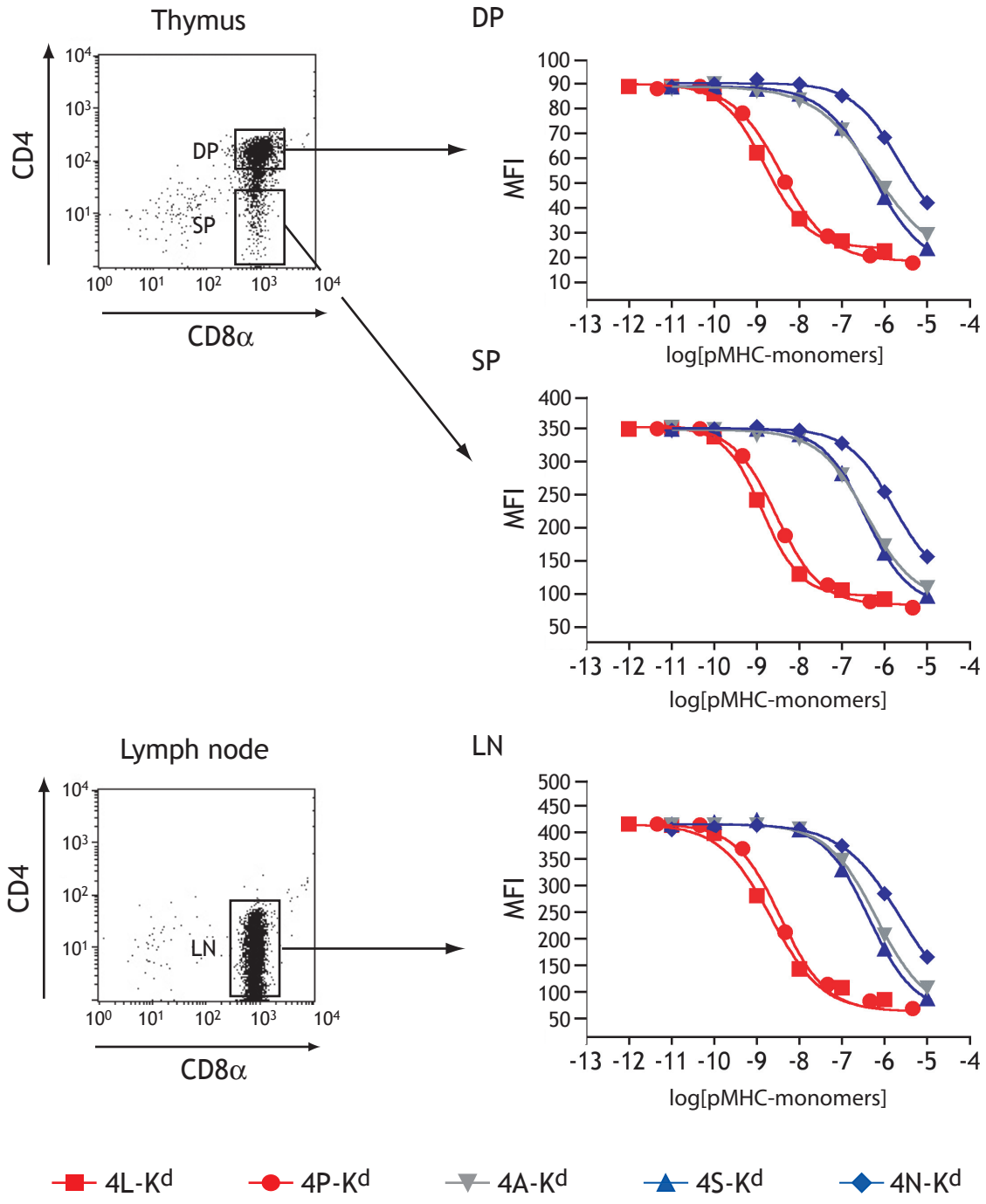

Figure 3.10: TCR ligand binding on T1 thymocytes and lymph node T cells. T1 thymocytes were incubated with various doses of photo-reactive, unlabeled monomers at 0°C and subsequent photo-crosslinking (~312nm); this was followed by incubation with 500nM 4P-K^d-Cy5 and a second round of photo-crosslinking (~312nm) according to the two step TCR labeling protocol. Cells were stained with fluorescently labeled α-CD4(RM4-5), α-CD8α(53-6.7), α-TCRβ(H57-597) mAbs. MFIs of Cy5 fluorescence signals obtained from DP thymoctyes (DP) or SP thymocytes (SP) and lymph node T cells (LN) are plotted as a function of primary ligand concentration (4L-K^d(■), 4P-K^d (●), 4A-K^d (▼), 4S-K^d (▲) or 4N-K^d (◆)).

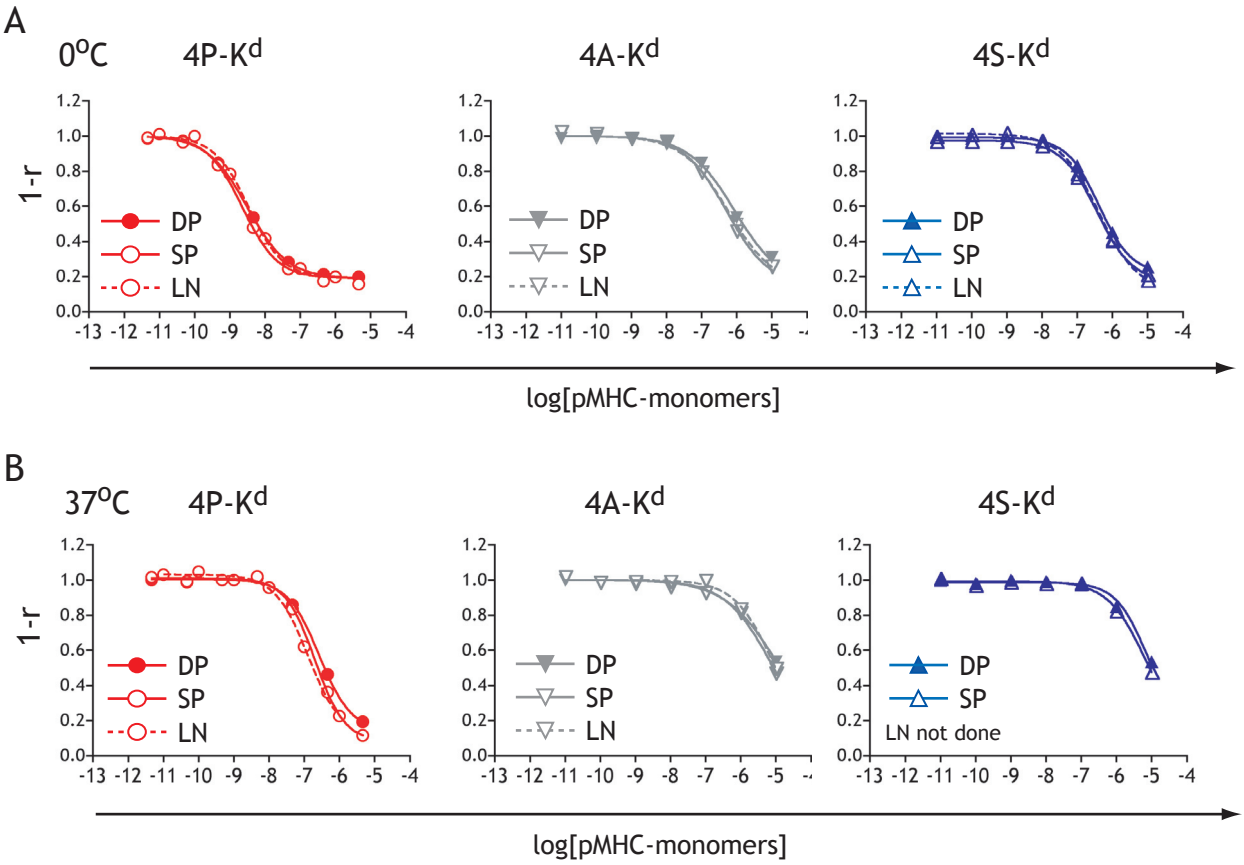

Figure 3.11: Comparisons of TCR ligand binding between DP thymocytes, SP thymocytes or lymph node T cells. Cy5 fluorescence signals obtained from two step labeling of T1 thymocytes and lymph node T cells were normalized for TCR expression levels. The curves representing the ratio of free TCRs (1-r) obtained from thymocytes and lymph node T cells were overlaid to allow direct comparison of changes in ligand binding at different stages of development. Symbols representing results obtained with DP thymocytes, SP thymocytes or lymph node T cells are shown in each panel. (A) Ratios of free TCRs observed with DP thymocytes (DP), SP thymocytes (SP) or lymph node T cells (LN) at 0°C are shown in three different panels representing either binding to 4P-K^d, 4A-K^d or 4S-K^d primary ligand. (B) Similar to (A) but from primary ligand bindings performed at 37°C.

two step TCR labeling at 37°C was also performed on lymph node T cells and no differences in the K_D values compared to the thymocytes were observed.

To further characterize the binding between the T1-TCR and pMHC monomer ligands, 'off-rate' studies were performed. In these studies the pMHC ligands tested were incubated with DP or SP thymocytes at concentrations leading to TCR saturation binding. Instead of UV photo-crosslinking the bound ligands the samples were diluted 200-fold in the presence of the α-H-2K^d (α1) mAb 20-8-4S which binds to the pMHC monomers and prevents rebinding to the TCR. Therefore, once diluted, pMHC ligands that were not bound to TCR were no longer able to rebind to T1-TCR molecules. Following dilution of the samples in the presence of the 20-8-4S antibody UV crosslinking was performed on aliquots of the cells at defined intervals. Subsequently cells were washed and labeled with ligand from the second step of the

Table IV: K_D values [M] determined for pMHC monomers bound to T1 thym. and LN T cells at 0°C and 37°C.

Temperature; Cell type	Ligands				
	4L-K^d	4P-K^d	4A-K^d	4S-K^d	4N-K^d
0°C					
DP	2.0×10^{-9}	3.4×10^{-9}	4.7×10^{-7}	5.7×10^{-7}	1.5×10^{-6}
SP	2.1×10^{-9}	2.9×10^{-9}	4.2×10^{-7}	5.7×10^{-7}	2.6×10^{-6}
LN	2.2×10^{-9}	3.5×10^{-9}	4.2×10^{-7}	5.7×10^{-7}	2.4×10^{-6}
ΔK_D (SP/DP)	**1.1 x**	**0.9 x**	**0.9 x**	**1.0 x**	**1.8 x**
37°C					
DP	6.5×10^{-8}	2.2×10^{-7}	5.4×10^{-6}	5.5×10^{-6}	5.9×10^{-5}
SP	6.5×10^{-8}	3.7×10^{-7}	7.6×10^{-6}	7.8×10^{-6}	8.1×10^{-5}
LN	not done	1.6×10^{-7}	7.5×10^{-6}	not done	not done
ΔK_D (SP/DP)	**1.0 x**	**1.7 x**	**1.4 x**	**1.4 x**	**1.3 x**

Mean values of at least two experiments are shown.

two step assay as described. This allowed to study the 'off-rates' of the T1-TCR/CD8-pMHC interactions. Figure 3.12 shows 'off-rates' of the 4P-K^d, the 4A-K^d and the 4S-K^d monomers when incubated on DP or SP thymocytes at 0°C. Similar to the observations made with the dose dependent ligand binding, no differences in the half-lives ($t_{1/2}$) of the TCR/CD8-pMHC interactions were observed between DP and SP thymocytes for all three ligands tested. Interestingly, at 0°C the differences in the half-lives (see Table V) between the 4P-K^d (23 min.) and the 4A-K^d (28 sec.) and 4S-K^d (27 sec.) ligands were between 50- and 60-fold, approximating the affinity differences between these ligands (see Table IV). This argues that the differences in affinity between different TCR ligands was largely due to differences in their 'off-rates'. Unfortunately the half-lives of the TCR/CD8-pMHC interactions could not be determined at 37°C due to very high 'off-rates' (TCR/CD8-4P-K^d: $t_{1/2}$< 5 sec.). In conclusion, these affinity comparisons between different stages of T cell development showed that the affinity of a given TCR/CD8-pMHC monomer interaction was equivalent on DP and SP thymocytes as well as on LN cells. Previous studies using pMHC multimers showed, that non-cognate pMHC multimers bound less avidly to SP and LN cells than to DP cells arguing for altered ligand binding when DP thymocytes were compared to SP thymocytes and lymphocytes (Daniels et al., 2001; Moody et al., 2001) and a correlation between the cell

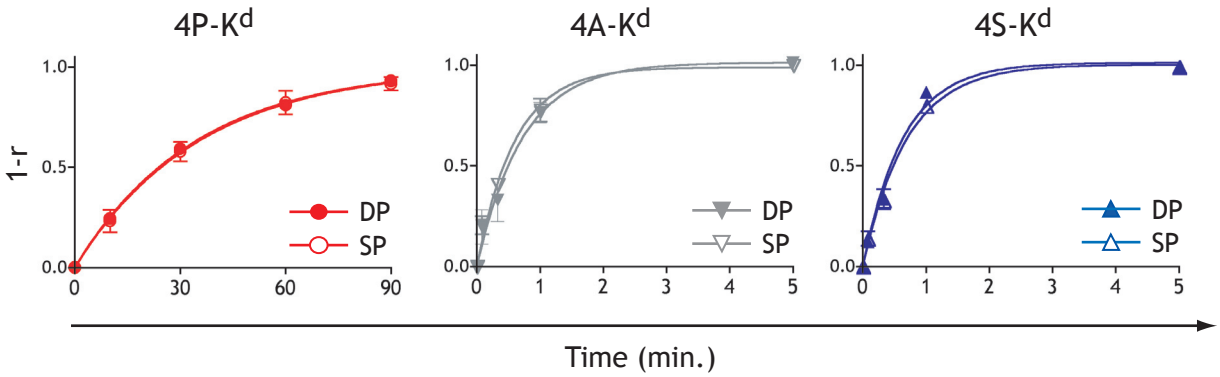

Figure 3.12: 'Off-rates' determined by two step labeling assays from DP and SP thymocytes. T1 thymocytes were incubated for 90 min. with either 100nM of 4P-K^d or 1µM of 4A-K^d or 4S-K^d prior to dilution in the presence of 20µg/ml α-H-2K^d(α1)(20-8-4S) mAb. Aliquots of the diluted cells were incubated for defined intervals and subjected to UV crosslinking (~312nm). The ratios of free TCRs (1-r) were determined by the two step assay. Cells were stained with fluorescence labeled α-CD4(RM4-5), α-CD8α(53-6.7), α-TCRβ(H57-597) mAbs. MFIs of Cy5 fluorescence signals obtained from DP and SP thymocytes are plotted as a function of time.

Table V: Half-lifes ($t_{1/2}$) of pMHC monomers bound to T1 thymocytes at 0^{o}C.

	Ligands		
Cell type	4P-K^d	4A-K^d	4S-K^d
DP	23 min. ± 4 min.	28 sec. ± 8 sec.	27 sec. ± 6 sec.
SP	24 min. ± 5 min.	30 sec. ± 8 sec.	26 sec. ± 7 sec.

Mean values of at least two experiments are shown.

surface protein glycosylation status and the binding capacity of pMHC multimer per TCR has been described (Casabo et al., 1994). It was proposed, that addition of a sialic acid residue to the CD8β coreceptor was responsible for the reduced CD8 mediated binding capacity of SP thymocytes compared to DP thymocytes. Removal of the sialic acid residues by enzymatic cleavage with neuraminidase increased the avidity of non-cognate tetramer binding on SP thymocytes to levels observed on DP thymocytes. To test the impact of neuraminidase on TCR mediated, cognate binding of monomeric pMHC ligands and to compare it to binding of pMHC multimers, binding studies with 4P-K^d-Cy5 monomers, 4P-K^d-Cy5 tetramers and 4A-K^d-Cy5 tetramers were performed using DP and SP thymocytes that were either untreated or pre-treated with neuraminidase prior to ligand binding.

3.1.12 Analysis of Cognate TCR-Ligand Binding Using pMHC Tetramers

To compare differences in cognate TCR/CD8 binding of pMHC monomers and tetramers, 4P-K^d-Cy5 monomers and tetramers were applied to T1 thymocytes. Moreover the differences in ligand binding between high affinity 4P-K^d and low affinity 4A-K^d tetramers were compared. To better compare the monomeric and tetrameric forms of the 4P-K^d ligand, these experiments were performed with directly labeled reagents. In a first step, the glycosylation status of the cells under study was examined using fluorescence labeled peanut agglutinin (PNA). PNA has been shown to bind to desialylated O-linked glycosylation branches on cell surface proteins of DP thymocytes including the CD8β molecule (Priatel et al., 2000). Due to developmental upregulation of sialyltransferases in DP thymocytes, sialic acid moieties are added to Galβ-1-3GalNac branches during positive selection; this leads to reduced PNA binding on SP thymocytes. To test the impact of differential glycosylation on ligand binding these studies were performed on freshly isolated thymocytes or on thymocytes which were pre-treated with neuraminidase. Neuraminidase reverts the effects of the sialyltransferases by enzymatic removal of the sialic acids on glycoproteins leading to an increase in PNA binding (Figure 3.13A). Untreated SP thymocytes showed the lowest PNA staining (MFI: 50) indicating that they express highly sialylated proteins on their surface. Neuraminidase treatment increased the PNA binding on DP and SP thymocytes to similarly high levels (MFI:~1000) indicating a reduction in sialylation.

Figure 3.13B shows ligand binding studies performed on DP and SP thymocytes which were either untreated (black curves) or neuraminidase treated (green curves). Two major observations were made concerning cognate binding of pMHC monomers and pMHC tetramers. First, as described for experiments using the two step labeling assay, no significant differences in ligand affinity was observed for 4P-K^d monomers, when bound to untreated DP (Panel I, black curve) or SP (Panel IV, black curve) thymocytes. In both cases the K_D values were ~4nM. 4P-K^d tetramers bound more avidly to DP (Panel II, black curve) and SP (Panel V, black curve) thymocytes compared to 4P-K^d monomers indicated by the lower concentrations needed to reach half-maximal TCR saturation (apparent K_D = 0.4nM).

Importantly, as in the case of 4P-K^d monomers, no significant difference in the concentration leading to half-maximal TCR saturation of cognate 4P-K^d tetramer binding was observed when SP thymocytes were compared to DP thymocytes. In the case of the 4A-K^d tetramers TCR saturation was not reached by the highest concentration of tetramers applied (Panels III and VI) and therefore half-maximal TCR saturation could not be determined. But as expected from the low affinities measured for the 4A-K^d monomers ($5.7x10^{-7}$ M, Table

A: Sialylation status

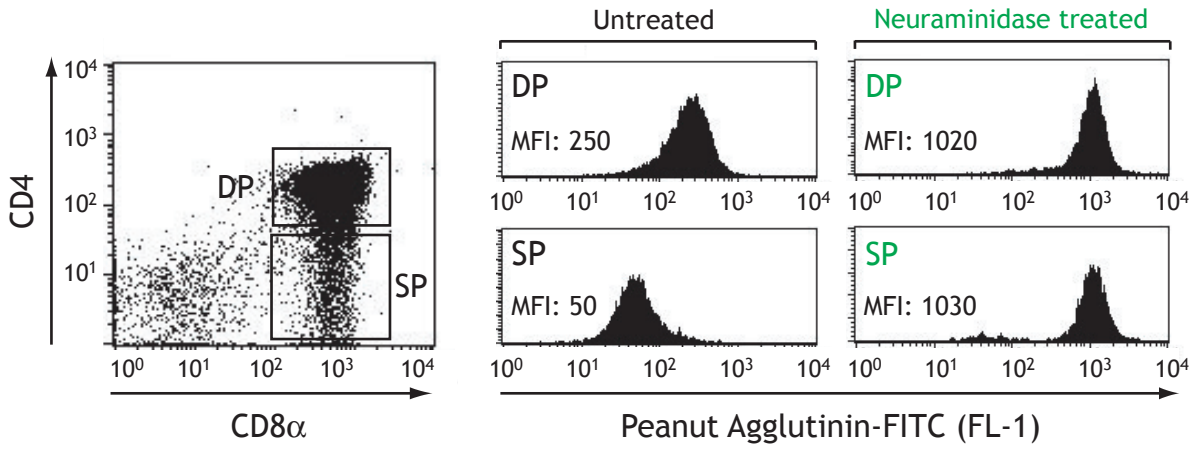

B: TCR ligand binding

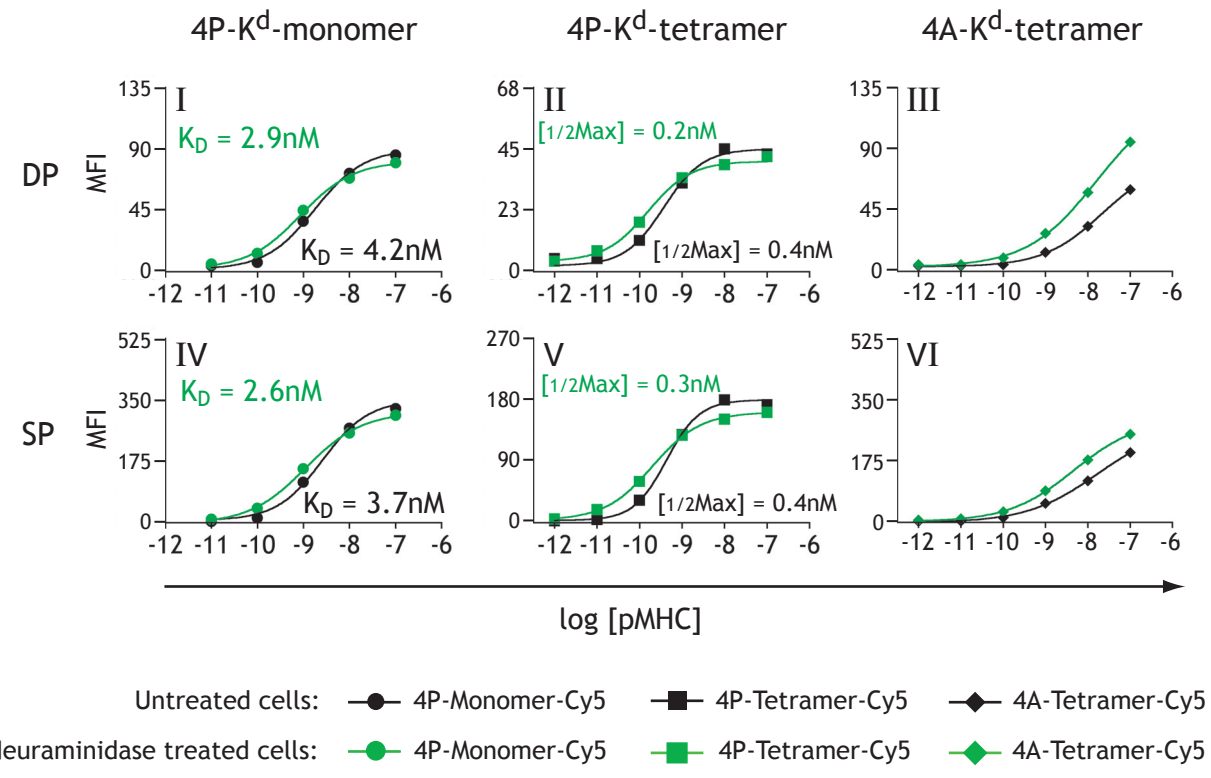

Figure 3.13: Direct photoaffinity labeling on T1 thymocytes using fluorescence labeled pMHC monomers or tetramers. (A) Neuraminidase treated or untreated thymocytes were incubated with 0.2µg/ml FITC-labeled peanut agglutinin (PNA) in the presence of α-CD4(RM4-5)-PerCP, α-CD8α(53-6.7)-APC and α-TCRβ(H57-597)-PE and analyzed by flow cytometry. Cells were electronically gated and the mean fluorescence of PNA binding to DP or SP thymoyctes was determined. (B) Neuraminidase treated (green curves) or untreated (black curves) thymocytes were incubated with varying doses of Cy5 labeled 4P-K^d monomer (panels I and IV), 4P-K^d tetramer (panels II and V) or 4A-K^d tetramer (panels III and VI). After UV-crosslinking (~312nm) cells were incubated with fluorescence labeled α-CD4(RM4-5), α-CD8α(53-6.7), α-TCRβ(H57-597) mAbs. DP (panels I, II and III) and SP thymocytes (panels IV, V and VI) were analyzed by flow-cytometry.

IV) the 4A-K^d tetramers bound less avidly to DP and SP thymocytes than 4P-K^d tetramers. Second, removal of sialic acid by neuraminidase treatment did not significantly alter the binding of 4P-K^d monomers to either DP (Panel I, green curve) or SP (Panel IV, green curve) thymocytes. Despite the slightly stronger binding at low concentrations and slightly weaker binding at high ligand concentrations the K_D values were not significantly affected by neuraminidase treatment. A very similar observation was made for the 4P-K^d tetramers, where neuraminidase treatment did not alter the apparent K_D (Panels II and V, green curves). In the case of the low avidity 4A-K^d tetramer, neuraminidase treatment led to increased binding on both DP thymocytes (Panel III, green curve) and SP thymocytes (Panel VI, green curve) at all ligand concentrations tested. Thus neuraminidase treatment increased ligand binding of the lower affinity tetramer.

In conclusion, using direct photoaffinity labeling on T1 thymocytes it was shown, that cognate TCR ligand binding to pMHC monomers and tetramers was not significantly different between DP thymocytes and SP thymocytes and that the different degrees of sialylation on these two populations had no significant influence on the TCR mediated cognate binding of monomeric or multimeric ligands.

3.1.13 Defining Positive and Negative Selecting Ligands

To be able to perform fetal thymic organ cultures (FTOC) the T1-TCR mice were bred to B10.D2; $Rg^{-/-}$; $\beta2m^{-/-}$ mice (see Material and Methods). As shown in Figure 3.14A, thymocytes of these T1-TCR; $Rg^{-/-}$; $\beta2m^{-/-}$ mice were arrested at the DP stage prior to positive and negative selection due to the lack of pMHC class I expression in $\beta2m^{-/-}$ mice. Using *ex vivo* cultures of fetal thymi in the presence of exogenous β2m and peptide (Hogquist et al., 1994) the developmental arrest was abrogated and depending on the potency of the peptide applied thymocytes were either positively or negatively selected (Fig. 3.14B). Downregulation of CD4 was indicative for positive selection (Fig. 3.14B; blue arrow) and downregulation of both CD4 and CD8 for negative selection (Fig. 3.14B; red arrow). The 5 peptides (Fig. 3.14C) used in the CD69 upregulation assays and the ligand binding studies were tested for their ability to induce positive or negative selection of T1-TCR; $Rag^{-/-}$; $b2m^{-/-}$ thymocytes in FTOC assays. 10μM of each peptide were applied to the FTOC cultures and thymocytes were analyzed for the CD4 and CD8β expression levels by flow-cytometry after 7 days of culture. Figure 3.14D shows representative dot blots for the 5 peptides tested. The 4L and 4P peptides induced negative selection, while the 4S and 4N peptides induced positive selection. The 4A peptide gave a mixed picture. Although 32% of the cells were CD8 SP and expressed CD8β (consistent with positive selection), most of the remaining cells were DN, expressing neither

coreceptor. The presence of the latter population was a product of negative selection. As the 4A peptide induces both types of selection, this peptide was referred to as transitional or 'borderline' selecting peptide.

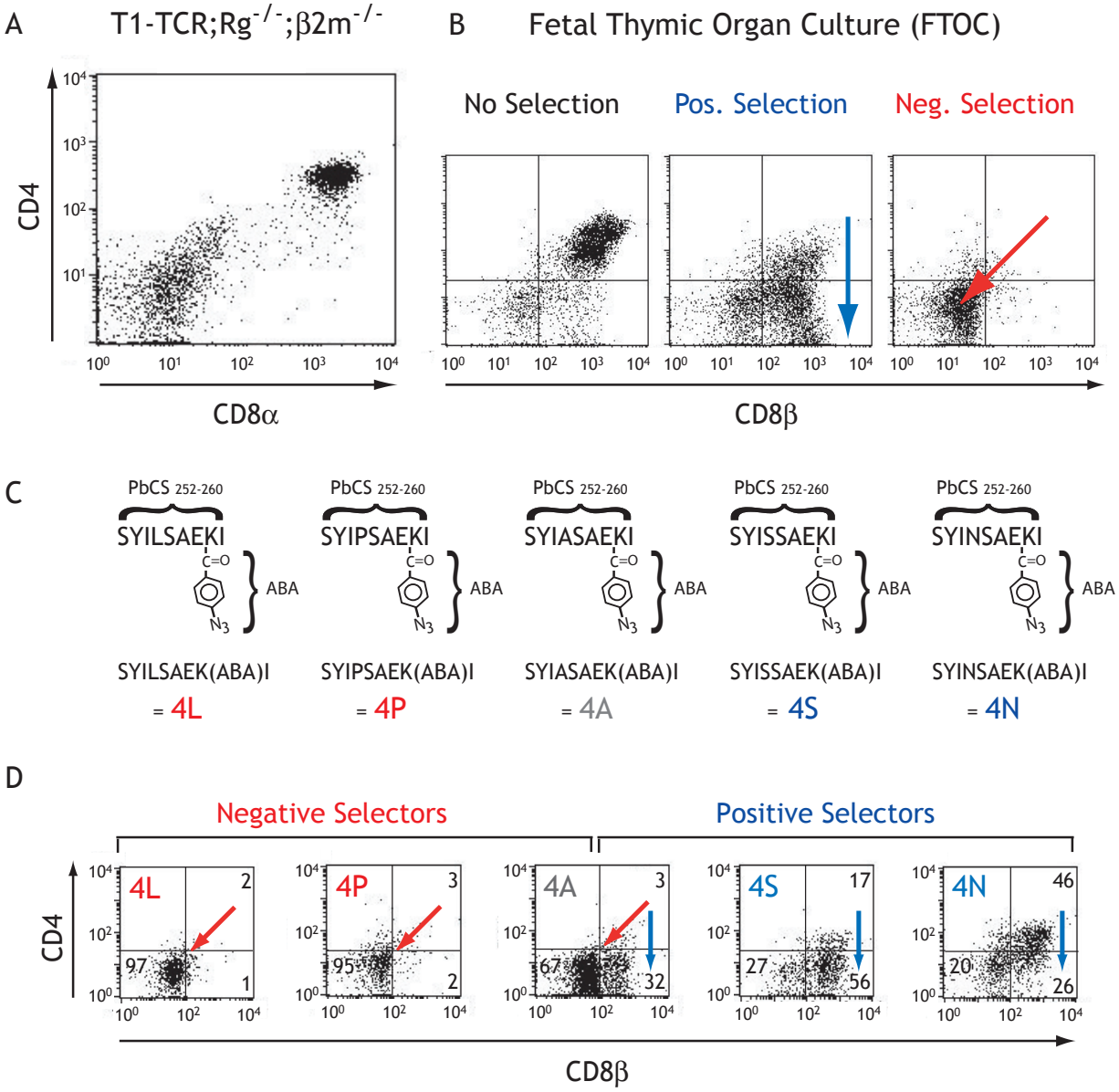

Figure 3.14: Defining positive and negative selecting peptides using fetal thymic organ culture (FTOC). (A) CD4 and CD8α expression on thymocytes from T1-TCR; Rag$^{-/-}$; β2m$^{-/-}$ mice. Thymic development in these mice is blocked at the DP stage due to the absence of β2m. (B) Defining positive and negative selecting peptides using FTOC: 7 day culture of fetal thymi (E14) in the presence of β2m and peptide did not affect CD4 and CD8 expression when 'null' peptides were added. Positive selecting ligands only induced downregulation of CD4 (blue arrow) while negative selecting peptides induced downregulation of both CD4 and CD8β (red arrow). (C) Peptides used in FTOCs. (D) Selection properties of various peptides added at 10μM final concentration to FTOC: 4L and 4P induced negative selection (red arrows). 4S and 4N induced positive selection (blue arrows). 4A induced negative selection on the majority of cells. Numbers indicate percentages of cells found in a quadrant.

3.1.14 Evidence for a Positive-Negative Selection Affinity Threshold

To further characterize the mixed phenotype that was observed with the 4A peptide, FTOCs were repeated including various concentrations of each peptide. Interestingly, the selection properties of the 4L, the 4P, the 4S and the 4N peptides were relatively concentration independent. In the case of the 4L and the 4P peptides, all concentrations tested led to negative selection, while in the case of the 4S and the 4N peptides all concentrations tested led to positive selection. In contrast, high concentrations of 4A led to negative selection, while low concentrations of 4A led to positive selection. This is illustrated in Figure 3.15A. These results combined with the finding, that the 4L and 4P peptides were considered strong peptides and the 4S and 4N peptide were considered weak peptides in CD69 upregulation assays while the 4A peptide was considered a moderate potency peptide (see Results 3.1.3; Fig. 3.3A), favoured the affinity model of thymic selection (see Introduction 1.4.1 and Reviewed by Starr et al., 2003) with the 4A peptide being at the affinity border between positive and negative selection.

Combining FTOC data with TCR-ligand binding data this argues that the affinity of the 4A-K^d ligand was too high to induce dose-independent positive selection and too low to induce a dose-independent negative selection. Therefore, the affinity of the TCR/CD8-4A-K^d interaction reflected the affinity threshold between positive and negative selection in the T1-TCR system. To directly compare the affinity and the selection properties, the affinity measurements of the 4L-K^d, the 4A-K^d and the 4S-K^d ligands were repeated on DP thymocytes from T1-TCR; $Rag^{-/-}$; $\beta2m^{-/-}$ mice at 37°C. These measurements revealed an affinity threshold defining positive and negative selection for the T1-TCR, which was 4µM.

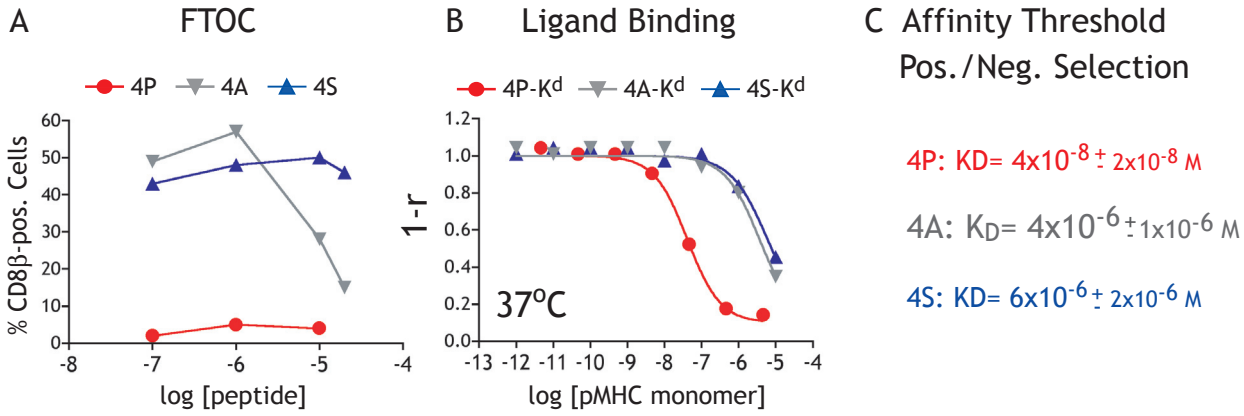

Figure 3.15: Comparison of thymic selection and ligand affinity. (A) Thymocyte positive and negative selection after 7 days of FTOC in the presence of various doses of 4P (●), 4A (▼) or 4S (▲) peptide. High percentages of $CD8\beta^+$ cells are indicative of positive selection and low percentages are indicative of negative selection. (B) Dose dependence of the ratio of free TCRs with the 4P-K^d (●) the 4A-K^d (▼) or the 4S-K^d (▲) monomers assessed on DP thymocytes from T1; $Rag^{-/-}$; $\beta2m^{-/-}$ mice using the two step labeling assay at 37°C. (C) K_D values representing the affinities of TCR ligand interactions determined from (B).

3.2 Role of the α-CPM in TCR-Ligand Binding and Function

3.2.1 The Role of the α-CPM in Thymocyte Development

The α-chain connecting peptide domain (α-CPM) is an evolutionary very conserved motif consisting of eight amino acids (FETDxNLN) located in the constant region of the TCRα chain in all vertebrates. Its function has been analyzed by several studies of mutant TCR molecules in which the α-CPM was replaced by a short amino acid sequence found in the corresponding constant region of TCRδ chains. Using hybridoma cell lines and transgenic mice expressing such α-CPM mutant TCRs, a series of defects were reported elucidating the importance of the evolutionary conservation of this motif (see Introduction 1.2.2.3). Most strikingly, TCR transgenic mice expressing mutant TCRs lacking the α-CPM showed a complete block of thymocyte development at the DP stage of T cell development (Backstrom et al., 1998; Werlen et al., 2000). It was shown that this defect was not due to a complete abrogation of TCR function, but specifically affected the TCR's ability to mediate positive selection; negative selection was unaffected by the absence of the α-CPM. Analysis of the signaling pathways revealed that the specific defect in positive selection was due to the absence of Erk MAP kinase signaling and altered CD3ζ and LAT phosphorylation in α-CPM deficient thymocytes stimulated with positive selecting ligands (Werlen et al., 2000). Although these studies described major defects in the signaling cascades by the absence of the α-CPM they did not address the question whether replacement of the α-CPM changed the pMHC ligand binding capacity of such mutant TCR receptors. To address this question, α-CPM mutant T1-TCRs were produced which allowed studying the impact of the α-CPM in TCR ligand binding by using the photoaffinity labeling technique (see Introduction 1.3.3.1).

3.2.2 Chimeric TCRs including or lacking the α-CPM

To study the role of the α-CPM in TCR-ligand binding the wildtype T1-TCR and two mutant, chimeric forms of the T1-TCR were generated. Mutant α-CPM deficient TCRs were produced by replacing parts of the TCRα chain constant regions by a sequence derived from the TCRδ chain constant region (more detailed explanations are found in the Introduction 1.1.3 and Results 3.2.4: Figure 1). Because it had previously been reported that TCRs consisting of such α-CPM deficient chimeric TCRα/δ chains were only expressed on the cell surface in conjunction with chimeric TCRβ/γ chains (Backstrom et al., 1996) the α-CPM mutant T1-TCRs did not only differ from the wildtype T1-TCRs by the absence of the α-CPM but also by the replacement of the transmembrane (TM) and cytosolic regions of the TCRα and TCRβ chains with homologous, corresponding sequences of TCRγ/δs. To be able to more

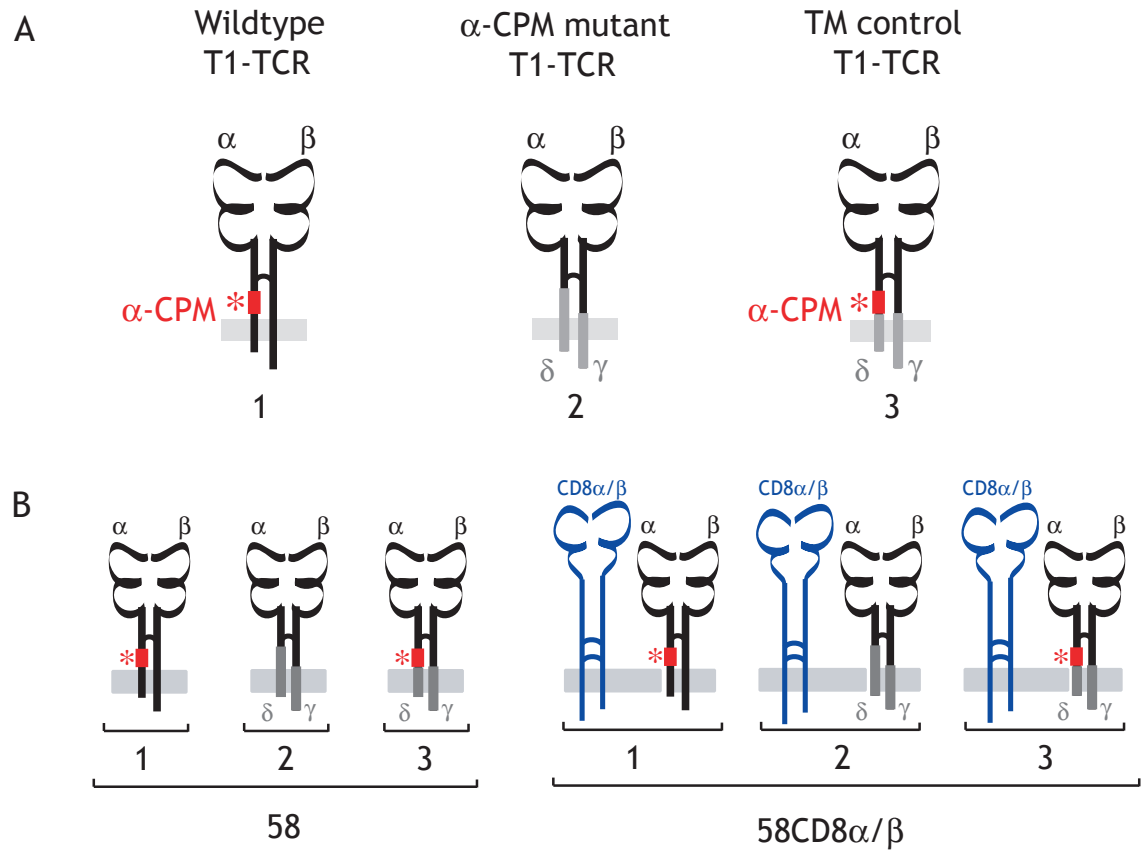

Figure 3.16: T1-TCR variants and hybridomas used to study the role of the α-CPM. (A) Schematic representation of wildtype (1), α-CPM mutant (2) and TM control (3) T1-TCRs. TCRα/β derived regions are shown in black; TCRγ/δ derived regions are shown in gray. The location of the α-chain connecting peptide motif (α-CPM) is shown in red. In the case of the α-CPM mutant (2) and TM control TCR (3) the transmembrane and cytosolic regions are derived from TCRγ/δ. In the case of the α-CPM mutant TCR, the α-CPM is replaced by homologous connecting peptide sequences derived from the TCRδ chain. For the amino-acid sequences see Results 3.2.4 (Fig. 1 in Naeher et al., 2002). (B) Wildtype T1-TCR (1), α-CPM mutant TCR (2) and TM control TCR (3) were independently transfected into 58 and 58CD8$\alpha^+\beta^+$ hybridomas.

specifically test the α-CPM mediated differences observed between the wildtype and the α-CPM mutant TCRs a third, transmembrane (TM) control T1-TCR was included in the studies. This chimeric TCR consisted of the same TCRβ/γ chimeric chain as the α-CPM mutant T1-TCR, but in contrast to the α-CPM mutant T1-TCR the TCRδ derived sequences were slightly shorter than those included in the α-CPM mutant chain. Therefore the TM control receptor contains the wildtype α-CPM motif. The three different T1-TCRs used in these studies are shown in Figure 3.16A.

3.2.3 Hybridoma Cell Lines Expressing WT or chimeric T1-TCRs

As a first step, measurements of T1-TCR-ligand binding and functional responses were performed on the thymoma derived '58' hybridoma cell line. This hybridoma cell line does

not express endogenous TCRs nor the CD4 or CD8 coreceptor molecules (Letourneur et al., 1989). To perform TCR-ligand binding studies including the three different T1-TCR variants in the presence or absence of the CD8α/β coreceptor the cDNAs of the T1-TCR variants were either introduced in the 58 hybridomas or 58CD8α/β hybridomas which had been previously transfected with the cDNAs of the CD8α/β coreceptor (Stotz et al., 1999). Figure 3.16B shows the TCRs and coreceptors expressed in six different hybridoma lines produced. Binding to T1-TCRs was assessed by UV induced crosslinking of TCR-bound H-2K^d monomers loaded with radioactive (^{125}I) variants of the PbCS$_{253\text{-}260}$(IASA)YIPSAEK(ABA)I peptides illustrated in Figure 3.17A (see Introduction 1.4.3.3). Therefore quantification of bound ligand could be assessed by immunoprecipitation of the T1-TCR, SDS-PAGE analysis and autoradiography. The results from the photoaffinity labeling experiments were compared to functional responses elicited by the peptides shown in Figure 3.17B when presented by the T2 hybridoma line (Cerundolo et al., 1990) expressing H-2K^d.

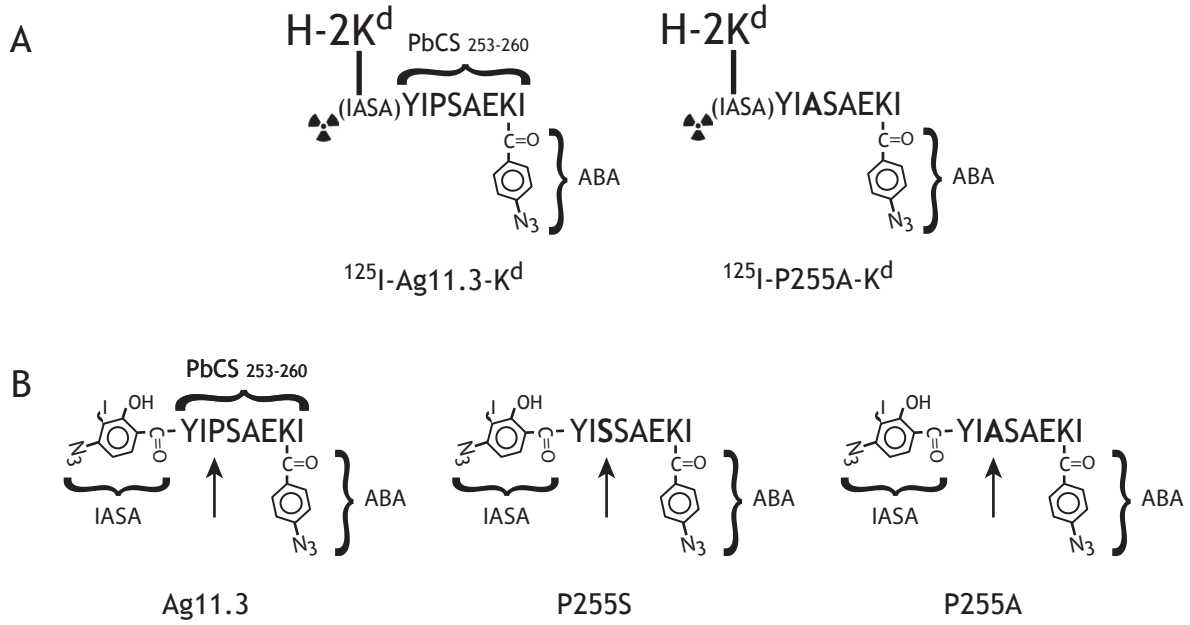

Figure 3.17: Ligands used in the studies performed with hybridomas. (A) Monomeric pMHC ligands used. The bifunctional, PbCS$_{253\text{-}260}$ derived, radioactively labeled ^{125}I-Ag11.3 peptide or the ^{125}I-P255A peptide variant were covalently crosslinked (UV irradiation at 350nm) to the H-2K^d heavy chain complexed with β2m. (B) Bifunctional IASA-YIPSAEK(ABA)I peptides were used for IL-2 assays. Arrows indicate the amino acid residues by which the peptide variants differ.

3.2.4 'A Role for the α-CPM in Mediating TCR/CD8 Cooperativity'

The results of these experiments were published in the Journal of Immunology (2002), 169:2964.

The Journal of Immunology

A Role for the α-Chain Connecting Peptide Motif in Mediating TCR-CD8 Cooperation

Dieter Naeher,* Immanuel F. Luescher,† and Ed Palmer[1]*

To generate peripheral T cells that are both self-MHC restricted and self-MHC tolerant, thymocytes are subjected to positive and negative selection. How the TCR discriminates between positive and negative selection ligands is not well understood, although there is substantial evidence that the CD4 and CD8 coreceptors play an important role in this cell fate decision. We have previously identified an evolutionarily conserved motif in the TCR, the α-chain connecting peptide motif (α-CPM), which allows the TCR to deliver positive selection signals. Thymocytes expressing α-CPM-deficient receptors do not undergo positive selection, whereas their negative selection is not impaired. In this work we studied the ligand binding and receptor function of α-CPM-deficient TCRs by generating T cell hybridomas expressing wild-type or α-CPM-deficient forms of the T1 TCR. This K^d-restricted TCR is specific for a photoreactive derivative of the *Plasmodium berghei* circumsporozoite $peptide_{252–260}$ IASA-YIPSAEK(ABA)I and is therefore amenable to TCR photoaffinity labeling. The experiments presented in this work show that α-CPM-deficient TCRs fail to cooperate with CD8 to enhance ligand binding and functional responses. *The Journal of Immunology,* **2002, 169: 2964–2970.**

During T cell development thymocytes are subjected to positive and negative selection, establishing a pool of mature T cells that is self-MHC restricted and self-MHC tolerant. TCR-mediated ligand recognition is essential for positive and negative selection of thymocytes. Although how the TCR generates distinct positive and negative selection signals is not completely understood, thymocytes are sensitive to ligand affinity in that low-affinity ligands induce positive selection and high-affinity ligands induce negative selection (1–3). The CD4 and CD8 coreceptors play an important role during thymic selection by enhancing ligand binding to the TCR (4–8). In addition, these coreceptors play a key role in lineage commitment. Several lines of evidence suggest that the strength of the signal delivered by the coreceptor determines whether a thymocyte will develop into a helper or a cytotoxic T cell (9–12). Although the precise role of coreceptor involvement on positive and negative selection is still unresolved, their importance in modulating TCR ligand binding and recruitment of the membrane proximal tyrosine kinase $p56^{lck}$ to the TCR-CD3 complex has been demonstrated (13–18). $p56^{lck}$-mediated phosphorylation of immunotyrosine-based activation motifs present in the cytoplasmic tails of the CD3 chains is necessary for the appropriate induction of the signaling cascades involved in both types of thymic selection (12, 19–22).

The TCR constant regions couple the αβ heterodimer to the CD3 complex. TCRαβ constant regions are composed of the cytosolic (Cyto),[2] the transmembrane (TM), the connecting peptide (CP), and the Ig-like domains. In terms of positive selection, a particularly important role is played by a motif located in the membrane proximal CP domain of the TCRα chain (23, 24). This α-chain connecting peptide motif (α-CPM) consists of seven highly conserved amino acids (FETDxNLN), is only found in TCRαβ, and is absent from TCRγδ. Thymocytes from mice expressing α-CPM mutant TCRs fail to undergo positive selection, while negative selection is not impaired. Characterization of thymocytes or hybridomas expressing α-CPM mutant TCRs revealed an impaired CD3ζ phosphorylation (23, 25), a defective activation of the $p56^{Fyn}$ protein kinase (26), and an impaired CD3δ association (24). CD3δ is also important for thymic selection signals because thymocytes from CD3δ knockout mice fail to undergo positive selection as well (27, 28). The defect observed with α-CPM mutant receptors is selective for low-affinity (positive-selecting) ligands. Low-affinity ligands fail to recruit tyrosine-phosphorylated isoforms of the signaling components *lck*, CD3-ζ, ZAP-70, and linker for activation of T cells into detergent-insoluble, membrane rafts in α-CPM mutant thymocytes (25). Why these defects are specific for positive-selecting ligands is still unclear.

To investigate whether the defects observed with α-CPM-deficient TCRs are mediated by altered ligand binding, we studied the T1 TCR, a receptor that was developed to investigate TCR-ligand interactions by photoaffinity labeling (29). In the T1 TCR system, photoaffinity labeling is used to cross-link soluble, monomeric, pMHC ligands to surface TCRs on living cells. This system is based on the *Plasmodium berghei* circumsporozoite (PbCS) peptide derivative, IASA-YIPSAEK(ABA)I, with two photoreactive groups, IASA and ABA, which can be selectively activated by UV light of different wavelengths. This bireactive peptide derivative can be covalently cross-linked to the K^d molecule by selective photoactivation of the IASA group, leaving the ABA group intact. After specific binding of these pMHC complexes to T1 TCRs, photoactivation of the ABA group allows covalent cross-linking of the pMHC ligand to the TCR.

In this study we generated the wild-type and two chimeric forms of the T1 TCR, in which the α-CPM was either present or absent. All receptors were expressed in $CD8^-$ and $CD8^+$ hybridomas. We were able to show that replacement of the α-CPM does not alter the binding of the T1 TCR to its pMHC ligand per se. However, these studies demonstrate that the α-CPM is required for mediating

*Laboratory of Transplantation Immunology and Nephrology, University Hospital, Basel, Switzerland; and †Ludwig Institute for Cancer Research, Lausanne Branch, University of Lausanne, Epalinges, Switzerland

Received for publication May 2, 2002. Accepted for publication July 9, 2002.

The costs of publication of this article were defrayed in part by the payment of page charges. This article must therefore be hereby marked *advertisement* in accordance with 18 U.S.C. Section 1734 solely to indicate this fact.

[1] Address correspondence and reprint requests to Dr. Ed Palmer, Laboratory of Transplantation Immunology and Nephrology, University Hospital, Hebelstrasse 20, CH-4031 Basel, Switzerland. E-mail address: ed.palmer@unibas.ch

[2] Abbreviations used in this paper: Cyto, cytosolic; α-CPM, α-chain connecting peptide motif; TM, transmembrane; CP, connecting peptide; PbCS, *Plasmodium berghei* circumsporozoite.

0022-1767/02/$02.00

TCR-CD8 cooperation to increase ligand binding. Furthermore, we show that the functional defects observed in hybridomas expressing α-CPM-deficient TCRs are CD8 mediated and most prominent with low-affinity ligands.

Materials and Methods

DNA constructs

The T1 TCR is derived from the K^d-restricted, PbCS derivative peptide$_{253–260}$ (IASA)-YIPSAEK(ABA)I (Ag11.3)-specific CTL clone, T1 (30). The cDNA encoding the TCRα chain was cloned into the G418-resistant retroviral vector, LXSN (31–33). Similarly, the T1 TCRβ chain was cloned into the puromycin-resistant retroviral vector, LXSP (23). The cDNAs encoding the T1 TCR αδ chimeras were constructed using the previously described αII and αIV chimeric cDNAs (23) specific for the 3BBM74 TCR (34) by replacing the VJC-containing *Eco*RI-*Spe*I fragment by T1 TCR VJC α-chain sequences. Similarly, the T1 TCR βγ chimera βIII was constructed by replacing the VDJC-containing *Eco*RI-*Xba*I fragment of the 3BBM74 chimeric β-chains by T1 TCR VDJC β-chain-containing sequences.

Cells

The TCR^-CD8^- T hybridoma, 58, and its TCR^-CD8^+ derivative, 58CD8αβ, have been described previously (35, 36). Retroviral infection was used to introduce the wild-type or chimeric T1 TCRα chains and the wild-type or chimeric T1 TCRβ chains into the 58 (TCR^-CD8^-) and the 58CD8αβ (TCR^-CD8^+) hybridomas. Transduced hybridomas were subsequently FACS-sorted for high TCR expression. All cells were grown in IMDM supplemented with 2% FCS, 2 mM L-glutamine, 100 U/ml penicillin, 100 μg/ml streptomycin, and 50 μM 2-ME. The T2-K^d cell line (generously provided by T. Potter, National Jewish Medical and Research Center, Denver, CO) used for peptide presentation was grown in IMDM with 10% FCS. The indicator cell line HT-2 (37) was grown in IMDM containing 10% FCS and 250 U/ml rIL-2. The ectotropic packaging cell line BOSC23 was purchased from American Type Culture Collection (Manassas, VA) and grown in IMDM containing 10% FCS.

Transduction of cDNAs

The BOSC23 packaging cell line was transfected as previously described (38). The supernatant containing retroviral particles was used to infect the TCR^-CD8^- cell line, 58, and its $CD8^+$ derivative, 58CD8αβ. In short, 5×10^5 58 or 58CD8αβ hybridomas were resuspended in 500 μl IMDM containing 4 μg/ml polybrene (Sigma-Aldrich, St. Louis, MO). After 24 h, 5 ml of fresh IMDM and the appropriate selective drugs were added (1 mg/ml G418 (Life Technologies, Rockville, MD), 3 μg/ml puromycin (Sigma-Aldrich), 2 mM histidinol (Sigma-Aldrich), or 0.5 mg/ml hygromycin B (Calbiochem, La Jolla, CA)). Surviving cells were analyzed after 4 days and sorted for high TCR surface expression by FACS. Transfected cells were continuously maintained in medium containing selective drugs.

Antibodies

The anti-TCR Cβ mAb H57-597 (39), the anti-CD3ε mAb 145-2C11 (40), and the anti-CD8β mAb H35-17 (41) were purified from culture supernatants using protein G (Amersham Pharmacia Biotech, Piscataway, NJ). The anti-CD8α mAb 53-6.7 and the anti-CD8β mAb 53-5.8 were purchased from BD PharMingen (San Diego, CA).

Quantitation of TCR surface expression

To calculate the relative amounts of the three different TCRs expressed on $CD8^+$ and $CD8^-$ hybridomas, the expression of the TCR, measured with the anti-TCR Cβ mAb H57-597, was normalized to the expression of the wild-type TCR measured on $CD8^+$ hybridomas. The following equation was used: relative TCR expression = MCF of TCR staining expressing variant TCR/MCF of TCR staining on $CD8^+$ hybridomas expressing the wild-type TCR.

K^d and TCR photoaffinity labeling

Soluble K^d molecules were produced and loaded with the ^{125}IASA-YIPSAEK(ABA)I peptide or the P255A derivative as previously described (29). TCR photoaffinity labeling was also performed as previously described (5). Briefly, 5×10^6 cpm of K^d-^{125}IASA-YIPSAEK(ABA)I were incubated with 10^7 T hybridoma cells either at 0°C for 2 h or at 37°C for 10 min, followed by UV irradiation at 312 ± 40 nm. After UV irradiation, cells (10^7 cells/ml) were washed twice and lysed in 1 ml lysis buffer containing 1% Triton X-100, 1% Nonidet P-40, 150 mM NaCl, 0.2 mM EDTA, 50 mM HEPES, 1 mM PMSF, 10 μg/ml leupeptin, 10 μg/ml aprotinin, and 10 μg/ml iodoacetamide for 2 h at 4°C. Postnuclear supernatants were subjected to immunoprecipitation with anti-TCR Cβ mAb H57-597. The immunoprecipitates were analyzed by reducing SDS-PAGE and quantified using a PhosphorImager and ImageQuant software (Molecular Dynamics, Sunnyvale, CA). To compare the photoaffinity labeling of the various receptors, the values were normalized for TCR expression and compared with the labeling value obtained on $CD8^+$ hybridomas expressing the wild-type T1 TCR. The following equation was used: relative binding = (CPM bound by variant TCR/CPM bound by $CD8^+$ hybridoma expressing wild-type TCR)/relative TCR expression.

IL-2 assays

A total of 80 μl IMDM containing 6×10^4 T2-K^d cells was plated in flat-bottom 96-well plates and incubated with the indicated amounts of peptide (see Fig. 4) for 2 h at 37°C. T hybridoma cells (6×10^4 in 100 μl IMDM) were subsequently added. After a further 24 h of incubation at 37°C, the supernatant was harvested and assayed for IL-2 using the indicator line HT-2 as previously described (23).

Calculation of relative receptor sensitivities

Relative receptor sensitivities were defined by determining the peptide concentration required for half-maximal IL-2 production from each hybridoma and peptide tested. These values were normalized to the concentration of P255S peptide required for half-maximal IL-2 production from the $CD8^+$ hybridomas expressing the wild-type T1 TCR. The following equation was used: relative receptor sensitivity = [P255S] required for 1/2 max IL-2 production of $CD8^+$ hybridomas expressing wild-type TCR/[pep] required for 1/2 max IL-2 production of hybridomas expressing a variant TCR

Results

Wild-type and chimeric T1 TCRs

To test whether altered ligand binding was responsible for the functional defects previously observed with mutant TCRs lacking the α-CPM domain (23–26), we analyzed the ligand binding properties of several chimeric T1 receptors. The T1 receptors are specific for photoreactive derivatives of a PbCS peptide$_{253–260}$ (IASA)YIPSAEK(ABA)I (29), which can be photo-cross-linked to K^d and the TCR. The CP, TM, and Cyto domains of the wild type and the two chimeric TCRs used in this study are schematically shown in Fig. 1*A*. Because a simple deletion or replacement of the α-CPM prevented TCR expression (data not shown), we generated chimeric TCRs in which the CP, TM, and Cyto domains were replaced with the corresponding domains from a TCRγδ. In Fig. 1*A*, TCRδ sequences, which replaced α-sequences, are shown in black and TCR-γ sequences, which replaced the TCRβ sequences, are shown in gray. The α-CPM mutant receptor is comprised of αIV and βIII chains. The αIV chain encodes V, D, J, and parts of the C region sequences from the T1 TCRα chain followed by Cδ sequences; this chain lacks the α-CPM (Fig. 1*B*). In the βIII chain, the TM and the Cyto domains of the β-chain were replaced by homologous Cγ sequences (Fig. 1*B*, boxed sequences); the βIII chain is required for expression of the αIV chain, which lacks the α-CPM. The control for the α-CPM mutant receptor is the TM control receptor, which expresses the βIII chain and the αII chain. The αII chain is identical to the αIV chain, except that it includes the α-CPM (Fig. 1*B*). Thus, the only difference between the α-CPM mutant and the TM control receptors is the absence of the α-CPM domain from the α-CPM mutant receptor.

Cell surface expression of wild-type and variant T1 TCRs

The expression of chimeric TCRs was examined on 58 ($CD8^-$) and 58CD8αβ ($CD8^+$) T cell hybridomas (Fig. 2 and data not shown). The wild-type and α-CPM mutant receptors were expressed at comparable, low levels while the TM control (α-CPM intact) receptor was expressed at higher levels. TCR expression was similar on $CD8^-$ and $CD8^+$ hybridomas (data not shown) and expression of a particular TCR did not significantly affect CD8

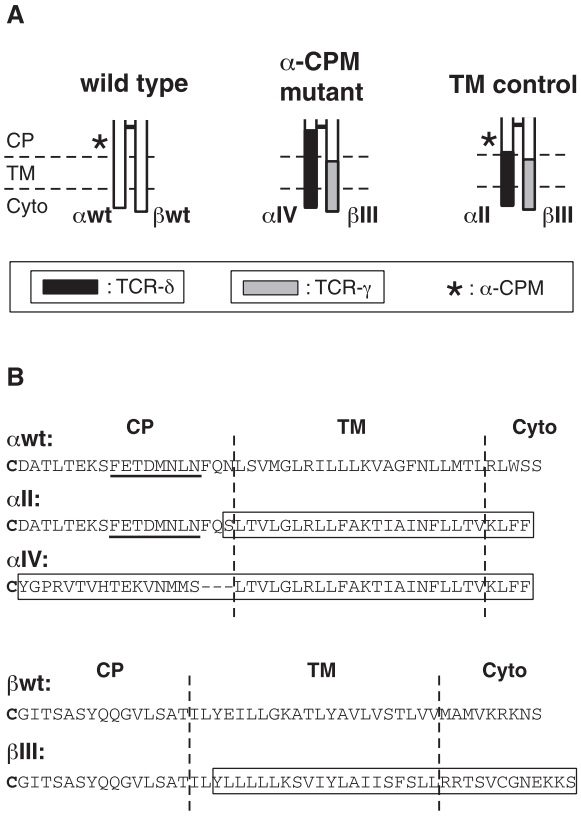

FIGURE 1. Sequences of the T1 TCRs used in this study. *A*, Schematic representation of the constant regions of the wild-type and chimeric TCRs used in this study. Only the CP, TM, and Cyto domains are shown. The complete α- and β-chain cDNAs have been described previously (29). Open bars, Cα and Cβ sequences; vetical filled bars, Cδ sequences; shaded bars, Cγ sequences. The interchain disulfide bond is represented by a filled horizontal bar. The location of the α-CPM domain is indicated by an asterisk. The α-CPM mutant receptor (αIV/βIII) is similar to the TM control (αII/βIII) receptor, except that the α-CPM has been removed and replaced by Cδ sequences in the αIV chain. *B*, Amino acid sequences of chimeric TCRα chains and TCRβ chains. Only the CP, TM, and Cyto domains of the TCR constant regions are shown. The sequences of the wild-type TCRα (αwt) and TCRβ (βwt) chains, two chimeric TCR$\alpha\delta$ chains (αII and αIV), and one chimeric TCR$\beta\gamma$ chain (βIII) are shown using the single letter amino acid code. The α-CPM is underlined. The boxes indicate Cδ-derived sequences in the case of the αII and αIV chains and a Cγ-derived sequence in the case of the βIII chain. The interchain Cys^{224} of the T1 TCRα chain and the interchain Cys^{257} of the T1 TCRβ chain are indicated by bold letters. The vertical dotted lines indicate the approximate boundary of the TM domain, defined using the Lasergene Navigator Protean Software program (DNAstar, Madison, WI).

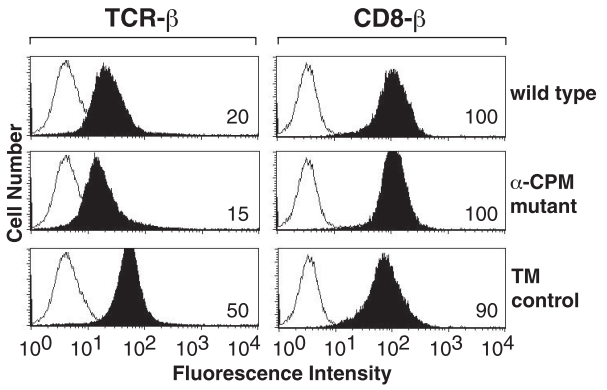

FIGURE 2. TCR and CD8 cell surface expression. $CD8^+$ (58CD8$\alpha\beta$) T cell hybridomas expressing wild-type or chimeric TCRs were stained with the anti-TCR Cβ mAb H57-597 or with the anti-CD8β mAb 53-5.8 and analyzed by flow cytometry. The open histograms represent the staining of untransfected 58 (TCR^-CD8^-) control hybridomas stained with the same Abs. Filled histograms represent the TCR or CD8β expression profiles for each $CD8^+$ hybridoma used in this study. The number in each panel indicates the mean fluorescence intensity observed with hybridomas expressing the indicated T1 TCRs or the CD8 coreceptor. TCR expression levels were similar in $CD8^-$ (58) hybridomas (data not shown). In all $CD8^+$ hybridomas, the mean fluorescence intensity for CD8α expression was 250, irrespective of the TCR expressed (data not shown).

expression (Fig. 2). Finally, CD8$\alpha\beta$ expression was similar in all $CD8^+$ cell lines used in this study (Fig. 2).

Ligand binding on wild-type and chimeric T1 TCRs

To test whether replacement of the α-CPM affects ligand binding, we performed photoaffinity labeling of wild-type and chimeric T1 TCRs using photoreactive ligands. To this end, hybridomas expressing the different T1 TCRs were incubated with monomeric K^d-peptide complexes. Two different ligands were used: the high-affinity Ag11.3 and the variant, P255A, which has a lower relative affinity for the T1 TCR (42). After incubating hybridomas expressing the different T1 TCRs with equal amounts of K^d-peptide complexes, TCR-bound K^d-peptide complexes were cross-linked by UV irradiation. TCRs were immunoprecipitated and analyzed by SDS-PAGE and phosphor imaging. Fig. 3*A* shows a representative experiment in which TCR photoaffinity labeling was performed on $CD8^-$ and $CD8^+$ hybridomas expressing the various T1 TCRs. The labeled material at 90 kDa represents the trimolecular complex consisting of the TCR, the peptide, and K^d. The material at 45 kDa represents a minor fraction of peptide-K^d complexes that were not cross-linked to but were coprecipitated with the T1 TCR. When TCR^- and $CD8^-$ hybridomas were incubated with peptide-K^d complexes under the same conditions, no signal could be detected, demonstrating that the binding of the peptide-K^d complexes was specific for the T1 TCR (Fig. 3*A*).

Fig. 3, *B–D*, shows a quantification of the signal intensities measured by phosphor imaging after correction for the different TCR expression levels and normalization to the signal observed on hybridomas expressing the wild-type T1 TCR on $CD8^+$ hybridomas at 0°C (see *Materials and Methods* for calculations).

Fig. 3*B* shows relative ligand binding observed for the different T1 TCRs upon incubation with ^{125}IASA-YIPSAEK(ABA)I-K^d (Ag11.3) complexes at 37°C. Importantly, ligand binding at 37°C was equivalent on all TCRs in the absence of CD8 (Fig. 3*B*, open bars), demonstrating that the α-CPM-deficient TCR binds ligand as well as the wild-type and TM control TCRs. In contrast, a significant increase in ligand binding was observed only on $CD8^+$ hybridomas (Fig. 3*B*, filled bars) expressing the wild-type or the TM control receptor, which contain an intact α-CPM. No increase in ligand binding was observed for $CD8^+$ hybridomas expressing the α-CPM mutant receptor, which lacks the α-CPM. Therefore, at 37°C only hybridomas expressing receptors with an intact α-CPM showed a CD8-mediated increase in ligand binding. We also performed affinity labeling of T1 TCRs using the weak ^{125}IASA-YIASAEK(ABA)I-K^d (P255A) ligand. Because the signals obtained with the weak ligand at 37°C were too weak to be accurately quantified, we repeated the experiments with the strong (Ag11.3) and the weak (P255A) ligands at 0°C where the signal intensities were higher, which is in accordance with previous observations (5).

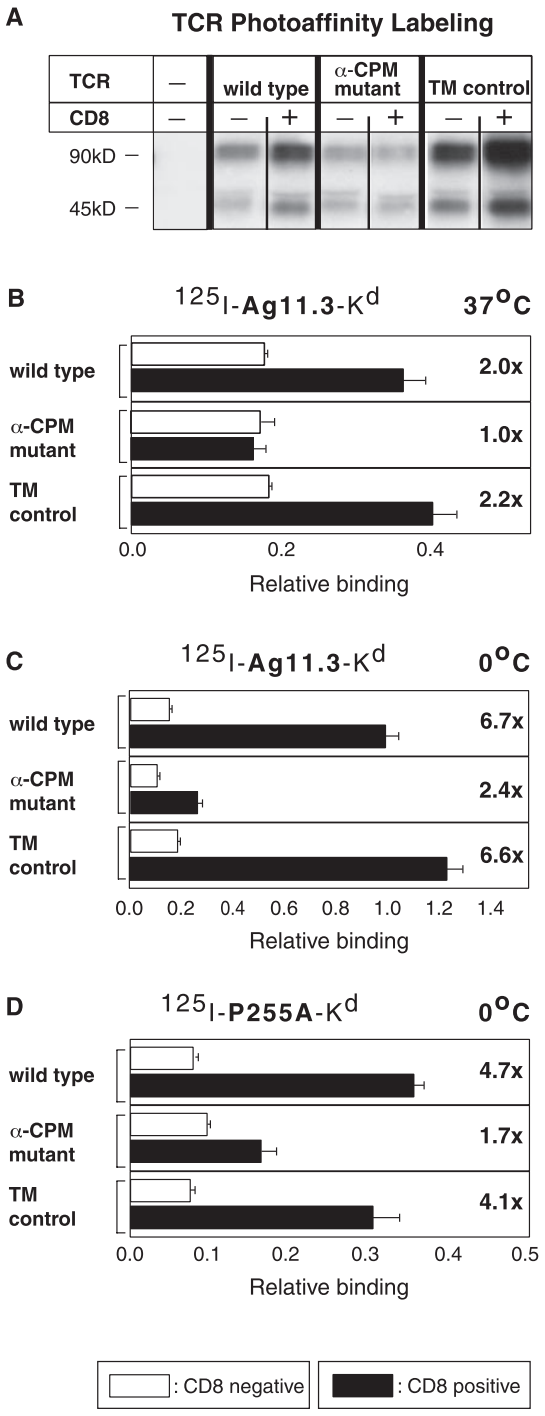

FIGURE 3. TCR photoaffinity labeling studies on CD8$^+$ or CD8$^-$ hybridomas using soluble, monomeric peptide-K^d complexes. *A*, Photoaffinity labeling of the untransfected 58 (TCR$^-$CD8$^-$) control hybridoma or the T cell hybridomas expressing the indicated T1 TCR variants in the absence (−) or presence (+) of CD8 coreceptors. Cells were incubated with equal amounts of radiolabeled soluble covalent complexes of monomeric K^d and the peptide derivative ^{125}IASA-YIPSAEK(ABA)I (Ag11.3) at 37°C. After UV irradiation at 312 nm, TCR-ligand complexes were immunoprecipitated and analyzed by SDS-PAGE as described in *Materials and Methods*. The 90-kDa bands representing the trimolecular, TCR-peptide-K^d complexes were quantified by a PhosphorImager. The 45-kDa band is the soluble pMHC ligand, which was immunoprecipitated with the TCR but was not covalently cross-linked. *B*, Normalized, relative ligand binding of CD8$^-$ (open bars) and CD8$^+$ hybridomas (filled bars) expressing the various T1 TCRs after incubation with the ^{125}I-Ag11.3-K^d ligand at 37°C. The numbers represent the fold increase in ligand binding mediated by CD8. The values representing the 90-kDa bands were corrected for the different mean values of TCR expression shown in Fig. 2. The corrected TCR ligand binding values were then normalized to the Ag11.3 binding observed at 0°C to CD8$^+$ hybridomas expressing the wild-type TCR ligand, which was defined as 1.0. Normalized binding of the ^{125}I-Ag11.3-K^d complexes is shown for wild-type and chimeric T1 TCRs either in the absence or presence of the CD8 coreceptor. *C*, Normalized, relative ligand binding observed with the ^{125}I-Ag11.3-K^d ligand at 0°C. See *B* for experimental details. *D*, Normalized, relative ligand binding with the ^{125}I-P255A-K^d ligand at 0°C. See *B* for experimental details.

As shown in Fig. 3, *C* and *D*, binding on CD8$^-$ hybridomas (open bars) was similar for all TCRs tested, irrespective of whether the strong (Ag11.3) ligand (Fig. 3*C*) or the weak (P255A) ligand (Fig. 3*D*) was used. In the presence of CD8, a significant increase in ligand binding was observed only on hybridomas expressing the wild-type and TM control receptors, while the α-CPM mutant TCR exhibited only a small increase in ligand binding mediated by CD8 (Fig. 3, *C* and *D*). Therefore, the impact of CD8 on ligand binding was more pronounced with receptors containing the α-CPM (wild type and TM control) compared with the receptor lacking this motif (α-CPM mutant) (Fig. 3). The importance of the α-CPM is illustrated when comparing the CD8-mediated ligand binding increase observed on the α-CPM mutant and the TM control TCRs. These two receptors differ only by the absence or presence of the α-CPM (Fig. 1*A*).

The ligand binding experiments were repeated on CD8$^+$ hybridomas expressing the chimeric T1 TCRs in the presence of a CD8β blocking mAb, H35-17. Ligand binding observed in the presence of this Ab was similar to the results obtained on CD8$^-$ hybridomas (data not shown). Because a mAb directed against the CD8β chain completely blocks the increase in ligand binding this enhancement can be attributed to CD8αβ heterodimers rather than CD8αα homodimers.

The fact that the absence of the α-CPM precludes proper CD8 participation in the binding of pMHC ligands suggests that the α-CPM is an important structural feature orchestrating TCR/CD8 cooperation.

IL-2 production of hybridomas expressing wild-type or chimeric T1 TCRs

We examined the ability of α-CPM mutant receptors to transduce a signal by measuring the IL-2 produced in response to peptide ligands. To determine whether the functional deficit observed with hybridomas expressing α-CPM-deficient TCRs was dependent on the potency of the peptide tested, we performed IL-2 assays using three ligands with varying potencies for the T1 TCR. Fig. 4*A* shows the IL-2 responses of CD8$^-$ and CD8$^+$ hybridomas expressing the various receptors when stimulated with ligands of high (Ag11.3; Fig. 4*A*, *a–c*), medium (P255S; Fig. 4*A*, *d–f*) or low (P255A; Fig. 4*A*, *g–i*) affinities. Stimulation of CD8$^-$ hybridomas (Fig. 4*A*, open symbols) generally resulted in lower IL-2 production than the stimulation of CD8$^+$ hybridomas (Fig. 4*A*, filled symbols). When comparing IL-2 production of the various hybridomas stimulated by the high-affinity Ag11.3 ligand, CD8 significantly increased the IL-2 responses of hybridomas expressing the wild-type, α-CPM mutant, or TM control receptor (Fig. 4*A*, *a–c*). A similar CD8-mediated increase in IL-2 production was observed when the various hybridomas were stimulated with the medium-affinity P255S peptide variant (Fig. 4*A*, *d–f*). Interestingly, a clear difference in the CD8 participation was observed when comparing

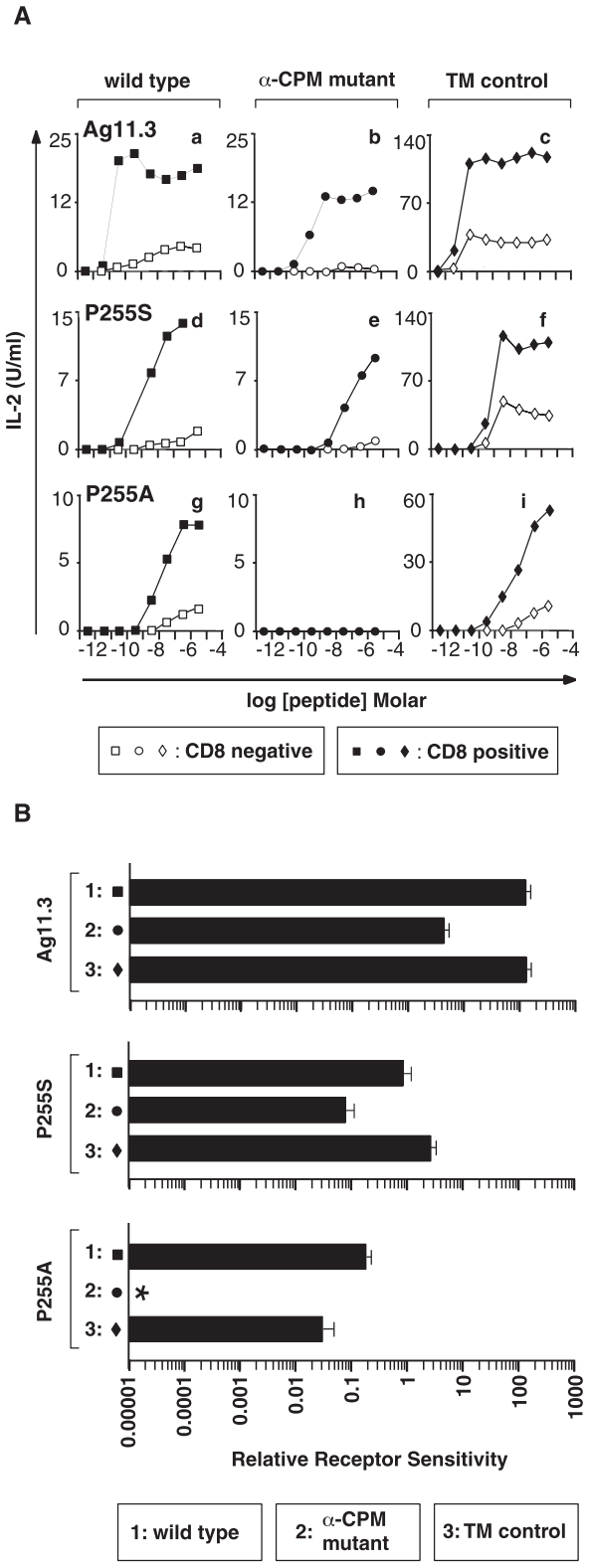

FIGURE 4. IL-2 responses of T1 TCR expressing $CD8^-$ and $CD8^+$ hybridomas to peptide ligands of varying potency. *A*, $CD8^-$ and $CD8^+$ hybridomas expressing different T1 TCRs were stimulated with the strong Ag11.3 peptide (*a–c*) or the lower-affinity derivatives P255S (*d–f*) or P255A (*g–i*) and their IL-2 production was measured. Results obtained from $CD8^-$ (□) and $CD8^+$ (■) hybridomas expressing the wild-type T1 TCR are shown in *a*, *d*, and *g*. Shown in *b*, *e*, and *h* are IL-2 responses of $CD8^-$ (○) and $CD8^+$ (●) hybridomas expressing the α-CPM mutant T1 TCR. Shown in *c*, *f*, and *i* are the IL-2 responses of hybridomas that express the TM control T1 TCR in the absence (◊) or presence (♦) of the CD8 coreceptor molecules. *B*, Receptor sensitivities of $CD8^+$ hybridomas to peptide ligands of varying potency. Relative receptor sensitivities of $CD8^+$ hybridomas expressing the various T1 TCRs were calculated from the peptide concentration required for half-maximal IL-2 synthesis in each hybridoma line and normalized to the receptor sensitivity calculated from $CD8^+$ hybridomas expressing the wild-type receptor responding to P255S (see *Materials and Methods* for calculation of receptor sensitivity). The numbers indicate the different T1 TCRs tested: 1, wild type; 2, α-CPM mutant; 3, TM control. Three different peptides were tested: Ag11.3, P255S, and P255A. The asterisk indicates that the α-CPM mutant receptor was at least 10,000-fold less sensitive to the low-affinity ligand, P255A, than the wild-type TCR. Data are expressed as the mean of triplicates from a representative experiment. IL-2 assays were independently conducted three times in the case of the Ag11.3 and the P255A peptides and twice with P255S peptide.

the responses to the low-affinity P255A ligand. Hybridomas expressing the wild-type T1 TCR (Fig. 4*Ag*) or the TM control TCR (Fig. 4*Ai*) showed a significant CD8-mediated increase in IL-2 production when stimulated with the weak P255A peptide. In contrast, α-CPM mutant hybridomas failed to produce any detectable IL-2, even when CD8 was present (Fig. 4*Ah*).

To quantify the CD8-mediated differences between the wild-type, α-CPM mutant, and TM control receptors, we reanalyzed the IL-2 data obtained with $CD8^+$ hybridomas to determine the sensitivity of each receptor for each Ag. We calculated the relative sensitivity of each TCR by determining the peptide concentration required for half-maximal IL-2 production for each hybridoma line and comparing it to the P255S concentration required for half-maximal IL-2 production from the $CD8^+$ hybridoma expressing wild-type receptor; this was defined as 1.0 (see *Materials and Methods* for calculation).

The results are shown in Fig. 4*B*, where the three ligands have been ordered according to their potency. Although the wild-type, α-CPM mutant, and TM control receptors showed the highest sensitivity for the high-affinity Ag11.3 peptide, the α-CPM mutant TCR displayed a 30-fold reduced sensitivity for this ligand. Similar observations were made with the intermediate-affinity P255S peptide. Again, the α-CPM mutant receptor was 10- to 30-fold less sensitive than the wild-type or TM control receptors. However, in response to the low-affinity P255A peptide, the α-CPM mutant receptor was strikingly unresponsive. Compared with the wild-type receptor, the α-CPM mutant TCR was at least 10,000-fold less responsive to this low-affinity ligand. Therefore, we conclude that the α-CPM is of particular importance in mediating TCR/CD8 cooperation in functional responses to weak ligands.

Discussion

To generate a functional T cell repertoire, αβ thymocytes expressing self-MHC-restricted TCRs survive and differentiate (positive selection), while thymocytes, whose receptors are self-MHC reactive, undergo apoptosis (negative selection) (43–47). Although thymocytes can discriminate between different antigenic ligands, which induce positive or negative selection, the mechanisms by which the TCR couples ligand binding to distinct cellular responses are still unclear.

We have previously identified a highly conserved motif in the constant region of the TCRα chain, α-CPM, which is required for the positive selection of thymocytes (24). Thymocytes expressing α-CPM mutant TCRs have specific signaling defects in responses to positive-selecting ligands, while their responses to negative-selecting ligands are unaffected (25). While it seems that the α-CPM

plays an important role in generating positive selection signals, how the α-CPM functions is still unclear.

To further characterize the defects observed with α-CPM mutant receptors, we used a hybridoma cell line that expressed a wild-type or α-CPM mutant form of the T1 TCR, in either the presence or the absence of the CD8 coreceptor. Because the α-CPM mutant and wild-type TCRs differ in their TM and cytoplasmic domains as well, we included the TM control TCR, which provides a direct control for the role of the α-CPM (Fig. 1).

To test whether α-CPM-deficient TCRs bind ligand defectively, we performed photoaffinity labeling studies (29) with the different TCR mutants expressed on hybridoma cell lines. Relative affinities were determined for the strong Ag11.3 ligand at 0°C and at 37°C, and for the weak P255A ligand at 0°C. Two major observations were made. First, there was no obvious (TCR-intrinsic) ligand binding defect observed with α-CPM mutant receptors when assessed on $CD8^-$ hybridomas (Fig. 3, *B–D*, open bars). Therefore, the α-CPM mutation does not decrease ligand binding per se. However, a significant difference in ligand binding was observed with $CD8^+$ hybridomas when comparing wild-type, TM, and α-CPM mutant TCRs (Fig. 3, *B–D*, filled bars). Our results clearly show that the α-CPM mutant TCR has a significant defect in engaging CD8 for ligand binding. Photoaffinity labeling performed with the weak P255A ligand variant showed a similar picture. The inability of CD8 to participate in ligand binding was due to the absence of the α-CPM, because ligand binding to the TM control TCR was comparable to that observed on the wild-type TCR (Fig. 3, *B* and *D*, filled bars). Taken together, these results imply that the α-CPM plays an important role in orchestrating the cooperation between the TCR and CD8, which is required to enhance the binding of both high- and low-affinity ligands.

The functional consequences of defective TCR/CD8 cooperation were also studied using IL-2 assays. Interestingly, CD8 enhanced IL-2 production from α-CPM mutant hybridomas when stimulated with ligands of high (Ag11.3) or medium (P255S) potency. However, no IL-2 production could be detected when hybridomas expressing the α-CPM mutant receptor were stimulated with the weak P255A ligand, not even in the presence of CD8 (Fig. 4*Ah*). Because $CD8^-$ hybridomas expressing the wild-type and TM control receptors showed a substantial IL-2 response to P255A peptide, loading limitations on the APC do not account for the failure of the α-CPM mutant hybridomas to respond.

When the IL-2 responses of $CD8^+$ hybridomas were analyzed for their peptide dose dependency, i.e., receptor sensitivity, similar observations were made. As shown in Fig. 4*B*, α-CPM mutant receptors were 10- to 30-fold less sensitive than wild-type and TM control receptors in response to peptides of high (Ag11.3) or medium (P255S) potencies. Strikingly, the differences mediated by the α-CPM were much more pronounced in the case of the weak P255A peptide. Comparing $CD8^+$ hybridomas, the α-CPM mutant receptor is 3,000- to 10,000-fold less sensitive in the response to P255A than the wild-type and TM control receptors. Furthermore, the wild-type receptor is only 10-fold less sensitive to the low-affinity ligand P255A compared with the medium-affinity ligand P255S. In contrast, the α-CPM mutant receptor is 10,000-fold less sensitive to the low-affinity P255A ligand compared with the medium-affinity P255S ligand. This underscores the particular importance of the α-CPM-mediated TCR/CD8 cooperation in response to weak ligands.

The fact that the functional defect of the α-CPM mutation is so pronounced with low-affinity ligands is surprising, because the binding of both strong (Ag11.3) and weak (P255A) ligands is similarly affected by the absence of the α-CPM (Fig. 3). Previous studies measuring the kinetics of the Ag11.3, the P255S, and the P255A binding to the wild-type T1 TCR showed a clear correlation between their off-rates and their functional potencies (42). Therefore, the high affinity (and slow off-rate) of the Ag11.3 ligand for the T1 TCR might compensate for the poor TCR/CD8 cooperation observed with the α-CPM mutant receptor. In this context, high-affinity pMHC ligands tend to be more CD8 independent. In contrast, the reduced TCR/CD8 cooperativity observed with the α-CPM mutant receptors has a catastrophic effect on weak ligands, which are more dependent on CD8 assistance to initiate intracellular signaling cascades. These observations are reminiscent of the phenotype displayed by thymocytes expressing α-CPM mutant TCRs. These mutant thymocytes cannot undergo positive selection and are specifically unresponsive to low-affinity ligands (25).

Although the precise mechanism responsible for mediating TCR/CD8 cooperation is not known, we propose a model in which the CD8αβ molecules are recruited to the TCR complex by the α-CPM. Support for such a model comes from crystallographic studies of many murine and human TCR-pMHC complexes, which show a conserved orientation of the pMHC over the TCR, placing the MHC coreceptor binding site over the α-chain side of the TCR (34, 48–53). Furthermore, certain Vα domains show a preference for selection into the CD4 or CD8 subset of mature T cells (54). This could be explained by a preference of certain Vα domains to physically interact with CD4 or CD8. Such an arrangement would likely recruit the membrane proximal domain of the coreceptor to the α-chain constant region, an event that requires an intact α-CPM.

Thymocytes from CD8β knockout mice were specifically blocked in undergoing positive selection (9, 15, 18, 55), which emphasizes the critical role played by the coreceptor in responding to weak ligands. While studies by Bosselut et al. (21) have clearly shown that the extracellular, TM, and cytoplasmic domains of CD8β contribute to its ability to support positive selection, little is known about the structural elements of the TCR, which mediate the engagement between the receptor and the coreceptor. The studies presented in this work suggest that the α-CPM is an important structural element mediating TCR/CD8 cooperation.

Whether the association of the CD8 coreceptor to the TCR is mediated by a direct interaction of CD8 with the α-CPM has not yet been ruled out. Because proper association of CD3δ to the TCRα chain also requires the α-CPM (24, 25), CD3δ may associate with the coreceptor as well. Consistent with this idea is the observation that thymocytes from CD3δ-deficient mice cannot undergo positive selection (27, 28).

These studies provide evidence that the α-CPM plays an important role in mediating TCR/CD8 cooperativity. Although not considered in these studies, a similar role might be played by the α-CPM in case of cooperation with the CD4 coreceptor, because the α-CPM mutation blocks the positive selection of a class II MHC-restricted TCR as well (24). The precise mechanism by which the cooperation between the TCR and its coreceptor allows a "reading" of ligand affinity and to what extent this controls the decisions taken during positive and negative selection require additional work.

Acknowledgments

We thank T. Potter for the APC line T2-K^d, S. Stotz for the 58 hybridoma line expressing CD8αβ, and Ramona Leibnitz for some of the cDNA constructs. We are grateful to T. Hayden, H. Kohler, and M. Dessing for flow cytometric support. We also thank J. Gatfield, E. Meier, and G. Werlen for valuable discussion and J. Gatfield, B. Hausmann, and G. Werlen for reviewing the manuscript.

References

1. Hogquist, K. A., S. C. Jameson, W. R. Heath, J. L. Howard, M. J. Bevan, and F. R. Carbone. 1994. T cell receptor antagonist peptides induce positive selection. *Cell 76:17.*

2. Alam, S. M., P. J. Travers, J. L. Wung, W. Nasholds, S. Redpath, S. C. Jameson, and N. R. Gascoigne. 1996. T-cell-receptor affinity and thymocyte positive selection. *Nature 381:616*.
3. Alam, S. M., G. M. Davies, C. M. Lin, T. Zal, W. Nasholds, S. C. Jameson, K. A. Hogquist, N. R. Gascoigne, and P. J. Travers. 1999. Qualitative and quantitative differences in T cell receptor binding of agonist and antagonist ligands. *Immunity 10:227*.
4. Konig, R., L. Y. Huang, and R. N. Germain. 1992. MHC class II interaction with CD4 mediated by a region analogous to the MHC class I binding site for CD8. *Nature 356:796*.
5. Luescher, I. F., E. Vivier, A. Layer, J. Mahiou, F. Godeau, B. Malissen, and P. Romero. 1995. CD8 modulation of T-cell antigen receptor-ligand interactions on living cytotoxic T lymphocytes. *Nature 373:353*.
6. Garcia, K. C., C. A. Scott, A. Brunmark, F. R. Carbone, P. A. Peterson, I. A. Wilson, and L. Teyton. 1996. CD8 enhances formation of stable T-cell receptor/MHC class I molecule complexes. *Nature 384:577*.
7. Hampl, J., Y. H. Chien, and M. M. Davis. 1997. CD4 augments the response of a T cell to agonist but not to antagonist ligands. *Immunity 7:379*.
8. Connolly, J. M., T. H. Hansen, A. L. Ingold, and T. A. Potter. 1990. Recognition by CD8 on cytotoxic T lymphocytes is ablated by several substitutions in the class I α_3 domain: CD8 and the T-cell receptor recognize the same class I molecule. *Proc. Natl. Acad. Sci. USA 87:2137*.
9. Itano, A., D. Cado, F. K. Chan, and E. Robey. 1994. A role for the cytoplasmic tail of the β chain of CD8 in thymic selection. *Immunity 1:287*.
10. Hernandez-Hoyos, G., S. J. Sohn, E. V. Rothenberg, and J. Alberola-Ila. 2000. Lck activity controls CD4/CD8 T cell lineage commitment. *Immunity 12:313*.
11. Legname, G., B. Seddon, M. Lovatt, P. Tomlinson, N. Sarner, M. Tolaini, K. Williams, T. Norton, D. Kioussis, and R. Zamoyska. 2000. Inducible expression of a $p56^{Lck}$ transgene reveals a central role for Lck in the differentiation of CD4 SP thymocytes. *Immunity 12:537*.
12. Trobridge, P. A., K. A. Forbush, and S. D. Levin. 2001. Positive and negative selection of thymocytes depends on Lck interaction with the CD4 and CD8 coreceptors. *J. Immunol. 166:809*.
13. Killeen, N., A. Moriarty, H. S. Teh, and D. R. Littman. 1992. Requirement for CD8-major histocompatibility complex class I interaction in positive and negative selection of developing T cells. *J. Exp. Med. 176:89*.
14. Ingold, A. L., C. Landel, C. Knall, G. A. Evans, and T. A. Potter. 1991. Coengagement of CD8 with the T cell receptor is required for negative selection. *Nature 352:721*.
15. Nakayama, K., I. Negishi, K. Kuida, M. C. Louie, O. Kanagawa, H. Nakauchi, and D. Y. Loh. 1994. Requirement for CD8 β chain in positive selection of CD8-lineage T cells. *Science 263:1131*.
16. Sebzda, E., M. Choi, W. P. Fung-Leung, T. W. Mak, and P. S. Ohashi. 1997. Peptide-induced positive selection of TCR transgenic thymocytes in a coreceptor-independent manner. *Immunity 6:643*.
17. Goldrath, A. W., K. A. Hogquist, and M. J. Bevan. 1997. CD8 lineage commitment in the absence of CD8. *Immunity 6:633*.
18. Fung-Leung, W. P., V. A. Wallace, D. Gray, W. C. Sha, H. Pircher, H. S. Teh, D. Y. Loh, and T. W. Mak. 1993. CD8 is needed for positive selection but differentially required for negative selection of T cells during thymic ontogeny. *Eur. J. Immunol. 23:212*.
19. Veillette, A., J. C. Zuniga-Pflucker, J. B. Bolen, and A. M. Kruisbeek. 1989. Engagement of CD4 and CD8 expressed on immature thymocytes induces activation of intracellular tyrosine phosphorylation pathways. *J. Exp. Med. 170:1671*.
20. Thome, M., P. Duplay, M. Guttinger, and O. Acuto. 1995. Syk and ZAP-70 mediate recruitment of $p56^{lck}$/CD4 to the activated T cell receptor/CD3/ζ complex. *J. Exp. Med. 181:1997*.
21. Bosselut, R., S. Kubo, T. Guinter, J. L. Kopacz, J. D. Altman, L. Feigenbaum, and A. Singer. 2000. Role of CD8β domains in CD8 coreceptor function: importance for MHC I binding, signaling, and positive selection of $CD8^+$ T cells in the thymus. *Immunity 12:409*.
22. Barber, E. K., J. D. Dasgupta, S. F. Schlossman, J. M. Trevillyan, and C. E. Rudd. 1989. The CD4 and CD8 antigens are coupled to a protein-tyrosine kinase ($p56^{lck}$) that phosphorylates the CD3 complex. *Proc. Natl. Acad. Sci. USA 86: 3277*.
23. Backstrom, B. T., E. Milia, A. Peter, B. Jaureguiberry, C. T. Baldari, and E. Palmer. 1996. A motif within the T cell receptor α chain constant region connecting peptide domain controls antigen responsiveness. *Immunity 5:437*.
24. Backstrom, B. T., U. Muller, B. Hausmann, and E. Palmer. 1998. Positive selection through a motif in the $\alpha\beta$ T cell receptor. *Science 281:835*.
25. Werlen, G., B. Hausmann, and E. Palmer. 2000. A motif in the $\alpha\beta$ T-cell receptor controls positive selection by modulating ERK activity. *Nature 406:422*.
26. Ulivieri, C., A. Peter, E. Orsini, E. Palmer, and C. T. Baldari. 2001. Defective signaling to Fyn by a T cell antigen receptor lacking the α-chain connecting peptide motif. *J. Biol. Chem. 276:3574*.
27. Dave, V. P., Z. Cao, C. Browne, B. Alarcon, G. Fernandez-Miguel, J. Lafaille, A. de la Hera, S. Tonegawa, and D. J. Kappes. 1997. CD3δ deficiency arrests development of the $\alpha\beta$ but not the $\gamma\delta$ T cell lineage. *EMBO J. 16:1360*.
28. Delgado, P., E. Fernandez, V. Dave, D. Kappes, and B. Alarcon. 2000. CD3δ couples T-cell receptor signalling to ERK activation and thymocyte positive selection. *Nature 406:426*.
29. Luescher, I. F., J. C. Cerottini, and P. Romero. 1994. Photoaffinity labeling of the T cell receptor on cloned cytotoxic T lymphocytes by covalent photoreactive ligand. *J. Biol. Chem. 269:5574*.
30. Luescher, I. F., F. Anjuere, M. C. Peitsch, C. V. Jongeneel, J. C. Cerottini, and P. Romero. 1995. Structural analysis of TCR-ligand interactions studied on $H\text{-}2K^d$-restricted cloned CTL specific for a photoreactive peptide derivative. *Immunity 3:51*.
31. Miller, A. D., and G. J. Rosman. 1989. Improved retroviral vectors for gene transfer and expression. *BioTechniques 7:980*.
32. Morgenstern, J. P., and H. Land. 1990. Advanced mammalian gene transfer: high titre retroviral vectors with multiple drug selection markers and a complementary helper-free packaging cell line. *Nucleic Acids Res. 18:3587*.
33. Mullen, C. A., M. Kilstrup, and R. M. Blaese. 1992. Transfer of the bacterial gene for cytosine deaminase to mammalian cells confers lethal sensitivity to 5-fluorocytosine: a negative selection system. *Proc. Natl. Acad. Sci. USA 89:33*.
34. DiGiusto, D. L., and E. Palmer. 1994. An analysis of sequence variation in the β chain framework and complementarity determining regions of an allo-reactive T cell receptor. *Mol. Immunol. 31:693*.
35. Letourneur, F., and B. Malissen. 1989. Derivation of a T cell hybridoma variant deprived of functional T cell receptor α and β chain transcripts reveals a nonfunctional α-mRNA of BW5147 origin. *Eur. J. Immunol. 19:2269*.
36. Stotz, S. H., L. Bolliger, F. R. Carbone, and E. Palmer. 1999. T cell receptor (TCR) antagonism without a negative signal: evidence from T cell hybridomas expressing two independent TCRs. *J. Exp. Med. 189:253*.
37. Watson, J. 1979. Continuous proliferation of murine antigen-specific helper T lymphocytes in culture. *J. Exp. Med. 150:1510*.
38. Bill, J., O. Kanagawa, J. Linten, Y. Utsunomiya, and E. Palmer. 1990. Class I and class II MHC gene products differentially affect the fate of Vβ5 bearing thymocytes. *J. Mol. Cell. Immunol. 4:269*.
39. Kubo, R. T., W. Born, J. W. Kappler, P. Marrack, and M. Pigeon. 1989. Characterization of a monoclonal antibody which detects all murine $\alpha\beta$ T cell receptors. *J. Immunol. 142:2736*.
40. Leo, O., M. Foo, D. H. Sachs, L. E. Samelson, and J. A. Bluestone. 1987. Identification of a monoclonal antibody specific for a murine T3 polypeptide. *Proc. Natl. Acad. Sci. USA 84:1374*.
41. Golstein, P., C. Goridis, A. M. Schmitt-Verhulst, B. Hayot, A. Pierres, A. van Agthoven, Y. Kaufmann, Z. Eshhar, and M. Pierres. 1982. Lymphoid cell surface interaction structures detected using cytolysis-inhibiting monoclonal antibodies. *Immunol. Rev. 68:5*.
42. Hudrisier, D., B. Kessler, S. Valitutti, C. Horvath, J. C. Cerottini, and I. F. Luescher. 1998. The efficiency of antigen recognition by $CD8^+$ CTL clones is determined by the frequency of serial TCR engagement. *J. Immunol. 161:553*.
43. Anderson, G., K. J. Hare, and E. J. Jenkinson. 1999. Positive selection of thymocytes: the long and winding road. *Immunol. Today 20:463*.
44. Goldrath, A. W., and M. J. Bevan. 1999. Selecting and maintaining a diverse T-cell repertoire. *Nature 402:255*.
45. Mariathasan, S., R. G. Jones, and P. S. Ohashi. 1999. Signals involved in thymocyte positive and negative selection. *Semin. Immunol. 11:263*.
46. Kishimoto, H., and J. Sprent. 2000. The thymus and negative selection. *Immunol. Res. 21:315*.
47. Sprent, J., and H. Kishimoto. 2001. The thymus and central tolerance. *Philos. Trans. R. Soc. Lond. B 356:609*.
48. Speir, J. A., K. C. Garcia, A. Brunmark, M. Degano, P. A. Peterson, L. Teyton, and I. A. Wilson. 1998. Structural basis of 2C TCR allorecognition of $H\text{-}2L^d$ peptide complexes. *Immunity 8:553*.
49. Teng, M. K., A. Smolyar, A. G. Tse, J. H. Liu, J. Liu, R. E. Hussey, S. G. Nathenson, H. C. Chang, E. L. Reinherz, and J. H. Wang. 1998. Identification of a common docking topology with substantial variation among different TCR-peptide-MHC complexes. *Curr. Biol. 8:409*.
50. Garboczi, D. N., P. Ghosh, U. Utz, Q. R. Fan, W. E. Biddison, and D. C. Wiley. 1996. Structure of the complex between human T-cell receptor, viral peptide and HLA-A2. *Nature 384:134*.
51. Garcia, K. C., M. Degano, R. L. Stanfield, A. Brunmark, M. R. Jackson, P. A. Peterson, L. Teyton, and I. A. Wilson. 1996. An $\alpha\beta$ T cell receptor structure at 2.5 A and its orientation in the TCR-MHC complex. *Science 274:209*.
52. Garcia, K. C., M. Degano, L. R. Pease, M. Huang, P. A. Peterson, L. Teyton, and I. A. Wilson. 1998. Structural basis of plasticity in T cell receptor recognition of a self peptide-MHC antigen. *Science 279:1166*.
53. Sun, R., S. E. Shepherd, S. S. Geier, C. T. Thomson, J. M. Sheil, and S. G. Nathenson. 1995. Evidence that the antigen receptors of cytotoxic T lymphocytes interact with a common recognition pattern on the $H\text{-}2K^b$ molecule. *Immunity 3:573*.
54. Sim, B. C., L. Zerva, M. I. Greene, and N. R. Gascoigne. 1996. Control of MHC restriction by TCR Vα CDR1 and CDR2. *Science 273:963*.
55. Crooks, M. E., and D. R. Littman. 1994. Disruption of T lymphocyte positive and negative selection in mice lacking the CD8 β chain. *Immunity 1:277*.

3.2.5 Summary of the Published Results

Three major findings were described in this paper. First, the bimolecular TCR-pMHC binding was not altered by replacement of the α-CPM. Second, replacement of the α-CPM led to reduced CD8 cooperativity in TCR/CD8-pMHC binding. Third, the decreased CD8 cooperativity observed with α-CPM mutant TCRs was similar for the strong I-Ag11.3-K^d and the weak I-P255A-K^d monomers. On the other hand, the functional deficiencies observed with α-CPM mutant TCRs were much more pronounced with weak ligands than with strong ligands. Therefore the functional defects observed in the Il-2 assays performed with hybridomas expressing α-CPM mutant T1-TCRs could not be completely explained by a simple decrease in the binding of weak ligands. Due to limitations in the production of radioactively labeled ligands, the maximal ligand concentration used was $5x10^{-10}$ M. As described for the T1 mice, these concentrations were far too low for TCR saturation and hence determinations of the dissociation constants (K_Ds) could not be achieved. Moreover, despite the similarities in the functional defects observed with the hybridomas expressing α-CPM mutant T1-TCRs and previously published observations of transgenic mice expressing α-CPM mutant TCRs, it could not be predicted to what degree the observations made on hybridomas reflected the features of developing thymoyctes. To circumvent these limitations, transgenic mice were produced which expressed the three different T1-TCR variants.

3.2.6 WT, α-CPM Mutant or TM control T1-TCR Transgenic Mice

Transgenic mice expressing the three different T1-TCRs were produced as described above (see Results 3.1.1). Figure 3.18A shows the flow-cytometric analysis of the thymocytes from wildtype, α-CPM mutant and transmembrane (TM) control T1; $Rag^{-/-}$ mice. As previously described for transgenic mice expressing α-CPM mutant TCRs with various specificities (Backstrom et al., 1998; Werlen et al., 2000) only very few SP thymocytes were observed in α-CPM mutant T1; $Rag^{-/-}$ mice. On the other hand, TM control mice did not show any reduction in their number of SP thymocytes compared to wildtype mice, attesting that the lack of SP thymocytes observed in α-CPM mutant mice was due to the absence of the α-CPM rather than the replacement of the transmembrane and cytosolic portions of the TCRα/β constant regions. Moreover the number of lymph node T cells ($6x10^6 \pm 3x10^6$) was similar for wildtype and TM control mice, while very few peripheral T cells were detected in the α-CPM mutant mice (data not shown). TCR and CD8α/β expression levels on DP thymocytes were similar in all three mouse lines studied as shown in Figure 3.18B. In the case

of the wildtype and the TM control T1; Rag$^{-/-}$ mice, where SP thymocytes and lymph node T cells could be analyzed, no significant differences in the TCR nor the CD8α/β expression levels were observed.

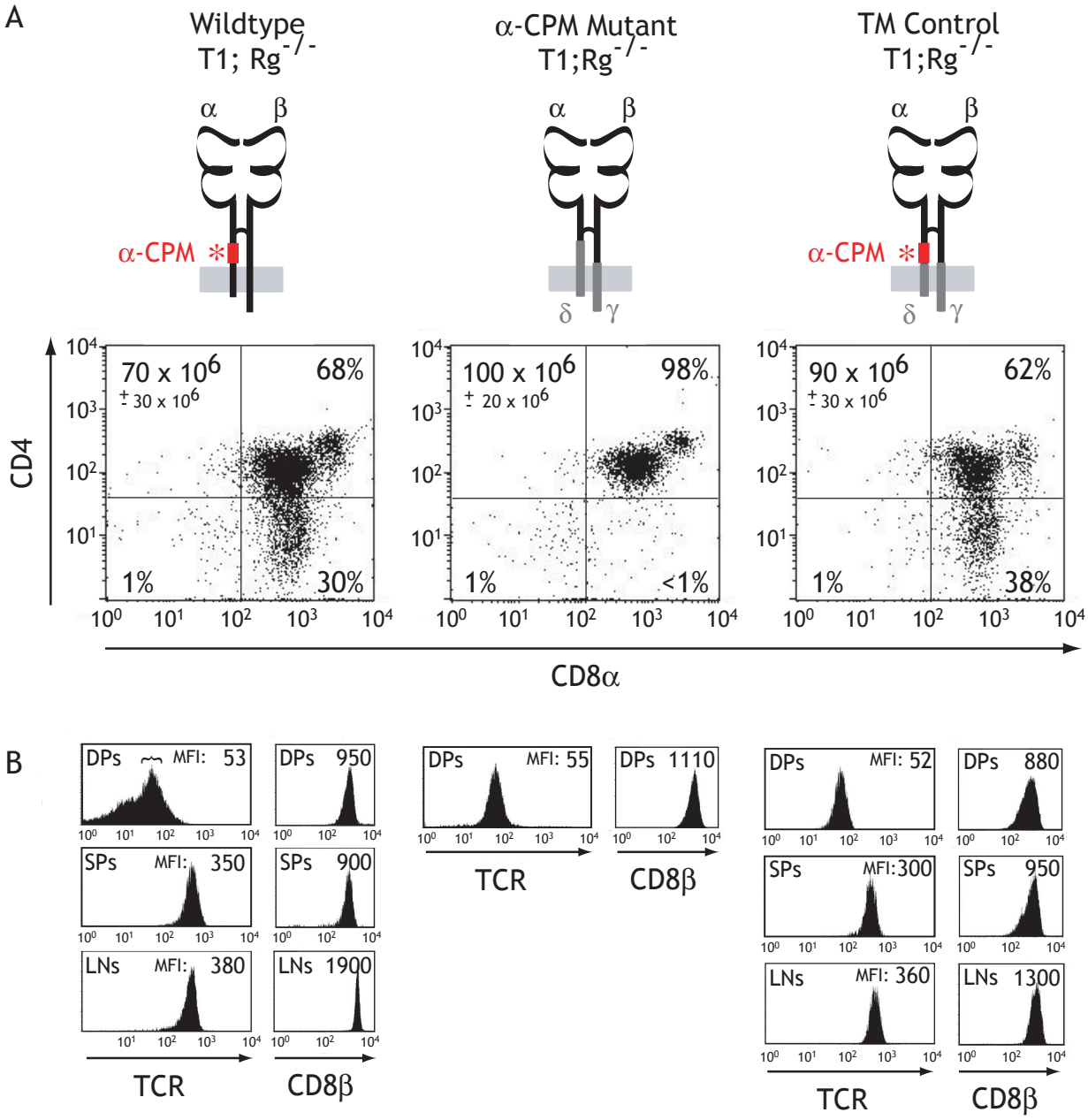

Figure 3.18: Flow cytometric analysis of thymocytes and lymph node cells from mice expressing either wildtype, α-CPM mutant or TM control T1-TCR. Thymocytes and lymph node cells from 6 to 8 weak old Balb/c;Rag$^{-/-}$ mice, which were either transgenic for the wildtype, the α-CPM mutant or the TM control T1-TCR were isolated and stained with fluorescence labeled α-CD4(RM4-5), α-CD8α(53-6.7), α-CD8β(53-5.8), α-TCRβ(H57-597). (A) CD4 and CD8α cell surface expression measured on thymocytes of mice expressing the T1 variants. Numbers in the upper left corner of each panel indicate total cell number of thymocytes per animal (SED indicated; n=3). Thymocytes were electronically gated and the percentages of double negative (DN), single positive (SP) and double positive (DP) determined. (B) Mean fluorescence intensities of TCRβ and CD8β were determined on DPs, SPs and lymph node T cells (LN) from each strain. MFI of TCR levels on DP thymocytes from wildtype T1 mice was determined for TCR^{intermediate} cells (upper left panel indicated by bracket).

3.2.7 Reduced Responsiveness of α-CPM Mutant Thymocytes

To analyze the functional differences between wildtype, α-CPM mutant and TM control thymocytes, CD69 upregulation assays were performed. As described in Section 3.1.3 these experiments were evaluated by plotting the percentage of cells undergoing CD69 upregulation as a function of peptide concentration. In the case of the DP thymocytes derived from wildtype mice, only 80% of all cells expressed T1-TCRs on the cell surface and therefore the maximal percentage of DP cells undergoing peptide specific CD69 upregulation was 80% in the case of the wildtype mice, while it was 100% in the case of the α-CPM mutant or the TM control mice. Figure 3.19 shows the dose response curves representing the cell surface expression of CD69 observed on thymocytes of the three different mouse lines tested. The responses to the 4L, 4P, 4A, 4S and 4N peptides characterized in Results 3.1.2 were analyzed. As indicated in Panels I, III, IV and V, very similar dose dependent CD69 upregulation was observed on DP thymocytes of wildtype and TM control mice. In contrast, the DP thymocytes of α-CPM mutant mice (Panel II) appeared to be dramatically less responsive to the weak 4A, 4S and 4N ligands, while the strong 4P and 4L ligands gave comparable levels of CD69 upregulation as observed for wildtype and TM control DP thymocytes. Indeed for the 4S and the 4N ligands, only a fraction of the α-CPM mutant thymocytes upregulated CD69, even at high peptide doses. Therefore the dose response curves of these peptides appeared to plateau at much lower percentages of $CD69^+$ cells (~40%) than in the case of the strong 4L and 4P peptides (100%). Therefore DP thymocytes of α-CPM mutant T1; $Rag^{-/-}$ mice showed defective CD69 upregulation compared to wildtype and TM mutant mice which was most prominent with weak ligands. This observation made with the α-CPM mutant T1; $Rg^{-/-}$ mice was in accordance with previous studies which similarly reported a specific defect in the response to weak ligands when cells expressing an α-CPM mutant TCR were analyzed (Werlen et al. 2000; Naeher et al., 2002). In contrast, the percentage of DP thymocytes upregulating CD69 was very similar for wildtype and TM control mice in response to all peptides tested.

In the case of the wildtype and TM control mice CD69 upregulation was also studied on SP thymocytes. Very similar dose response curves were observed for the 4L, 4P, 4A and 4S peptides underlining functional similarity of the wildtype and the TM control receptors. However, when the percentage of SP thymocytes upregulating CD69 in response to the 4N peptide was analyzed a slightly reduced maximum in the percentage of responding cells was observed in TM control mice (70%) compared to wildtype mice (90%). Panels VI, VII and VIII illustrate the results obtained from CD69 upregulation assays in the presence of the α-H-$2K^d$(α3) mAb SF1-1.1. This antibody blocks the CD8 binding site on H-$2K^d$ molecules

and hence allows one to study the impact of the CD8-pMHC interaction on the functional responses. Blocking the binding site for CD8 on the pMHC molecules of the APCs led to distinct results concerning the CD69 upregulation in response to weak or strong peptides. The responses to weak peptides (blue curves) were much more affected by the presence of the blocking antibody than responses to strong peptides (red curves). Considering the wildtype and TM control DP thymocytes, the responses to the weak ligands (4A, 4S and 4N) were dramatically inhibited by blocking CD8. On the other hand, the responses to the strong ligands, 4L and 4P were only modestly reduced by this blocking mAb. This pattern was even more pronounced with DP thymocytes expressing the α-CPM mutant receptor. The response to strong ligands was modestly inhibited, while the response to weak ligands was eliminated (Panel VII). It is interesting that the peptide responses of wildtype and TM control thymocytes in the presence of the CD8 blocking mAb were very similar to the peptide responses of α-CPM mutant thymocytes in the absence of this mAb (Panels VI and VIII compared to Panel II in Fig. 3.19). This implied that α-CPM mutant thymocytes might suffer from a disturbed TCR-CD8 cooperativity in ligand binding. To compare these differences in a more quantitative way, the EC_{50} values representing the sensitivity of cells for a given ligand were determined. Table VI summarizes the EC_{50} values determined for the five different peptides tested on thymocytes of wildtype, α-CPM mutant and TM control mice. The EC_{50} values represent the peptide concentrations at which 50% of the responding cells upregulated CD69. In those cases where the maximal percentage of cells responding was reduced the EC_{50} value potentially overestimated the sensitivity of the cells; these values are therefore marked with an asterisk. As described above (see Results 3.1.4 and Table II), the EC_{50} values were higher for SP thymocytes than for DP thymocytes reflecting the sensitivity drop generally observed between these two stages of thymocyte development. This sensitivity drop was more pronounced with weak 4S and 4N peptides and correlated with the CD8 dependence of the thymocyte sensitivity for the various peptides, as shown by the increased EC_{50} values determined in the presence of the SF1-1.1 antibody. Importantly, the EC_{50} values observed on DP and SP thymocytes of TM control mice were equivalent to those determined on wildtype DP and SP thymocytes. In contrast, the sensitivities of α-CPM DP thymocytes were lower for all peptides tested compared to wildtype and TM control mice and the biggest differences were observed for the intermediate (4A) and the weak (4S and 4N) peptides tested.

Table VII shows a direct comparison of EC_{50} values obtained from TM control and α-CPM mutant thymocytes. While the EC_{50} values of the α-CPM mutant DP thymocytes were 8-fold higher for the 4L peptide and 17-fold higher for the 4P peptide compared to wildtype or

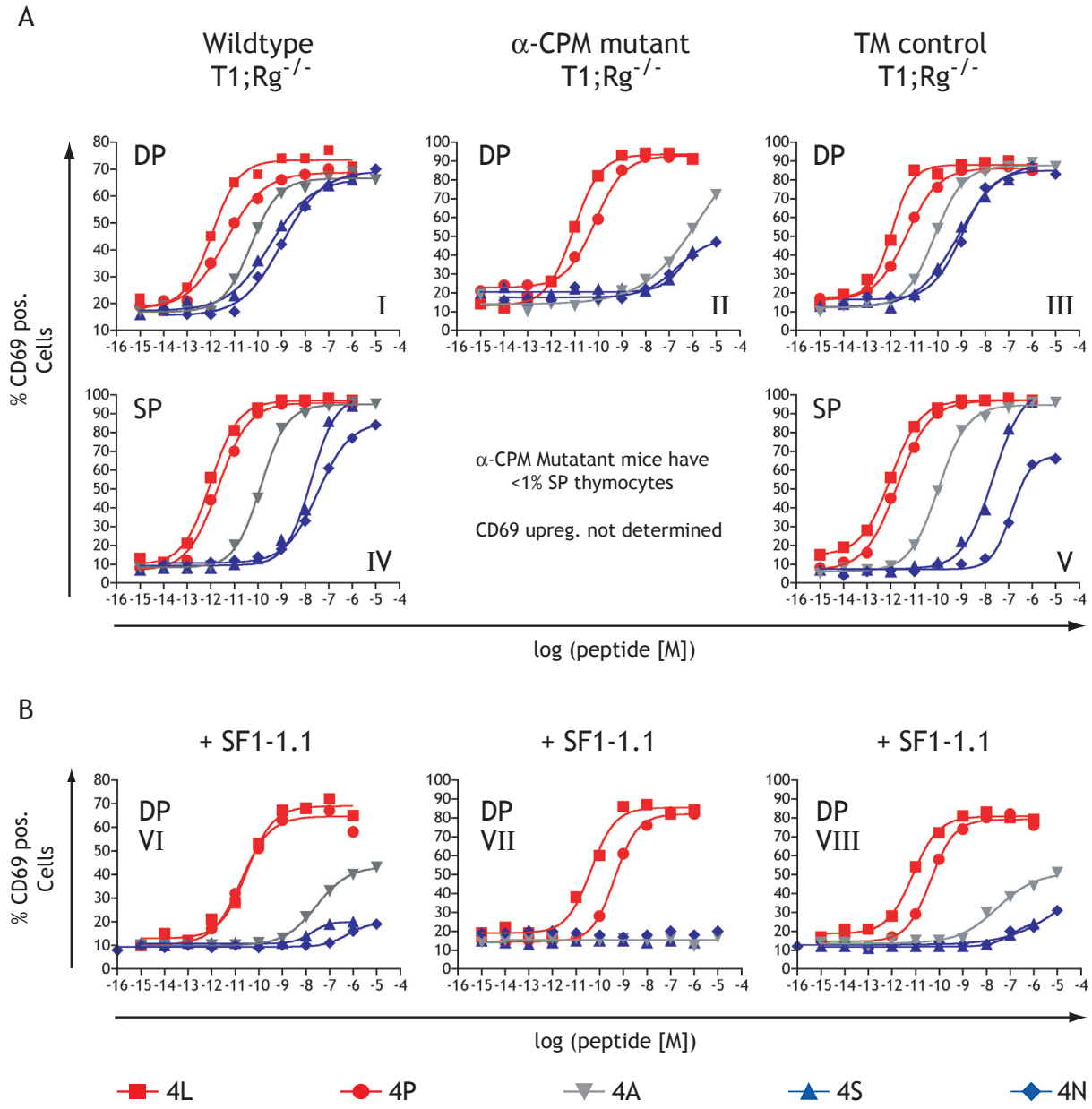

Figure 3.19: Peptide dose dependent CD69 upregulation on thymocytes from wildtype, α-CPM mutant or TM control T1 thymocytes. Thymocytes from wildtype, α-CPM mutant or TM control mice were stimulated for 18 hrs. with various doses of 4L(■), 4P(●), 4A(▼), 4S(▲) or 4N(◆) peptides presented on T2-K^d cells in the presence or absence of α-H-$2K^d$(SF1-1.1) (20μg/ml) and subsequently stained with fluorescence labeled α-CD4(RM4-5), α-CD8α(53-6.7), α-CD69(H1.2F3) mAbs. Percentage of DP and SP thymocytes of the three mouse strains were analyzed. (A) Percentages of DP thymocytes and SP thymocytes expressing surface CD69, in the absence of α-H-$2K^d$(α3)(SF1-1.1) mAb. (B) Percentages of DP thymocytes and SP thymocytes expressing surface CD69, stimulated in the presence of α-H-$2K^d$(α3)(SF1-1.1) mAb. A representative experiment from a total of at least two independent experiments is shown.

TM control thymocytes, the EC_{50} values of the α-CPM mutant thymocytes for the 4A peptide were more than 17000-fold higher compared to wildtype and TM control thymocytes. For the even weaker 4S and 4N peptides this differences in sensitivity could not accurately be quantified due to the fact that only very few thymocytes from α-CPM mutant mice up-

Table VI: EC_{50} values [M] determined for wildtype, α-CPM mutant or TM control T1 thymocytes.

Strain: Cell type; mAb	Peptides				
	4L	4P	4A	4S	4N
A. Wildtype					
DP	1.2×10^{-12}	3.1×10^{-12}	5.2×10^{-11}	3.3×10^{-10}	1.1×10^{-9}
SP	1.0×10^{-12}	4.3×10^{-12}	1.3×10^{-10}	$1.8 \times 10^{-8*}$	$3.6 \times 10^{-8*}$
DP + SF1-1.1 mAb	3.0×10^{-11}	1.8×10^{-11}	$2.8 \times 10^{-8*}$	$1.7 \times 10^{-8*}$	$5.4 \times 10^{-7*}$
B. α-CPM mutant					
DP	9.0×10^{-12}	7.4×10^{-11}	$>9.0 \times 10^{-7}$	$5.0 \times 10^{-7*}$	$2.3 \times 10^{-7*}$
SP	not done	not done	not done	not done	not done
DP + SF1-1.1 mAb	4.3×10^{-11}	4.4×10^{-10}	$>1.0 \times 10^{-4*}$	$>1.0 \times 10^{-4*}$	$>1.0 \times 10^{-4*}$
C. TM control					
DP	1.2×10^{-12}	4.3×10^{-12}	5.2×10^{-11}	3.3×10^{-10}	1.1×10^{-9}
SP	1.0×10^{-12}	2.1×10^{-12}	1.3×10^{-10}	1.8×10^{-8}	$3.6 \times 10^{-8*}$
DP + SF1-1.1 mAb	3.0×10^{-11}	1.8×10^{-11}	$2.8 \times 10^{-8*}$	$1.7 \times 10^{-8*}$	$>5.0 \times 10^{-7}$

Mean values of at least two experiments are shown. (*) less than 50% of all cells responded.

Table VII: α-CPM mediated differences in EC_{50} values [M] of DP T1 thymocytes.

Strain; Cell type	Peptides				
	4L	4P	4A	4S	4N
TM control; DP	1.2×10^{-12}	4.3×10^{-12}	5.2×10^{-11}	3.3×10^{-10}	1.1×10^{-9}
α-CPM mutant; DP	9.0×10^{-12}	7.4×10^{-11}	8.9×10^{-7}	$5.0 \times 10^{-7*}$	$2.3 \times 10^{-7*}$
ΔEC_{50} ($\pm$ α-CPM)	**8 x**	**17 x**	**>17000 x**	**>>1400 x**	**>200 x**

Mean values of at least two experiments are shown. (*) less than 50% of all cells responded

regulated CD69 at all and therefore the EC_{50} values for these peptides were substantially overestimating the responsiveness of the cells. The developmental consequences of these differences were tested using FTOCs.

3.2.8 Wildtype, α-CPM Mutant and TM Control T1; $Rag^{-/-}$; $\beta2m^{-/-}$ Mice

The three different T1; $Rag^{-/-}$ mouse lines were backcrossed onto β2m deficient B10D2; $Rag^{-/-}$; $\beta2m^{-/-}$ mice. As previously described, absence of the β2m protein abolished the class I MHC expression in these mice and led to an arrest of thymocyte development at the DP stage (prior to positive and negative selection). Figure 3.20 shows the CD4, CD8 and TCR expression profiles of thymocytes from wildtype, α-CPM mutant and TM control T1; $Rag^{-/-}$; $\beta2m^{-/-}$ mice measured by flow-cytometry. The dot plots show that a majority of thymocytes were DP due to the developmental block resulting from the lack of MHC class I expression.

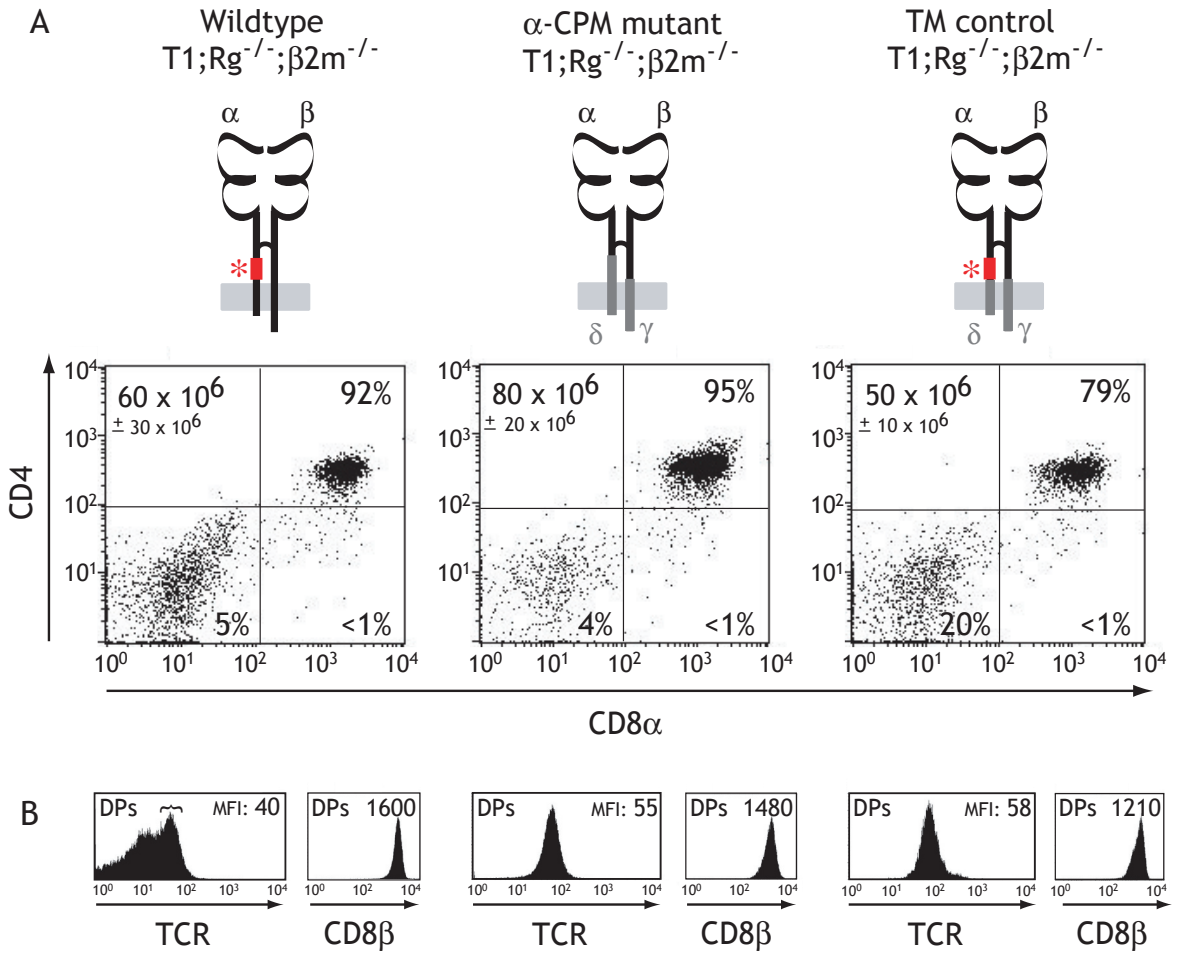

Figure 3.20: Flow cytometric analysis of thymocytes from B10.D2; $Rag^{-/-}$; $\beta2m^{-/-}$ mice expressing either wildtype, α-CPM mutant or TM control T1-TCR. Thymocytes and lymph node cells from 6 to 8 week old B10.D2; $Rag^{-/-}$; $\beta2m^{-/-}$ mice which were either transgenic for the wildtype, the α-CPM mutant or the TM control T1 TCR were isolated and stained with fluorescence labeled α-CD4(RM4-5), α-CD8α(53-6.7), α-CD8β(53-5.8), α-TCR(H57-597) mAbs. (A) CD4 and CD8α cell surface expression measured on thymocytes of the mice expressing the T1 variants. Numbers in the upper left corner of each panel indicate total cell number of thymocytes per animal (SED indicated; n=3). The percentages of double negative (DN), single positive (SP) and double positive (DP) thymocytes were determined. (B) Expression levels of TCRβ and CD8β on DP thymocytes. MFI of TCR levels on DP thymocytes from wildtype T1-TCR; $Rag^{-/-}$; $\beta2m^{-/-}$ mice was determined for $TCR^{intermediate}$ cells (left panel, bracket).

The number of SP thymocytes in wildtype and TM control mice was dramatically reduced due to the absence of positive selection in these $\beta 2m^{-/-}$ mice (Fig. 3.20A). Interestingly, thymocytes of TM control T1; $Rag^{-/-}$; $\beta 2m^{-/-}$ mice had increased levels of DN cells compared to wildtype and α-CPM mutant mice. Dependent on the age of the mice, the percentage of DN cells varied considerably, being higher in young mice (2-5 week old) and decreasing with time. In 6 weak old TM control T1; $Rag^{-/-}$; $\beta 2m^{-/-}$ mice ~20% of all thymocytes were DN (Figure 3.20A, right panel).

The T1-TCR expression levels (Fig. 3.20B) were similar to the TCR expression levels observed with T1; $Rag^{-/-}$ mice (Fig. 3.18B). Similar to T1;$Rag^{-/-}$ mice, not all DP thymocytes from wildtype T1; $Rag^{-/-}$; $\beta 2m^{-/-}$ mice expressed the TCR. Nevertheless ~60% of all T1; $Rag^{-/-}$; $\beta 2m^{-/-}$ DP thymocytes expressed the T1-TCR at levels comparable to the α-CPM mutant and the TM control mice (Fig. 3.20B). CD8α and CD8β levels were comparable on all DP thymocytes of the three T1; $Rag^{-/-}$; $\beta 2m^{-/-}$ mouse lines. To study the thymic selection properties of the three different T1-TCR mouse lines wildtype, α-CPM mutant and TM control T1; $Rag^{-/-}$; $\beta 2m^{-/-}$ mice were used to perform FTOCs.

3.2.9 Positive Selection Defect in α−CPM Mutant Mice

Fetal thymic organ cultures (FTOCs) were used to study the role of the α-CPM motif as well as the α/β transmembrane (TM) and cytosolic regions. As described in Section 3.1.13 and shown in Figure 3.21, culturing of fetal thymi from wildtype T1; $Rag^{-/-}$; $\beta 2m^{-/-}$ mice in the presence of exogenous β2m and peptide led to different levels of CD4 and CD8β downregulation indicative for positive or negative selection of the DP thymocytes. FTOCs from mice expressing the wildtype T1 receptor gave different results depending on the peptide used in the culture. The strong peptides, 4L and 4P induced negative selection as evidenced by the predominance of DN thymocytes and the absence of DP and SP thymocytes in FTOCs (Figure 3.21A). The weak peptides, 4S and 4N induced positive selection given the presence of many CD8α/β SP thymocytes and relatively few DN thymocytes. The 4A peptide gives a mixed picture of positive and negative selection. FTOCs incubated with this peptide generated some CD8α/β SP thymocytes but many DN thymocytes as well. For this reason, 4A was considered a transitional selector (see Results 3.1.14). The results for the TM control FTOCs are similar (Figure 3.21C) indicating that the substitution of TM and cytoplasmic domains does not change the relationship of pMHC affinity and the outcome of thymic selection. FTOCs from thymi expressing the α-CPM mutant T1 TCR provided interesting results (Figure 3.21B). The 4P and 4L peptides induced negative selection, similar to wildtype and TM control FTOCs. The weak ligands, 4S and 4N failed to induce positive selection, which was

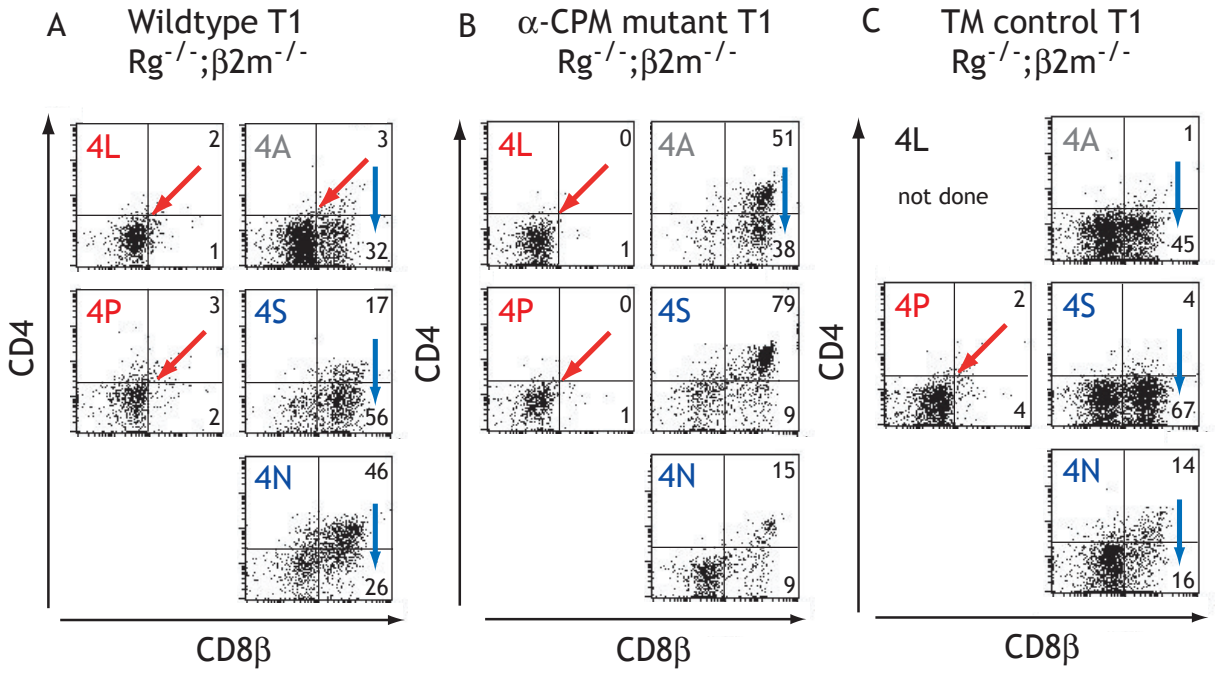

Figure 3.21: α-CPM mutant thymocytes are defective in undergoing positive selection. FTOC were performed with fetal thymi derived from wildtype (A), α-CPM mutant (B) or TM control (C) T1-TCR; $Rag^{-/-}$;$\beta2m^{-/-}$ mice. The percentage of cells in each quadrant are indicated. The 4L (not done for TM control mice) and 4P peptides induced negative selection indicated by the downregulation of CD4 and CD8β (red arrows) after 7 days of FTOC. Positive selection monitored by CD4 downregulation (blue arrow) was observed with wildtype and TM control thymocytes in response to 4A, 4S and 4N, while it was only observed with the 'borderline' 4A peptide when thymocytes from α-CPM mutant mice were tested. α-CPM mutant thymocytes were not positively selected when the 4S and the 4N peptides were used.

expected from an α-CPM mutant receptor. Interestingly, the 4A peptide induced positive selection in α-CPM FTOCs indicating that positive selection can be achieved through an α-CPM mutant receptor, but that a higher affinity ligand is required.

3.2.10 Binding of Strong Ligands to Wildtype and Chimeric T1-TCRs

To directly compare TCR/CD8-pMHC interactions on DP thymocytes of wildtype, α-CPM mutant or TM control T1; $Rg^{-/-}$; $b2m^{-/-}$ mice two step TCR labeling assays (see Section 3.1.7) were performed at 0°C, 24°C and 37°C. The studies included the 4L-K^d, 4P-K^d, 4A-K^d, 4S-K^d and 4N-K^d pMHC monomers which allowed CD8 binding to the α3 domain of the K^d molecules. In addition the 4P-$K^d_{\Delta223/227}$ pMHC monomers were used for which the charge mutations at position 223 and 227 led to abrogated CD8-K^d binding. Figures 3.22 and 3.23 show the two step labeling experiments for each pMHC ligand performed on thymocytes of either wildtype, αCPM mutant or TM control mice. As the TCR ligand binding interactions were shown to be substantially temperature dependent (see Figure 3.9), the ligand binding assays were performed at 0°C, 24°C and 37°C. In the case of the 4P peptide, the experi-

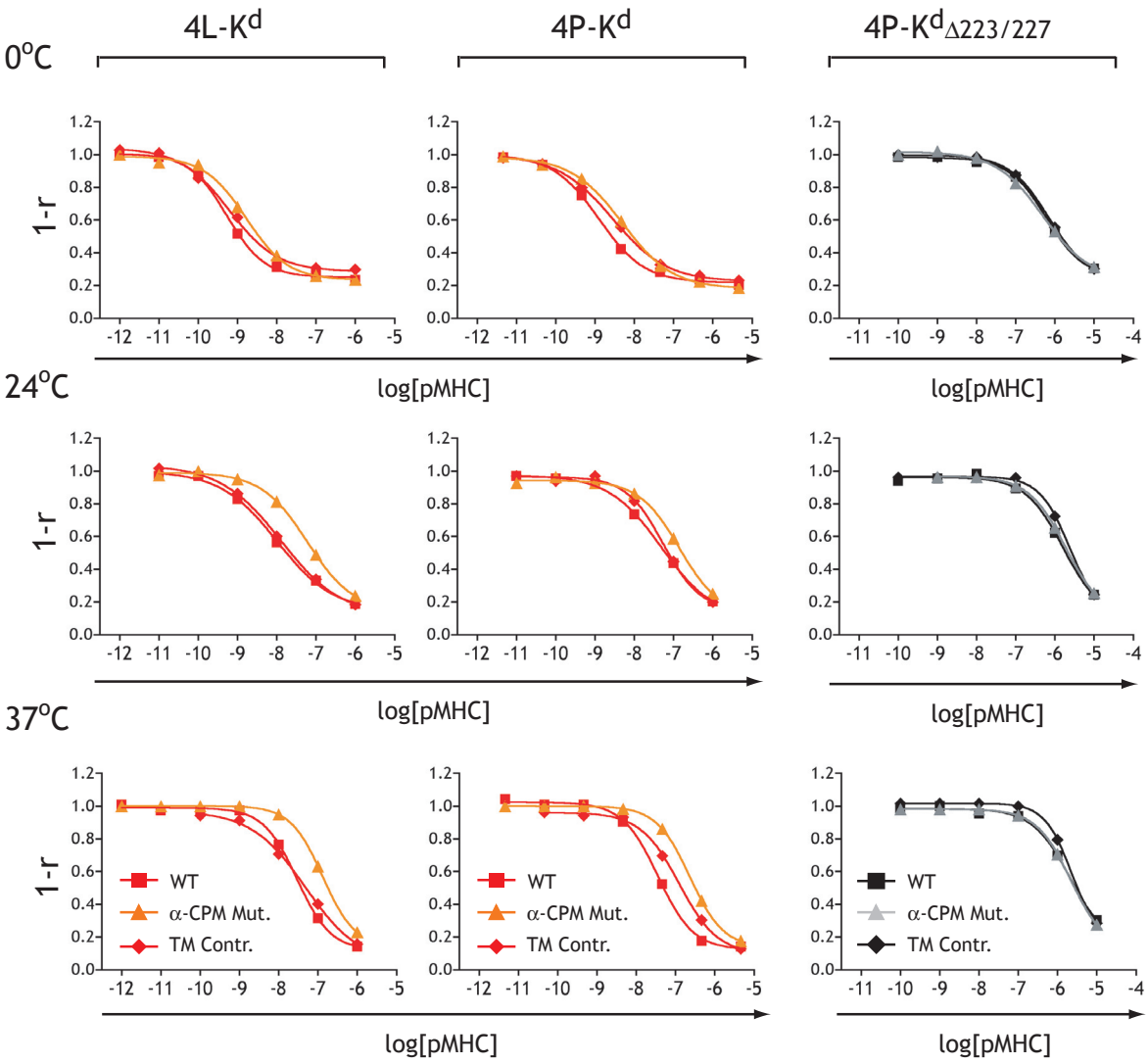

Figure 3.22: Binding of strong ligands to thymocytes from wild type, α-CPM mutant or TM control T1-TCR; Rag$^{-/-}$; β2m$^{-/-}$ mice. The ratios of free TCRs (1-r) obtained from two step labeling experiments performed either on wildtype (■ or ■), α-CPM mutant (▲ or ▲) or TM control mice (◆ or ◆) were overlaid to allow direct comparisons of binding differences mediated by the replacement of the α-CPM. Experiments representing dose dependent binding of the 4L-K^d, the 4P-K^d or the 4P-K$^d_{\Delta 223/227}$ primary ligands at 0°C, 24°C or 37°C are shown in individual panels. A representative experiment from a total of at least two independent experiments is shown.

ments were also performed with the 4P-K$^d_{\Delta 223/227}$ pMHC monomers which are defective in CD8 binding. This mutant ligand allowed the study of the bimolecular TCR-pMHC interaction in the absence of coreceptor binding. Figure 3.22 summarizes the results obtained from titration studies including pMHC monomers loaded with the strong, negative selecting 4P and 4L peptides. For all temperatures tested the 4L-K^d and the 4P-K^d monomers bound with slightly lower affinity to α-CPM mutant thymocytes than to wildtype and TM control thymocytes. In contrast, no significant differences between wildtype, α-CPM mutant and TM control thymocytes were observed when the binding to the 4P-K$^d_{\Delta 223/227}$ monomers was

studied. This implied that the α-CPM mutation *per se* does not alter binding of the pMHC to the TCR. Rather the effect of the α-CPM mutation on ligand binding involves CD8. This was in accordance with the observation made on hybridoma cells, where a CD8 mediated defect in ligand binding was evident when hybridomas expressing the α-CPM mutant T1-TCR were analyzed. The binding defects observed with α-CPM mutant thymocytes were not very pronounced at 0°C but clearly increased with rising temperatures. At 37°C binding of the 4L-K^d and 4P-K^d monomers was clearly reduced on thymocytes expressing α-CPM mutant TCRs compared to thymocytes expressing wildtype TCRs. In contrast to the data observed on hybridomas, the TM control thymocytes showed also slightly reduced binding to the 4L-K^d and the 4P-K^d monomers compared to wildtype thymocytes, especially at 37°C. Therefore the binding defect mediated by the replacement of the α-CPM was relatively small. On the other hand, the functional defects observed with α-CPM mutant thymocytes for the strong 4L and 4P peptides were also small (see Fig. 3.19) and negative selection in response to 4L and 4P peptides was unaffected as shown by the FTOC experiments (Fig. 3.21). Thus the very small functional defects observed in responses of α-CPM mutant thymocytes to strong ligands were also reflected in a slightly decreased capacity of the α-CPM mutant TCR to bind strong ligands (Fig. 3.22).

3.2.11 Binding of Weak Ligands to Wildtype and Chimeric T1-TCRs

The binding of the weak 4A-K^d, 4S-K^d and 4N-K^d ligands to TCRs expressed on DP thymocytes was also examined (Fig. 3.23). The data show that at 0°C and 24°C α-CPM mutant thymocytes bound weak pMHC ligands almost as well as wildtype and TM control thymocytes. However at 37°C the binding of weak ligands to the α-CPM mutant receptor is notably weaker than their binding decrease in the wildtype and the TM control TCRs. This ligand binding may partially explain the functional defects in CD69 upregulation and positive selection with α-CPM mutant thymocytes.

3.2.12 TCR-Ligand Affinity Determinations

Table VIII summarizes the dissociation constants (K_D) determined from the two step TCR labeling curves shown in Figures 3.22 and 3.23. Values marked with asterisks indicate extrapolated values from curves which did not reach half-maximal TCR saturation even at the highest concentrations tested. While the affinities of the 4P-$K^d_{\Delta 223/227}$ reflecting 4P-MHC monomers which cannot bind to CD8 were very similar for all mouse strains and temperatures tested, pMHC ligands which can interact with CD8 showed very strong temperature

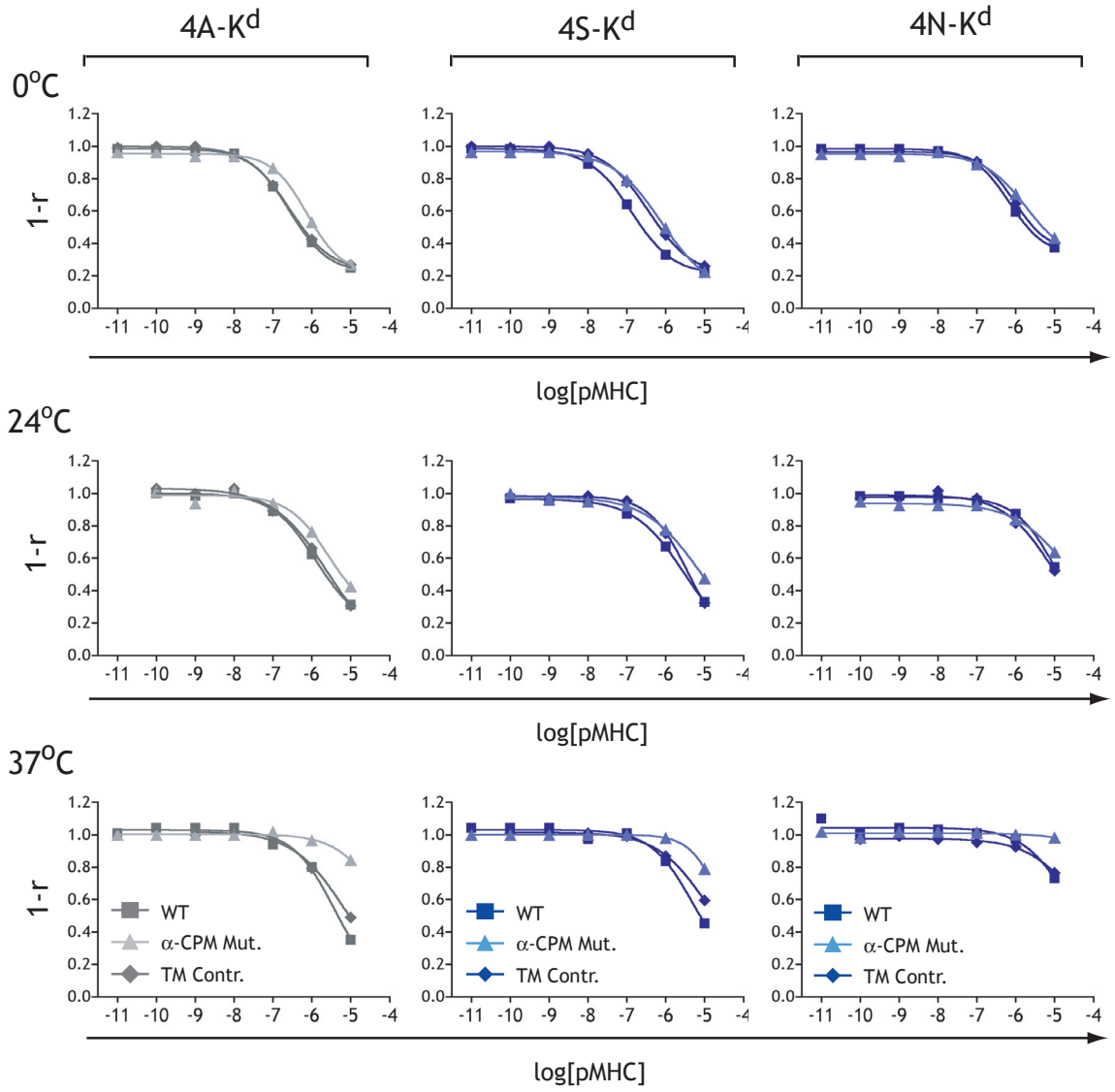

Figure 3.23: Binding of weak ligands to thymocytes from wildtype, α-CPM mutant or TM control T1-TCR; Rag$^{-/-}$; β2m$^{-/-}$ mice. The ratios of free TCRs (1-r) obtained from two step labeling experiments performed either on wildtype (■), α-CPM mutant (▲) or TM control mice (◆) were overlaid to allow for direct comparisons of ligand binding differences mediated by the replacement of the α-CPM. Experiments representing dose dependent binding of the 4A-K^d, the 4S-K^d or the 4A-K$^d_{\Delta 223/227}$ primary ligands at 0°C, 24°C or 37°C are shown in individual panels. A representative experiment from a total of at least two independent experiments is shown.

dependence. The K_D for each ligand is approximately 30- to 50-fold higher at 37°C compared to 0°C. The K_D values of the α-CPM mutant receptors were 2- to 5-fold higher than the K_D values for wildtype and TM control receptors. Interestingly, the relative affinity differences between α-CPM mutant and wildtype/TM control receptors were similar for both high and low affinity ligands.

Table VIII: K_D values [M] determined for pMHC monomers bound to wildtype, α-CPm mutant or TM control DP T1 thymocytes and α-CPM mediated affinity differences (ΔK_D).

Temperature; Strain	Ligands					
	4L-K^d	4P-K^d	4A-K^d	4S-K^d	4N-K^d	4L-$K^d_{\Delta 223/227}$
0°C						
Wildtype	6.9×10^{-10}	1.1×10^{-9}	1.2×10^{-7}	1.9×10^{-7}	7.1×10^{-7}	5.9×10^{-7}
α-CPM mutant	1.9×10^{-9}	4.0×10^{-9}	4.6×10^{-7}	7.1×10^{-7}	2.7×10^{-6}	5.7×10^{-7}
TM control	6.2×10^{-10}	2.2×10^{-9}	2.9×10^{-7}	3.5×10^{-7}	1.6×10^{-6}	7.9×10^{-7}
ΔK_D (± α-CPM)	**3.0 x**	**1.8 x**	**1.6 x**	**2.0 x**	**1.7 x**	**0.7 x**
24°C						
Wildtype	9.9×10^{-9}	3.9×10^{-8}	1.4×10^{-6}	2.0×10^{-6}	$9.1 \times 10^{-6*}$	1.0×10^{-6}
α-CPM mutant	3.5×10^{-8}	8.8×10^{-8}	3.3×10^{-6}	4.2×10^{-6}	$1.9 \times 10^{-5*}$	1.2×10^{-6}
TM control	1.0×10^{-8}	5.6×10^{-8}	1.9×10^{-6}	1.4×10^{-6}	$1.0 \times 10^{-5*}$	1.1×10^{-6}
ΔK_D (± α-CPM)	**3.5 x**	**1.6 x**	**1.7 x**	**3.0 x**	**1.9 x**	**1.1 x**
37°C						
Wildtype	2.4×10^{-8}	4.4×10^{-8}	3.6×10^{-6}	$6.3 \times 10^{-6*}$	$2.2 \times 10^{-5*}$	1.9×10^{-6}
α-CPM mutant	1.1×10^{-7}	3.9×10^{-7}	$3.3 \times 10^{-5*}$	$1.7 \times 10^{-5*}$	$1.7 \times 10^{-5*}$	1.9×10^{-6}
TM control	4.1×10^{-8}	1.5×10^{-7}	6.1×10^{-6}	$1.2 \times 10^{-5*}$	$4.7 \times 10^{-5*}$	2.1×10^{-6}
ΔK_D (± α-CPM)	**2.6 x**	**2.7 x**	**5.4 x**	**1.4 x**	**0.4 x**	**0.9 x**

Mean values of at least two experiments are shown. (*) half-maximal TCR saturation was not reached.

3.2.13 TCR-Ligand 'Off-rate' Determinations

To test whether the α-CPM replacement affected ligand dissociation from TCR, 'off-rates' were determined and compared. The results of these experiments are shown in Figure 3.24. At 0°C the 'off-rates' were ~2-fold faster for α-CPM mutant thymocytes compared to wildtype and TM control thymocytes irrespective of the ligand tested. In the case of the 4P-K^d monomers, the half-life of the TCR/CD8-pMHC interactions was ~12 minutes for α-CPM mutant thymocytes while it was ~20 minutes for the wildtype and the TM thymocytes (see Table IX). A similar observation was made for the low affinity 4S-K^d monomers, for which the half-lives of the α-CPM mutant thymocytes were faster (~14 sec.) compared to wildtype and TM control thymocytes (~21 sec.). Determining the 'off-rates' at higher temperatures was hampered by the extremely short half-lives of the TCR/CD8-pMHC interactions. However, 'off-rate' of the high affinity 4P-K^d monomers could be assessed at 24°C. Similar to the values obtained at 0°C, the half-life of 4P-K^d was 2-fold shorter on α-CPM mutant thymocytes (~10 sec.) than on wildtype or TM control thymocytes (~25 sec.).

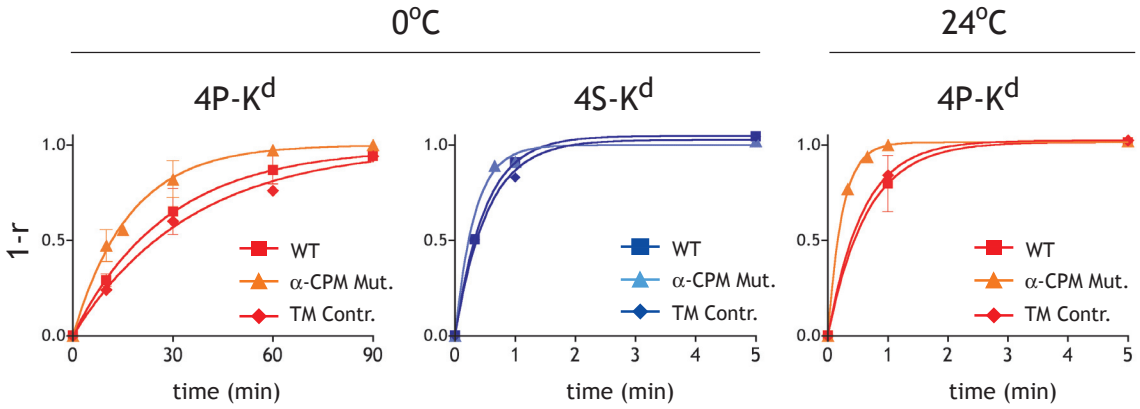

Figure 3.24: 'Off-rates' determined by two step labeling assays from DP and SP thymocytes from wildtype, α-CPM mutant or TM control T1-TCR; Rag$^{-/-}$; β2m$^{-/-}$ mice. T1 thymocytes were incubated for 90 min. with either 100nM of 4P-K^d or 1μM of 4A-K^d or 4S-K^d prior to dilution in the presence of 20μg/ml α-H-2K^d(α1)(20-8-4S) mAb. Aliquots of the diluted cells were incubated for defined intervals and subjected to UV crosslinking (~312nm). The ratios of free TCRs were determined by the two step assay. Cells were stained with fluorescence labeled α-CD4(RM4-5), α-CD8α(53-6.7), α-TCRβ(H57-597) mAbs. MFIs of Cy5 fluorescence signals obtained from DP and SP thymocytes are plotted as a function of time.

Table IX: Half-lives ($t_{1/2}$) of pMHC monomers bound to wildtype, α-CPM mutant or TM control DP T1 thymocytes at 0°C or 24°C.

	Ligand; 0°C		Ligand; 24°C
Strain	4P-K^d	4S-K^d	4P-K^d
Wildtype	19 min. ±4 min.	21 sec. ±9 sec.	27 sec. ±15 sec.
α-CPM mutant	12 min. ±7 min.	14 sec. ±11 sec.	10 sec. ±6 sec.
TM control	24 min. ±8 min.	22 sec. ±8 sec.	24 sec. ±8 sec.

Mean values of at least two experiments are shown.

3.3.14 CD8 Impact on Ligand Binding

The relative affinity differences measured between α-CPM mutant and wildtype or TM control T1-TCRs were between 2- and 10-fold, depending on the ligand tested and the temperature at which the experiments were performed. These affinity differences were also reflected in similar differences in the half-lives of a given TCR/CD8-pMHC interaction. The affinity measured with the 4P-K$^d_{\Delta 223/227}$ monomers was similar for all T1-TCR variants tested (Table VIII); this implied that the bimolecular TCR-pMHC was not altered by the replacement of the α-CPM. To test the impact of CD8 on ligand binding the binding curves obtained from 4P-K$^d_{\Delta 223/227}$ and 4P-K^d monomers were compared. As shown in Figure 3.25, at 37°C, CD8 participation increased the affinity of the wildtype T1-TCR for the 4P-pMHC monomers

by 50-fold. This difference was 25-fold in the case of the TM control TCR indicating that the replacement of the TCRα/β transmembrane regions by TCRγ/δ transmembrane regions further reduced the CD8 impact in ligand binding by a factor of 2. The impact of CD8 on pMHC binding to α-CPM mutant thymocytes was only 10-fold, which represents a 5-fold reduction to wildtype and a 2.5-fold reduction compared to TM control thymocytes. These data clearly show that the α-CPM mutation has a significant impact on the CD8 contribution to ligand binding.

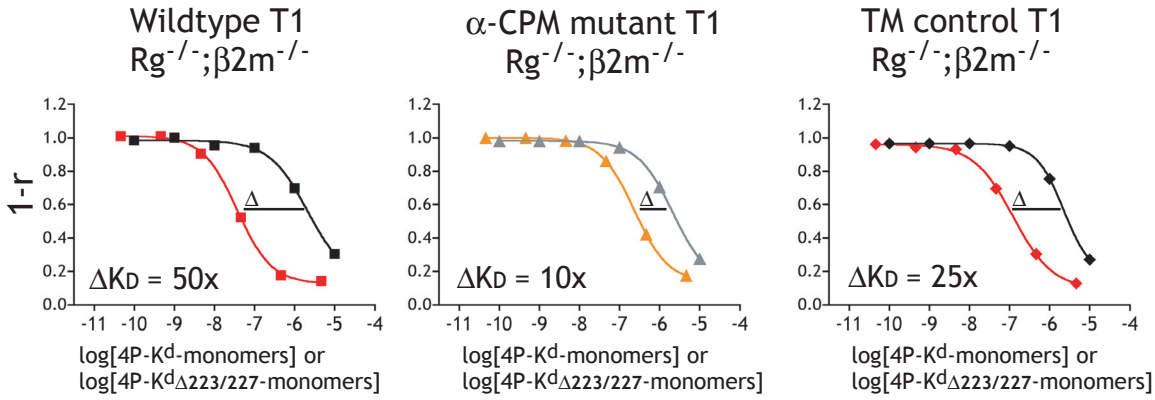

Figure 3.25: CD8 mediated binding increase on thymocytes of wildtype, α-CPM mutant or TM control T1; Rag$^{-/-}$; β2m$^{-/-}$ mice at 37°C. Results obtained from two step labeling with the 4P-K^d or the 4P-K$^d_{\Delta 223/227}$ primary ligands at 37°C were compared for each different mouse strain. Labeling curves with 4P-K^d (■) wt, (▲) α-CPM Mutant, (◆) TM control) or with 4P-K$^d_{\Delta 223/227}$ (■) wt, (▲) α-CPM mutant, (◆) TM control) are shown. The CD8 mediated fold differences in the affinities at 37°C are indicated in the lower left of each panel.

In conclusion, these results are consistent with the ligand labeling studies of hybridomas expressing wildtype, TM control or α-CPM mutant receptors. The relatively mild binding defect observed with α-CPM mutant TCRs due to reduced TCR-CD8 cooperativity was paralleled by dramatic functional deficits leading to the abrogation of positive selection. Whether the α-CPM phenotype can be completely explained by these differences in ligand binding remains an open question.

4. Discussion

In this thesis, hybridomas and transgenic mice expressing the T1-TCR were used to study the role of TCR-ligand affinity in the development of pMHC class I restricted T cells. Photoaffinity labeling experiments using soluble, monomeric pMHC complexes were performed on thymocytes and lymph node T cells from T1-TCR transgenic mice to study TCR ligand binding at various developmental stages. TCR affinities were compared to biological responses elicited by the various peptide derivatives. These studies revealed a direct correlation between TCR ligand affinities and the thymic selection properties of the various ligands. The role of TCR ligand binding in thymic selection was studied in further detail using a mutant form of the T1-TCR, i.e. α-CPM mutant T1-TCR, which was unable to induce positive selection of thymocytes. The results of these studies are discussed here in the context of previous studies on TCR ligand binding and thymic selection performed by others.

4.1 TCR Ligand Binding Measurements: Technical Considerations

TCR ligand binding measurements have been broadly used to study the role of TCR in T cell development and activation (Reviewed in Davis et al., 1998; Gascoigne et al., 2001; van der Merwe et al., 2003). Despite the development of invaluable techniques to study these interactions, it has not yet been possible to perform real-time analysis of TCR ligand interactions on live T cells or thymocytes interacting with pMHC expressing APCs. Instead, several techniques were developed which allowed to study TCR ligand interactions with solubilized forms of at least one of the binding partners. Most of the TCR ligand binding data available today were obtained from either using the surface-plasmon resonance (SPR; BIACore®: reviewed in Rudolph et al., 2002b) or soluble pMHC multimers (Altman et al., 1996; Ogg et al., 1998; Daniels et al., 2000). Many TCR-pMHC interactions and several CD4-MHC or CD8-MHC interactions have been studied using the SPR technique. These studies led to the determination of the affinities between specific TCR-pMHC interactions and coreceptor-pMHC interactions (Reviewed by van der Merwe et al., 2003). While the SPR technique allowed for detailed studies of TCR-ligand binding kinetics including 'on-rates', 'off-rates' and steady state binding affinities between bimolecular TCR-pMHC or coreceptor-pMHC interactions, it did not allow to study the impact of coreceptors in the trimeric TCR/coreceptor-pMHC interactions due to its plate based, cell free configuration. Neither was it possible to study developmental differences of these interactions as all the binding partners were derived from recombinantly produced molecules in either bacteria or non T

cell related fibroblast cell lines.

The development of fluorscence labeled, soluble pMHC ligands has been very useful to study the binding of soluble pMHC complexes to intact T cells and thymocytes. Unfortunately, measurements of pMHC monomers were hampered by the very fast 'off-rates' generally observed with TCR-pMHC interactions. On the other hand, the usage of pMHC multimers allowed binding measurements on live T cells and thymocytes and could be used to study both, either cognate TCR-pMHC or non-cognate coreceptor-pMHC interactions. Due to the multiple TCR binding sites on pMHC multimers these measurements determined the avidities of such interactions, representing a mixture of TCR-ligand affinity and the TCR crosslinking efficiency of the multiple pMHCs in a multimer complex.

Therefore, while the SPR technique allowed bimolecular TCR ligand affinity measurements using cell-free assays, pMHC multimers applied on live cells were used to measure ligand avidity. Despite the invaluable measurements performed by these two assays, they were unsuitable for TCR-pMHC affinity measurements on live cells. This limitation was overcome by the development of the photoaffinity labeling technique developed by Immanuel Lüscher. Using TCRs specific for photo-reactive, monomeric pMHC ligands, UV-crosslinking of TCR bound pMHC molecules led to covalent fixation of the TCR ligand interaction and therefore allowed for flow-cytometrical or biochemical analysis of bivalent TCR-pMHC interactions (see Introduction 1.3.3.2). This technique has been intensively used to study the role of TCR and CD8 coreceptors in ligand binding and signaling of activated T cells and T cell hybridomas (Lüscher et al., 1991; Lüscher et al., 1992; Lüscher et al., 1994; Lüscher et al., 1995a; Lüscher et al., 1995b; Anjuere et al., 1997; Kessler et al., 1997a; Kessler et al., 1997b; Hudrisier et al., 1998; Doucey et al. 2001; Gillaume et al., 2003;).

4.2 Photoaffinity Labeling on T Cells of T1-TCR Transgenic Mice

To study ligand affinities of TCRs expressed on T cells of different developmental stages T1-TCR transgenic mice were produced. Co-expressing transgenic T1-TCRα and TCRβ chains in Rag2 deficient mice allowed photoaffinity labeling ligand binding studies and functional analysis of DP thymocytes, SP thymocytes and lymph node T cells (Fig. 3.1), which uniquely expressed T1-TCRs in the absence of endogenously rearranged TCR molecules.

4.3 TCR-Cognate and Non-Cognate Binding on T1 Thymocytes

The use of Cy5 labeled photo-reactive pMHC monomers and analysis of TCR ligand bind-

ing by flow-cytometry was considered optimal to study TCR ligand affinities on thymocytes and lymph node T cells. By the means of electronic gating, DP and SP thymocytes were easily distinguished based on their CD4 and CD8 expression patterns. Titrations of 4P-K^d-Cy5 monomers (Fig. 3.5A) and photoaffinity labeling led to fluorescence signals which were dependent on the concentration of the ligand and the TCR expression levels of the cells analyzed (Fig. 3.5B and C). As indicated by the arrow in Figure 3.5C and the black curve in Figure 3.6B, using >10^{-6}M 4P-K^d-Cy5 led to fluorescence signals which were unexpectedly high, in particular on DP thymocytes. More detailed analysis of this phenomenon (Fig. 3.6) revealed that CD8 mediated non-cognate binding of the pMHC monomers to these cells. Despite the low affinity of CD8 coreceptor for MHC class I molecules (CD8α/β-H-2K^b: K_D=135µM at 25°C, Leishman et al. 2001) it is likely that the expression of high levels of unsialylated CD8 on DP thymocytes (Casabo et al., 1994) enhances non-cognate interactions on DP thymocytes and leads to the crosslinking of 4P-K^d-Cy5 to thymocytes. Non-cognate binding to CD8 was reported for MHC class I tetramers (Daniels et al., 2001; Moody et al., 2001). Therefore at concentrations higher than 10^{-6}M the fluorescence signals represented a mixture of cognate TCR-pMHC interactions and non-cognate CD8 MHC interactions. It is unclear whether the target of this non-cognate binding was CD8 itself or another surface protein. However, this non-cognate binding makes it difficult to determine the K_D of low affinity ligands since high ligand concentrations are required to saturate the TCR.

4.4 Affinity Measurements Using the Two Step Labeling Assay

To avoid non-cognate fluorescence signals, an assay was developed which used 4P-K^d-Cy5 at concentrations that were too low to be influenced by non-cognate CD8-MHC interactions. As described above (see Results 3.1.7) and illustrated in Figure 3.7 a first round of ligand titrations and photoaffinity labelings was performed with unlabeled pMHC monomers of varying affinity and at different temperatures, followed by washing and a second round of incubation performed on ice with a constant concentration (5x10^{-7}M) of the Cy5 labeled 4P-K^d-Cy5 ligand and subsequent photoaffinity labeling. As a result of this two step labeling assay, the fraction of the TCR on a cell, which remained free after the first round of photoaffinity labeling was measured. Direct comparison of direct photo-affinity labeling and two step labeling performed on DP thymocytes, SP thymocytes and lymph node T cells at 0°C and 37°C confirmed the accuracy of the K_D values determined by the two step labeling assay.

4.5 Temperature Dependent CD8 Participation in TCR Ligand Binding

These studies revealed a substantial temperature dependence of the K_D values, i.e. affinities (Fig. 3.9 and Table III). TCR ligand affinity dramatically increased at low temperatures in that the K_D of a ligand for the T1-TCR was 11- to 63-fold higher at 37°C than at 0°C (Fig. 3.9C). This change in affinity was much less pronounced, when mutant pMHC complexes were used that were unable to bind CD8α/β due to charge inversions in the α3 domain (D223K and D227K) of H-2K^d. Therefore the increased ligand affinity at low temperatures was due to an enhanced CD8 participation at 0°C. These findings are in accordance with a previous study, which showed only a small temperature mediated difference in ligand binding in the absence of CD8 but substantial temperature dependence in ligand binding when CD8α/β was present (Lüscher et al., 1995). Therefore it can be speculated that the temperature dependence is due to stability of CD8 recruited to the TCR. The reduced lateral mobility of these molecules in the plasma membrane at low temperatures would stabilize the trimeric (TCR/CD8-pMHC) complex and decrease the ligand 'off-rate' thereby increasing the affinity of the interaction. Reduced lateral mobility due to decreased membrane fluidity at low temperature would also lead to slower recruitment of CD8 to the TCR by pMHC ligands. Indeed, steady state binding of pMHC ligands was reached after only 90 minutes at 0°C while it took only 15 minutes at 24°C and less than 2 minutes at 37°C (data not shown). Upon simultaneous binding of TCR and CD8 to pMHC, reduced membrane fluidity at low temperatures would lead to slower lateral 'escape' of the CD8 coreceptor from the TCR-pMHC complex, assuming that the 'off-rates' measured for the CD8 MHC interaction is much faster than the 'off-rate' of most pMHC interactions. This is indeed the case, the dissociation kinetic constant k_{off} has been determined for several CD8 MHC interactions and was >20 s^{-1} while the 'off-rates' of bivalent cognate TCR-pMHC interaction were much slower (0.01-0.2 s^{-1}) (Reviewed in van der Merwe et al., 2003). Such a temperature dependent correlation of the 'off-rates' was observed (~20 min. at 0°C, ~30 sec. at 24°C (see Fig. 3.24) and < 20 sec. at 37°C (data not shown). Reducing the lateral mobility of TCR and CD8 leading to a 'concentration' of CD8 around TCR-pMHC complexes would reduce the rate-limiting CD8 recruitment step and lead to a bigger impact on the stability (e.g. lowering the 'off-rate') of the TCR-pMHC interaction. Therefore reduced lateral mobility of the molecules on the surface of a cell could explain the enhanced increase in TCR/CD8-pMHC binding observed for high affinity ligands (63-fold for 4P-K^d between 0°C and 37°C) compared to low affinity ligands (11-fold for 4S-K^d between 0°C and 37°C).

4.6 TCR-Ligand Affinity Does Not Change During Development

Thymocytes and peripheral T cells elicit very different responses to TCR ligands. While strong TCR stimuli lead to activation of T cells in the periphery, the same stimuli lead to negative selection and apoptosis in the thymus. Along the same line, weak TCR stimuli lead to positive selection and differentiation into the CD4 or the CD8 lineage, but they do not induce any measurable biological response in peripheral T cells (Hogquist et al., 1995; Davey et al., 1998; Lucas et al., 1999). It was not clear whether these developmentally regulated changes in the responses of T cells were in some measure mediated by changes in the affinity of the TCR for its ligands.

The use of photoaffinity labeling together with the production of T1-TCR transgenic mice allowed for the first time to study TCR ligand affinities at various stages of T cell development. Using the two step labeling assay, the affinities of the cognate TCR/CD8-pMHC interactions were studied at all three stages of T cell development. Labeling studies involving 5 different pMHC ligands of distinct affinity revealed no developmentally regulated change in TCR affinity (see Fig. 3.10 and 3.11). Similarly, when the dissociation kinetics of trimeric TCR/CD8-pMHC complexes were analyzed, equal 'off-rates' were measured on DP and SP thymocytes (see Fig. 3.12). These results clearly showed, that TCR ligand affinity does not change during T cell development.

This finding is particularly interesting in the light of studies using pMHC multimers, which showed differences in the non-cognate CD8-MHC avidity when DP thymocytes were compared to SP thymocytes and peripheral T cells (Daniels et al., 2001; Moody et al., 2001). In these studies it was shown that high concentrations of pMHC tetramers (~$1x10^{-7}$M) lead to TCR independent, CD8 mediated binding to DP thymocytes, while this type of binding was much weaker on SP thymocytes. These differences were explained by developmentally controlled addition of sialic acid residues to O-linked glycans on CD8β which occurs during the transition from DP to SP thymocytes (Casabo et al., 1994). It was proposed that addition of sialic acid causes conformational changes in the structure of the CD8α/β heterodimer reducing its ability to bind class I MHC. Whether this leads to changes in the CD8 dependent, TCR mediated cognate binding of pMHC ligands was not resolved.

The affinity measurements using pMHC monomers presented in this thesis argue against an influence of altered CD8 glycosylation on cognate TCR ligand binding. Nevertheless, as shown by direct photoaffinity labeling with monomeric 4P-K^d-Cy5 pMHCs (see Figure 3.6), TCR independent, CD8 mediated non-cognate binding was also observed with monomeric

pMHC ligands, when applied at very high concentrations (>10^{-6}M). Although it was shown, that DP thymocytes of T1 mice had less sialic acid present on their surface compared to SP thymocytes (Figure 3.13A) the affinities of the cognate TCR mediated binding of 4P-K^d monomers measured on these two cell populations were not significantly different (Fig. 3.13, Panels I and IV). Furthermore, using tetramers of 4P-K^d it was shown that the same was true for multimers of high affinity ligands (Fig. 3.13, Panels II and V). Binding data obtained using tetramers of the low affinity ligand 4A-K^d were hard to interpret because even at 10^{-7}M, TCR saturation was not observed (Fig. 3.13, Panels III and VI, black curves). The increase in binding between DP (Panel III) and SP (Panel VI) thymocytes was most likely due to increased TCR expression rather than a change in the sialic acid status between DP and SP thymocytes. However neuraminidase treatment led to a marked increase in 4A-K^d tetramer binding (Fig. 3.13, Panels III and VI, green curves). Thus, it is unclear whether differences in the sialylation status between these developmental stages could influence the avidity of low affinity ligands.

In conclusion, the data presented in this thesis (see Results 3.1.11 and 3.1.12) argue clearly against a developmentally controlled change in TCR affinity despite the changes observed for non-cognate CD8-MHC interactions. Furthermore the decrease in sensitivity of SP thymocytes to weak (4S and 4N) ligands can not be explained by changes in the TCR-ligand affinity. The changes in sialylation that occur with thymocyte maturation may decrease responsivness to low affinity ligands without affecting ligand binding *per se*. The fact that sialylation of thymocytes in the transition from DPs to SPs does not change the cognate TCR ligand affinity does not exclude an important role of glycosylation changes in T cell development. Studies using mice deficient in the sialyltransferase ST3Gal-I showed relatively normal thymic development but a 90% reduction of the peripheral CD8 T cell pool; CD4 T cell numbers were only slightly affected (Priatel et al., 2000). This emphasizes the importance of proper sialylation for thymic emigration and peripheral survival. In terms of thymocyte and T cell trafficking, reduction of the CD8 avidity on SP thymocytes could indeed be very important, as it was shown, that DP thymocytes could be strongly adsorbed to surface bound MHC class I, while SP thymocytes and mature T cells were not (Daniels et al., 2001). Interestingly, studies using pMHC dimers showed altered cognate TCR-pMHC binding upon activation of peripheral CD8 T cells (Fahmy et al., 2001). Unfortunately differential glycosylation was not studied in this work, but interestingly, desialylation of CD8β was described to happen upon activation of peripheral CD8 T cells (Casabo et al., 1994). Therefore it is possible that the activation of mature T cells by multimeric pMHC ligands is influenced

by these changes in the glycosylation status of CD8. On the other hand, disruption of CD8β sialylation did not significantly change the numbers of positively selected thymocytes, arguing against a pivotal role in the thymocyte selection *per se* (Priatel et al., 2000).

4.7 Evidence for an Affinity Threshold in Thymic Selection

The fact that T1-TCR ligand affinities did not change during T cell development has important consequences for the interpretation of how thymocytes and T cells recognize their ligands. For DP thymocytes undergoing positive or negative selection it was proposed that strong antigenic signals lead to negative selection, while weak antigenic signals lead to positive selection. Despite the broad acceptance of such a model of T cell selection, there is an intensive debate regarding the mechanisms leading to 'weak' or 'strong' antigenic signals.

Two different models were proposed of how TCR-ligand interaction intensities are interpreted by thymocytes undergoing thymic selection processes. In the avidity model, high numbers of ligand engaged TCRs ('strong signal') lead to negative selection, while low numbers of engaged TCRs ('weak signal') lead to positive selection. In this model the affinity of a given TCR-ligand interaction is not a direct measure of the selection outcome, because high affinity ligands applied at low concentrations would only occupy low numbers of TCRs and therefore lead to positive selection, while low affinity ligands applied at high concentrations would occupy many TCRs and thus lead to negative selection. Therefore in the avidity model, the affinity of a given pMHC complex in conjunction with its concentration is critical for the selection outcome. Some studies propose that the dose of pMHC ligand is critical for the thymic selection outcome (Sebzda et al., 1994; Ashton-Rickard et al., 1994; Liu et al., 1998; Smith et al., 1998). In contrast, the affinity model of thymic selection proposes that the affinity of the TCR-ligand interaction *per se* decides whether thymocytes get positively or negatively selected. In this model, the decision whether a thymocyte gets positively or negatively selected is ligand concentration independent. In the affinity model, it is predicted that high affinity pMHC ligands induce negative selection, even at low concentrations, while low affinity ligands lead to positive selection, even when presented at high ligand concentrations. Several previous reports were favoring the affinity model of thymic selection (Hogquist et al., 1994; Hogquist et al., 1995; McKeithan et al. 1995., Alam et al., 1996).

To study the thymic selection properties of the variant ligands tested in this thesis, FTOC assays were performed with fetal thymi from T1-TCR; $Rag^{-/-}$; $\beta 2m^{-/-}$ mice. Fig. 3.14 shows that the high affinity 4L and 4P ligands induced negative selection, while the low affinity

ligands 4A, 4S and 4N induced positive selection. Importantly, positive and negative selection were relatively concentration independent (see Fig. 3.15A) which support the affinity model of thymic selection. Nevertheless, the 4A peptide is an interesting exception. Unlike the other peptides high doses of 4A led to negative selection, while low peptide doses led to positive selection (see Fig. 3.15B). These results are consistant with the affinity model of thymic selection, assuming that the 4A ligand has an affinity for the T1-TCR which defines the border between positive and negative selection.

Analysis of the CD69 data and the TCR ligand affinity data supported this assumption. As illustrated in Figure 3.3A, the 4L peptide showed the strongest potency to upregulate CD69 in DP thymocytes, followed by the 4P, the 4A, the 4S and the 4N peptides. This hierarchy in ligand potencies was preserved on SP thymocytes and lymph node T cells. The peptides could be grouped into two distinct classes based on their ability to stimulate DP and SP thymocytes. In the first group consisting of the strong peptides 4L and 4P, both DP and SP thymocytes were similarly sensitive to these ligands. Furthermore DP and SP thymocytes were able to upregulate CD69 even in the presence of a mAb which blocked CD8 binding to K^d (see Fig. 3.3B). The second group of ligands consisted of the 4S and 4N peptides. Compared to DP cells SP thymocytes were substantially less sensitive to these positive selecting ligands (see Fig. 3.3A) and CD69 upregulation was severely reduced in the absence of CD8 participation in this group (see Fig. 3.3B). The 4A peptide seemed to share properties with the strong and weak potency groups. SP thymocytes were only slightly less sensitive to 4A compared to DP cells, which is a characteristic of strong ligands. On the other hand, the response to 4A was significantly CD8 dependent (see Fig. 3.3B), which is a characteristic of low potency ligands. Based on these criteria, the 4A peptide was considered a moderate potency ligand. Therefore, it may not be surprising that the 4A peptide can mediate positive and negative selection depending on the dose. The hierarchy of these peptides in functional assays is reflected in their affinity hierarchy (4L ~ 4P >> 4A > 4S > 4N). Therefore, as in the case of the CD69 assay and the FTOC assay, the 4A ligand affinity was lower than the affinity of strong, negative selecting ligands (4L-K^d and 4P-K^d) and slightly higher than weak, positive selecting ligands (4S-K^d and 4N-K^d). Based on these correlations of ligand potency, affinity and selection property, it can be reasoned that the outcome of thymic selection is determined by pMHC affinity for the TCR, with the 4A-K^d ligand (K_D = 4μM at 37°C) defining the affinity threshold between positive and negative selection for the T1 thymocytes.

4.8 A Role for the α-CPM in Mediating TCR-CD8 Cooperativity

Development of a general hypothesis describing the mechanism of TCR function in T cell activation and thymocyte selection has proven to be very difficult, given the enormous numbers of clonotypically different TCR molecules in each individual. The classical approaches used to unravel the mechanisms of TCR binding and function employed the study of many different TCRs of various specificities (Reviewed by Davis et al., 1998; Gascoigne et al., 2001; van der Merwe et al., 2003).

Another approach was taken by analysis of the TCR constant regions which are uniform in all individuals of a given species. Comparison of TCR constant regions from various species led to the identification of the α-CPM, an eight amino acid residue (FETDxNLN) motif, which has been evolutionarily conserved for the last 500 million years (Backstrom et al., 1996). Its biological importance has been shown by the finding that replacement of the α-CPM with non-homologous residues from the TCRδ connecting peptide, led to a complete block of thymocyte development in mice expressing such α-CPM mutant TCRs (Backstrom et al., 1998; Werlen et al., 2000). Analysis of the defects observed with α-CPM mutant mice, revealed specific defects in the signaling cascades involved in positive selection of thymocytes (Werlen et al., 2000). To investigate the role of the α-CPM in TCR ligand binding, studies on α-CPM mutant T1-TCR expressed in hybridomas and transgenic mice were performed using the photoaffinity labeling system. Using radioactively labeled, monomeric pMHCs (see Fig. 3.17A), ligand binding was compared between wildtype, α-CPM mutant or TM control T1-TCRs (Fig. 3.16A). To test the role of CD8 co-engagement in TCR ligand binding, these TCRs were either expressed in CD8 deficient '58' hybridomas or in 58CD8α/β hybridomas, which co-expressed CD8α/β (see Fig. 3.16B). TCR and TCR/CD8 mediated binding between the three different T1-TCRs variants were compared. Three observations were made concerning the effect of the replacement of the α-CPM in TCR ligand binding (Naeher et al., 2002; herein Results 3.2.4).

First, bimolecular TCR-pMHC binding in the absence of CD8 was similar for all three T1-TCR variants tested. This demonstrated that the α-CPM mutation *per se* does not decrease TCR affinity. Second, the α-CPM mutant TCRs were defective in mediating TCR-CD8 cooperativity in ligand binding. CD8 increased ligand binding 6.7-fold in the case of the wildtype and the TM control TCRs but only 2.4-fold in the case of the α-CPM mutant TCR. At 37°C, the CD8 mediated increase in ligand binding was 2-fold in the case of wildtype and TM control TCRs while no increase at all was observed for the α-CPM mutant TCR. It is important to note, that the TCR binding studies performed on hybridomas were using very

low concentrations (~5x10^{-10}M) of the radioactive ligands and therefore it was not possible to test, whether this absence of CD8 help in binding was due to a complete defect in TCR-CD8 cooperation at physiological temperatures or if it was due to a reduction in the TCR/CD8-pMHC affinity. To further investigate the role of the α-CPM in TCR ligand binding and function different transgenic mice were produced which expressed the T1-TCR variants. As illustrated in Figure 3.18 the replacement of the α-CPM led to a severe block of thymocyte development indicated by the absence of SP thymocytes in these mice. The fact that the percentage and numbers of SP thymocytes in TM control T1 mice was comparable to wild-type T1 mice, formally proved that the developmental block observed with α-CPM mutant mice was due to the replacement of the α-CPM rather than due to the replacement of the transmembrane and cytosolic regions of TCRα/β (by TCRγ/δ derived sequences). This was also obvious when the CD69 responses of thymocytes in response to various ligands were tested (see Fig. 3.19). While the peptide dose curves between wildtype and the TM control T1 thymocytes were very similar, thymoctes from α-CPM mutant mice showed severely reduced responses to weak ligands (see Fig. 3.19, panel II). Replacement of the α-CPM led to an 8- (4P) to 17-fold (4L) increase in the EC_{50} values for strong ligands, while the EC_{50} values of 4A were 17'000-fold increased (Table VII). For the weak 4S and 4N peptides the EC_{50} values for the α-CPM mutant thymocytes increased >>1400 fold and >>200 fold respectively.

Interestingly, the responses of wildtype and TM control thymocytes were similarly reduced when the binding of CD8 to H-2K^d was blocked with the SF1-1.1 mAb (see Fig. 3.19, panels VI and VIII). Therefore, abolished CD8 participation in ligand binding of the wildtype and TM control TCRs led to similar CD69 upregulation profiles as observed with α-CPM mutant thymocytes (see Fig. 3.19 panels II, VI and VIII). This functional defect involving impaired CD8 participation was reminiscent of the ligand binding defect observed on hybridomas expressing α-CPM mutant TCRs. To measure TCR ligand affinities and thymic selection capacities of wildtype, α-CPM mutant and TM control thymocytes, the different T1-TCR transgenes were bred to Rag2 and β2m double deficient mice. As expected, given the absence of class I MHC expression, thymocyte development of all three strains was arrested at the DP stage (see Fig. 3.20A). Fetal thymic organ cultures revealed that the replacement of the α-CPM did not affect negative selection (see Fig. 3.21, red arrows), while proper positive selection was only observed with wildtype and TM control thymocytes (see Fig. 3.21, blue arrows). This was in agreement with the positive selection defects observed with two other α-CPM mutant TCRs of distinct specificities (Backstrom et al., 1998; Werlen et al., 2000) and underlining the requirement of the α-CPM for positive selection of thymocytes expressing TCRα/β.

To characterize the ligand binding properties of α-CPM mutant TCRs defects, two step labeling assays were performed on the pre-selection thymocytes from T1; $Rag^{-/-}$; $\beta 2m^{-/-}$ mice. When monomers were used which were unable to bind CD8 (see Fig. 3.22) no significant affinity differences were observed between wildtype, α-CPM mutant and TM control TCRs. This confirmed the results obtained with the CD8 negative '58' hybridomas and showed that the bivalent TCR-pMHC binding was not affected by replacement of the α-CPM. On the other hand, the trimolecular TCR/CD8-pMHC binding was reduced on α-CPM mutant thymocytes for all ligands and temperatures tested as indicated by the two step assay binding curves in Figure 3.22 and 3.23. But clearly, in all cases there was a small shift to higher ligand concentrations (i.e. an increase in the K_D) when the ligand binding curves obtained from α-CPM mutant thymocytes were compared to TM control thymocytes. As indicated in Table VIII the affinity differences were small but reproducible, indicated by the 2- to 5-fold differences in the K_D values between α-CPM mutant and TM control TCRs. Along the same line, the dissociation kinetics of the 4P-K^d (at 0°C and 24°C) and the 4S-K^d complexes (at 0°C) were maximally 2-fold faster with the α-CPM mutant TCRs compared to the wildtype and the TM control TCRs (see Fig. 3.24). Considering the dramatic functional defects observed with α-CPM mutant thymocytes concerning CD69 upregulation in response to weak ligands and abrogated positive selection, these relatively small defects in ligand binding which affect strong and weak ligands similarly (2- to 5-fold) do not reflect the dramatic differences in the EC_{50} values (> 17'000-fold in the case of 4A) observed from CD69 assays. How can this discrepancy by explained?

Thymocyte positive selection is critically dependent on proper CD8 co-engagement in ligand binding. In mice expressing CD8β chimeric molecules, where the extracellular region of CD8β was replaced by the extracellular region of CD8α, the number of SP thymocytes dropped by 50%. Exchange of the transmembrane and cytosolic part of CDβ by CD8α regions led to the same phenotype (Bosselut et al., 2000) and knocking out CD8β (leading to CD8α/α homodimer expression) was detrimental for thymocyte positive selection as well (Fung-Leung et al., 1993; Itano et al,. 1994; Nakayama et al., 1994; Crooks et al., 1994; Bosselut et al., 2000). This indicated that the presence of CD8β is absolutely required for positive selection of class I MHC restricted T cells and that CD8 fulfilled a dual function in terms of ligand binding and signaling. While the extracellular region of CD8β is very important in contributing to the ligand binding, the cytosolic regions were shown to be important to coordinate the recruitment of CD8α associated p56lck to the TCR/CD3 complex to initiate TCR signaling (Arcaro et al., 2000). Regarding the CD69 assays shown in Figure 3.19, replacement of the α-CPM or blocking of the interaction between CD8 and MHC on

wildtype T1 thymocytes led to equal functional defects. Given the membrane proximal location of the α-CPM, it seems unlikely that replacement of the α-CPM directly affected the interaction between CD8 and MHC. That α-CPM mutant TCRs bind ligands almost as well as wildtype and TM control receptors supports this idea. Nevertheless, in the absence of the α-CPM, thymocytes responded to weak ligands in the same way as if the CD8 MHC interaction would not have taken place, i.e. similar to the response of wildtype and TM control thymocytes in the presence of an the SF1-1.1 mAb that blocks CD8 engagement of class I MHC. The data support the idea that mutation of the α-CPM rather has a minimal impact on ligand binding but a profound effect on initializing TCR mediated signals, particularly from low affinity ligands. Interestingly, this was not the case for strong ligands. Neither the replacement of the α-CPM nor the disruption of the CD8 MHC interaction by mAbs led to a dramatic decrease in CD69 upregulation. This argues for a model in which the response to strong ligands is relatively independent of CD8 binding to MHC. There are many reports supporting this idea. As described above disruption of CD8β affected positive selection much more than negative selection (Fung-Leung et al., 1993; Itano et al,. 1994; Nakayama et al., 1994; Crooks et al., 1994) and that CD8 was only pivotal for responses to weak ligands, while the cells were not dependent on CD8 to respond to strong ligands (Kerry et al., 2003). Interestingly, while α-CPM mutant thymocytes were unable to induce any measurable Erk induction in response to weak, positive selecting ligands, the same ligands were able to induce p38 and Jnk, indicative of a second signaling pathway which was independent of the α-CPM (Werlen et al., 2000).

Taken together these studies suggest, that only weak TCR ligand interactions required the simultaneous binding of CD8 to the same pMHC molecule. Transmission of the information, that CD8 and the TCR are simultaneously bound to the same pMHC requires an intact α-CPM. It is conceivable that engagement of CD8 and the TCR near the plasma membrane is mediated by the α-CPM and the membrane proximal stalk of CD8β. This co-engagement would make it possible for low affinity ligands to initiate positive selection signals. The fact that mutation of the α-CPM has a small impact on the ability of CD8 to stabilize pMHC binding makes it unlikely that the α-CPM is just a 'docking' site for CD8. If 'docking' of CD8 to the TCR was needed to stabilize the trimeric, weak affinity TCR/CD8-pMHC interactions, replacement of the α-CPM should have led to a severe decrease in affinity or 'off-rate'. This was not observed. Subsequent to ligand binding there might be a very transient interaction between the CD8 and the α-CPM which allows the TCR to 'sense' the presence of CD8, without substantially altering the 'off-rate'. How this is achieved is not yet clear. A study using the '58CD8α/β' hybridomas described above, assigned a role to CD3δ in building a

functional link between the TCR and CD8 which was dependent on the presence of the α-CPM (Doucey et al., 2002). Interestingly mice lacking CD3δ or expressing mutant CD3δ chains lacking the extracellular region were also unable to undergo positive selection while negative selection was not affected (Dave et al., 1997; Delgado et al., 2000), similarly to CD8β deficient mice. Furthermore crystallographic studies showed a conserved orientation of the pMHC over the TCR, placing the MHC coreceptor binding site over the α-chain side of the TCR (Sun et al., 1995; Garcia et al., 1996; Garboczi et al., 1996; Teng et al., 1998; Speir et al., 1998). Evolution seems to have selected a pMHC orientation that places the coreceptor on the 'α-side' of the TCR, a side of the α/β heterodimer that also contains the α-CPM. In conclusion, the observations made with α-CPM mutant T1-TCRs combined with the data gained from CD8β and CD3δ mutant mice argue for a pivotal role of the α-CPM in 'sensing' TCR-CD8 cooperativity. This cooperativity allows thymocytes responding to weak TCR ligands to initiate signals leading to positive selection. Clearly more studies need to be performed to understand how the α-CPM 'reads' TCR/CD8-pMHC interactions and how it 'tells' it to the signaling machinery of the cell.

5. References

Abastado, J. P., Casrouge, A., and Kourilsky, P. (1993). Differential role of conserved and polymorphic residues of the binding groove of MHC class I molecules in the selection of peptides. J Immunol 151, 3569-3575.

Alam, S. M., Davies, G. M., Lin, C. M., Zal, T., Nasholds, W., Jameson, S. C., Hogquist, K. A., Gascoigne, N. R., and Travers, P. J. (1999). Qualitative and quantitative differences in T cell receptor binding of agonist and antagonist ligands. Immunity 10, 227-237.

Alam, S. M., Travers, P. J., Wung, J. L., Nasholds, W., Redpath, S., Jameson, S. C., and Gascoigne, N. R. (1996). T-cell-receptor affinity and thymocyte positive selection. Nature 381, 616-620.

Altman, J. D., Moss, P. A., Goulder, P. J., Barouch, D. H., McHeyzer-Williams, M. G., Bell, J. I., McMichael, A. J., and Davis, M. M. (1996). Phenotypic analysis of antigen-specific T lymphocytes. Science 274, 94-96.

Anjuere, F., Kuznetsov, D., Romero, P., Cerottini, J. C., Jongeneel, C. V., and Luescher, I. F. (1997). Differential roles of T cell receptor alpha and beta chains in ligand binding among H-2Kd-restricted cytolytic T lymphocyte clones specific for a photo-reactive Plasmodium berghei circumsporozoite peptide derivative. J Biol Chem 272, 8505-8514.

Arcaro, A., Gregoire, C., Boucheron, N., Stotz, S., Palmer, E., Malissen, B., and Luescher, I. F. (2000). Essential role of CD8 palmitoylation in CD8 coreceptor function. J Immunol 165, 2068-2076.

Ashton-Rickardt, P. G., Bandeira, A., Delaney, J. R., Van Kaer, L., Pircher, H. P., Zinkernagel, R. M., and Tonegawa, S. (1994). Evidencefor a differential avidity model of T cell selection in the thymus. Cell 76, 651-663.

Ashwell, J. D., Chen, C., and Schwartz, R. H. (1986a). High frequency and nonrandom distribution of alloreactivity in T cell clones selected for recognition of foreign antigen in association with self class II molecules. J Immunol 136, 389-395.

Ashwell, J. D., Fox, B. S., and Schwartz, R. H. (1986b). Functional analysis of the interaction of the antigen-specific T cell receptor with its ligands. J Immunol 136, 757-768.

Ashwell, J. D., and Schwartz, R. H. (1986). T-cell recognition of antigen and the Ia molecule as a ternary complex. Nature 320, 176-179.

Backstrom, B. T., Milia, E., Peter, A., Jaureguiberry, B., Baldari, C. T., and Palmer, E. (1996). A motif within the T cell receptor alpha chain constant region connecting peptide domain controls antigen responsiveness. Immunity 5, 437-447.

Backstrom, B. T., Muller, U., Hausmann, B., and Palmer, E. (1998). Positive selection through a motif in the alpha/beta T cell receptor. Science 281, 835-838.

Baker, B. M., Gagnon, S. J., Biddison, W. E., and Wiley, D. C. (2000). Conversion of a T cell antagonist into an agonist by repairing a defect in the TCR/peptide/MHC interface: implications for TCR signaling. Immunity 13, 475-484.

Bassing, C. H., Swat, W., and Alt, F. W. (2002). The mechanism and regulation of chromosomal V(D)J recombination. Cell 109 Suppl, S45-55.

Bosselut, R., Kubo, S., Guinter, T., Kopacz, J. L., Altman, J. D., Feigenbaum, L., and Singer, A. (2000). Role of CD8beta domains in CD8 coreceptor function: importance for MHC I binding, signaling, and positive selection of CD8+ T cells in the thymus. Immunity 12, 409-418.

Casabo, L. G., Mamalaki, C., Kioussis, D., and Zamoyska, R. (1994). T cell activation results in physical modification of the mouse CD8 beta chain. J Immunol 152, 397-404.

Cerundolo, V., Alexander, J., Anderson, K., Lamb, C., Cresswell, P., McMichael, A., Gotch, F., and Townsend, A. (1990). Presentation of viral antigen controlled by a gene in the major histocompatibility complex. Nature 345, 449-452.

Crooks, M. E., and Littman, D. R. (1994). Disruption of T lymphocyte positive and negative selection in mice lacking the CD8 beta chain. Immunity 1, 277-285.

Daniels, M. A., Devine, L., Miller, J. D., Moser, J. M., Lukacher, A. E., Altman, J. D., Kavathas, P., Hogquist, K. A., and Jameson, S. C. (2001). CD8 binding to MHC class I molecules is influenced by T cell maturation and glycosylation. Immunity 15, 1051-1061.

Daniels, M. A., and Jameson, S. C. (2000). Critical role for CD8 in T cell receptor binding and activation by peptide/major histocompatibility complex multimers. J Exp Med 191, 335-346.

Dave, V. P., Cao, Z., Browne, C., Alarcon, B., Fernandez-Miguel, G., Lafaille, J., de la Hera, A., Tonegawa, S., and Kappes, D. J. (1997). CD3 delta deficiency arrests development of the alpha/beta but not the gamma/delta T cell lineage. Embo J 16, 1360-1370.

Davey, G. M., Schober, S. L., Endrizzi, B. T., Dutcher, A. K., Jameson, S. C., and Hogquist, K. A. (1998). Preselection thymocytes are more sensitive to T cell receptor stimulation than mature T cells. J Exp Med 188, 1867-1874.

Davis, M. M., Boniface, J. J., Reich, Z., Lyons, D., Hampl, J., Arden, B., and Chien, Y. (1998a). Ligand recognition by alpha/beta T cell receptors. Annu Rev Immunol 16, 523-544.

Davis, S. J., Ikemizu, S., Wild, M. K., and van der Merwe, P. A. (1998b). CD2 and the nature of protein interactionsmediating cell-cell recognition. Immunol Rev 163, 217-236.

Degano, M., Garcia, K. C., Apostolopoulos, V., Rudolph, M. G., Teyton, L., and Wilson, I. A. (2000). A functional hot spot for antigen recognition in a superagonist TCR/MHC complex. Immunity 12, 251-261.

Delgado, P., Fernandez, E., Dave, V., Kappes, D., and Alarcon, B. (2000). CD3delta couples T-cell receptor signaling to ERK activation and thymocyte positive selection. Nature 406, 426-430.

Denkberg, G., Cohen, C. J., and Reiter, Y. (2001). Critical role for CD8 in binding of MHC tetramers to TCR: CD8 antibodies block specific binding of human tumor-specific MHC-peptide tetramers to TCR. J Immunol 167, 270-276.

DiGiusto, D. L., and Palmer, E. (1994). An analysis of sequence variationin the beta chain

framework and complementarity determining regions of an allo-reactive T cell receptor. Mol Immunol 31, 693-699 Issn: 0161-5890.

Ding, Y. H., Baker, B. M., Garboczi, D. N., Biddison, W. E., and Wiley, D. C. (1999). Four A6-TCR/peptide/HLA-A2 structures that generate very different T cell signals are nearly identical. Immunity 11, 45-56.

Doucey, M. A., Goffin, L., Naeher, D., Michielin, O., Baumgartner, P., Guillaume, P., Palmer, E., and Luescher, I. F. (2003a). CD3 delta establishesa functional link between the T cell receptor and CD8. J Biol Chem 278, 3257-3264.

Doucey, M. A., Legler, D. F., Faroudi, M., Boucheron, N., Baumgaertner, P., Naeher, D., Cebecauer, M., Hudrisier, D., Ruegg, C., Palmer, E., et al. (2003b). The beta1 and beta3 integrins promote T cell receptor-mediated cytotoxic T lymphocyte activation. J Biol Chem 278, 26983-26991.

Fahmy, T. M., Bieler, J. G., Edidin, M., and Schneck, J. P. (2001). Increased TCR avidity after T cell activation: a mechanism for sensing low-density antigen. Immunity 14, 135-143.

Fukui, Y., Ishimoto, T., Utsuyama, M., Gyotoku, T., Koga, T., Nakao, K., Hirokawa, K., Katsuki, M., and Sasazuki, T. (1997). Positive and negative CD4+ thymocyte selection by a single MHC class II/peptide ligand affected by its expression level in the thymus. Immunity 6, 401-410.

Fung-Leung, W. P., Wallace, V. A., Gray, D., Sha, W. C., Pircher, H., Teh, H. S., Loh, D. Y., and Mak, T. W. (1993). CD8 is needed forpositive selection but differentially required for negative selection of T cells during thymic ontogeny. Eur J Immunol 23, 212-216.

Gakamsky, D. M., Luescher, I. F., and Pecht, I. (2004). T cell receptor-ligand interactions: a conformational pre-equilibrium or an induced fit. Proc Natl Acad Sci U S A 101, 9063-9066.

Gao, G. F., and Jakobsen, B. K. (2000). Molecular interactions of coreceptor CD8 and MHC class I: the molecular basis for functional coordination with the T-cell receptor. Immunol Today 21, 630-636.

Gao, G. F., Tormo, J., Gerth, U. C., Wyer, J. R., McMichael, A. J., Stuart, D. I., Bell, J. I., Jones, E. Y., and Jakobsen, B. K. (1997). Crystal structure of the complex between human CD8alpha(alpha) and HLA-A2. Nature 387, 630-634.

Garboczi, D. N., Ghosh, P., Utz, U., Fan, Q. R., Biddison, W. E., and Wiley, D. C. (1996). Structure of the complex between human T-cell receptor, viral peptide and HLA-A2. Nature 384, 134-141.

Garcia, K. C., Degano, M., Pease, L. R., Huang, M., Peterson, P. A., Teyton, L., and Wilson, I. A. (1998). Structural basis of plasticity in T cell receptor recognition of a self peptide-MHC antigen. Science 279, 1166-1172.

Garcia, K. C., Degano, M., Stanfield, R. L., Brunmark, A., Jackson, M. R., Peterson, P. A., Teyton, L., and Wilson, I. A. (1996a). An alpha/beta T cell receptor structure at 2.5 A and its orientation in the TCR-MHC complex. Science 274, 209-219.

Garcia, K. C., Scott, C. A., Brunmark, A., Carbone, F. R., Peterson, P. A., Wilson, I. A., and Teyton, L. (1996b). CD8 enhances formation of stable T-cell receptor/MHC class I molecule

complexes. Nature 384, 577-581.

Garcia, K. C., Tallquist, M. D., Pease, L. R., Brunmark, A., Scott, C. A., Degano, M., Stura, E. A., Peterson, P. A., Wilson, I. A., and Teyton, L. (1997). Alpha/beta T cell receptor interactions with syngeneic and allogeneic ligands: affinity measurements and crystallization. Proc Natl Acad Sci U S A 94, 13838-13843.

Garcia, K. C., Teyton, L., and Wilson, I. A. (1999). Structural basis of T cell recognition. Annu Rev Immunol 17, 369-397.

Gascoigne, N. R., Zal, T., and Alam, S. M. (2001). T-cell receptor binding kinetics in T-cell development and activation. Expert Rev Mol Med 2001, 1-17.

Germain, R. N. (2002). T-cell developmentand the CD4-CD8 lineage decision. Nat Rev Immunol 2, 309-322.

Germain, R. N., and Stefanova, I. (1999). The dynamics of T cell receptor signaling: complex orchestration and the key roles of tempo and cooperation. Annu Rev Immunol 17, 467-522.

Germain, R. N., Stefanova, I., and Dorfman, J. (2002). Self-recognition and the regulation of CD4+ T cell survival. Adv Exp Med Biol 512, 97-105.

Gil, D., Schamel, W. W., Montoya, M., Sanchez-Madrid, F., and Alarcon, B. (2002). Recruitment of Nck by CD3 epsilon reveals a ligand-induced conformational change essential for Tcell receptor signaling and synapse formation. Cell 109, 901-912.

Guillaume, P., Legler, D. F., Boucheron, N., Doucey, M. A., Cerottini, J. C., and Luescher, I. F. (2003). Soluble major histocompatibility complex-peptide octamers with impaired CD8 binding selectively induce Fas-dependent apoptosis. J Biol Chem 278, 4500-4509.

Hennecke, J., Carfi, A., and Wiley, D. C. (2000). Structure of a covalently stabilized complex of a human alpha/beta T-cell receptor, influenza HA peptide and MHC class II molecule, HLA-DR1. Embo J 19, 5611-5624.

Hogquist, K. A., Jameson, S. C., and Bevan, M. J. (1994a). The ligand for positive selection of T lymphocytes in the thymus. Curr Opin Immunol 6, 273-278.

Hogquist, K. A., Jameson, S. C., and Bevan, M. J. (1995). Strong agonist ligands for the T cell receptor do not mediate positive selection of functional CD8+ T cells. Immunity 3, 79-86.

Hogquist, K. A., Jameson, S. C., Heath, W. R., Howard, J. L., Bevan, M. J., and Carbone, F. R. (1994b). T cell receptor antagonist peptides induce positive selection. Cell 76, 17-27.

Holler, P. D., and Kranz, D. M. (2003). Quantitativeanalysis of the contribution of TCR/pMHC affinity and CD8 to T cell activation. Immunity 18, 255-264.

Hudrisier, D., Kessler, B., Valitutti, S., Horvath, C., Cerottini, J. C., and Luescher, I. F. (1998). The efficiency of antigen recognition by CD8+ CTL clones is determined by the frequency of serial TCR engagement. J Immunol 161, 553-562.

Irie, H. Y., Ravichandran, K. S., and Burakoff, S. J. (1995). CD8 beta chain influencesCD8

alpha chain-associated Lck kinase activity. J Exp Med 181, 1267-1273.

Itano, A., Cado, D., Chan, F. K., and Robey, E. (1994). A role for the cytoplasmic tail of the beta chain of CD8 in thymic selection. Immunity 1, 287-290.

Janeway, C. (1989). Immunogenicity signals 1,2,3 ... and 0. Immunol Today 10, 283-286.

Jonsson, U., Fagerstam, L., Ivarsson, B., Johnsson, B., Karlsson, R., Lundh, K., Lofas, S., Persson, B., Roos, H., Ronnberg, I., and et al. (1991). Real-time biospecific interaction analysis using surface plasmon resonance and a sensor chip technology. Biotechniques 11, 620-627.

Jung, D., and Alt, F. W. (2004). Unraveling V(D)J recombination; insights into gene regulation. Cell 116, 299-311.

Kearse, K. P., Roberts, J. L., Munitz, T. I., Wiest, D. L., Nakayama, T., and Singer, A. (1994a). Developmental regulation of alpha beta T cell antigen receptor expression results from differential stability of nascent TCR alpha proteins within the endoplasmic reticulum of immature and mature T cells. Embo J 13, 4504-4514.

Kearse, K. P., Williams, D. B., and Singer, A. (1994b). Persistenceof glucose residues on core oligosaccharides prevents association of TCR alpha and TCR beta proteins with calnexin and results specificallyin accelerated degradation of nascent TCR alpha proteins within the endoplasmic reticulum. Embo J 13, 3678-3686.

Kerry, S. E., Buslepp, J., Cramer, L. A., Maile, R., Hensley, L. L., Nielsen, A. I., Kavathas, P., Vilen, B. J., Collins, E. J., and Frelinger, J. A. (2003). Interplay between TCR affinity and necessity of coreceptor ligation: high-affinity peptide-MHC/TCR interaction overcomes lack of CD8 engagement. J Immunol 171, 4493-4503.

Kersh, G. J., Kersh, E. N., Fremont, D. H., and Allen, P. M. (1998). High- andlow-potency ligands with similar affinitiesfor the TCR: the importance of kinetics in TCR signaling. Immunity 9, 817-826.

Kessler, B., Hudrisier, D., Cerottini, J. C., and Luescher, I. F. (1997a). Role of CD8 in aberrant function of cytotoxic T lymphocytes. J Exp Med 186, 2033-2038.

Kessler, B. M., Bassanini, P., Cerottini, J. C., and Luescher, I. F. (1997b). Effects of epitope modification on T cell receptor-ligand binding and antigen recognition by seven H-2Kd-restricted cytotoxic T lymphocyte clones specific for a photo-reactive peptide derivative. J Exp Med 185, 629-640.

Leishman, A. J., Naidenko, O. V., Attinger, A., Koning, F., Lena, C. J., Xiong, Y., Chang, H. C., Reinherz, E., Kronenberg, M., and Cheroutre, H. (2001). T cell responses modulated through interaction between CD8alpha/alpha and the nonclassical MHC class I molecule, TL. Science 294, 1936-1939.

Letourneur, F., and Klausner, R. D. (1992). A novel di-leucine motif and a tyrosine-based motif independently mediate lysosomal targeting and endocytosis of CD3 chains. Cell 69, 1143-1157.

Letourneur, F., and Malissen, B. (1989). Derivation of a T cell hybridoma variant deprived of functional T cell receptor alpha and beta chain transcripts reveals a nonfunctional alpha-

mRNA of BW5147 origin. Eur J Immunol 19, 2269-2274.

Liu, C. P., Crawford, F., Marrack, P., and Kappler, J. (1998). T cell positive selection by a high density, low affinity ligand. Proc Natl Acad Sci U S A 95, 4522-4526.

Lucas, B., Stefanova, I., Yasutomo, K., Dautigny, N., and Germain, R. N. (1999). Divergent changes in the sensitivity of maturing T cells to structurally related ligands underlies formation of a useful T cell repertoire. Immunity 10, 367-376.

Luescher, I. F., Anjuere, F., Peitsch, M. C., Jongeneel, C. V., Cerottini, J. C., and Romero, P. (1995a). Structural analysis of TCR-ligand interactions studied on H-2Kd- restricted cloned CTL specific for a photoreactive peptide derivative. Immunity 3, 51-63.

Luescher, I. F., Cerottini, J. C., and Romero, P. (1994). Photoaffinity labeling of the T cell receptor on cloned cytotoxic T lymphocytes by covalent photoreactive ligand. J Biol Chem 269, 5574-5582.

Luescher, I. F., Loez, J. A., Malissen, B., and Cerottini, J. C. (1992). Interaction of antigenic peptides with MHC class I molecules on living cells studied by photoaffinity labeling. J Immunol 148, 1003-1011.

Luescher, I. F., Romero, P., Cerottini, J. C., and Maryanski, J. L. (1991). Specific binding of antigenic peptides to cell-associated MHC class I molecules. Nature 351, 72-74.

Luescher, I. F., Vivier, E., Layer, A., Mahiou, J., Godeau, F., Malissen, B., and Romero, P. (1995b). CD8 modulation of T-cell antigen receptor-ligand interactions on living cytotoxic T lymphocytes. Nature 373, 353-356.

Maenaka, K., Juji, T., Nakayama, T., Wyer, J. R., Gao, G. F., Maenaka, T., Zaccai, N. R., Kikuchi, A., Yabe, T., Tokunaga, K., et al. (1999). Killer cell immunoglobulin receptors and T cell receptors bind peptide-major histocompatibility complex class I with distinct thermodynamic and kinetic properties. J Biol Chem 274, 28329-28334.

McKeithan, T. W. (1995). Kinetic proofreading in T-cell receptor signal transduction. Proc Natl Acad Sci U S A 92, 5042-5046.

Miller, A. D., and Rosman, G. J. (1989). Improved retroviral vectors for gene transfer and expression. Biotechniques 7, 980-982, 984-986, 989-990.

Moody, A. M., Chui, D., Reche, P. A., Priatel, J. J., Marth, J. D., and Reinherz, E. L. (2001a). Developmentally regulated glycosylation of the CD8alpha/beta coreceptor stalk modulates ligand binding. Cell 107, 501-512.

Moody, A. M., Xiong, Y., Chang, H. C., and Reinherz, E. L. (2001b). The CD8alpha/beta co-receptor on double-positive thymocytes binds with differing affinities to the products of distinct class I MHC loci. Eur J Immunol 31, 2791-2799.

Naeher, D., Luescher, I. F., and Palmer, E. (2002). A role for the alpha-chain connecting peptide motif in mediatingTCR-CD8 cooperation. J Immunol 169, 2964-2970.

Nakayama, K., Negishi, I., Kuida, K., Louie, M. C., Kanagawa, O., Nakauchi, H., and Loh, D. Y. (1994). Requirement for CD8 beta chain in positive selection of CD8-lineage T cells. Science

263, 1131-1133.

Newton, K., Harris, A. W., Bath, M. L., Smith, K. G., and Strasser, A. (1998). A dominant interfering mutant of FADD/MORT1 enhances deletion of autoreactive thymocytes and inhibits proliferation of mature T lymphocytes. Embo J 17, 706-718.

Nikolich-Zugich, J., Slifka, M. K., and Messaoudi, I. (2004). The many importantfacets of T-cell repertoire diversity. Nat Rev Immunol 4, 123-132.

O'Herrin, S. M., Lebowitz, M. S., Bieler, J. G., al-Ramadi, B. K., Utz, U., Bothwell, A. L., and Schneck, J. P. (1997). Analysis of the expression of peptide-major histocompatibility complexes using high affinity soluble divalent T cell receptors. J Exp Med 186, 1333-1345.

Ogg, G. S., and McMichael, A. J. (1998). HLA-peptide tetrameric complexes. Curr Opin Immunol 10, 393-396.

Pear, W. S., Nolan, G. P., Scott, M. L., and Baltimore, D. (1993). Production of high-titer helper-free retroviruses by transient transfection. Proc Natl Acad Sci U S A 90, 8392-8396.

Pircher, H., Mak, T. W., Lang, R., Ballhausen, W., Ruedi, E., Hengartner, H., Zinkernagel, R. M., and Burki, K. (1989). T cell tolerance to Mlsa encoded antigens in T cell receptor V beta 8.1 chain transgenic mice. Embo J 8, 719-727.

Priatel, J. J., Chui, D., Hiraoka, N., Simmons, C. J., Richardson, K. B., Page, D. M., Fukuda, M., Varki, N. M., and Marth, J. D. (2000). The ST3Gal-I sialyltransferase controls CD8+ T lymphocyte homeostasis by modulating O-glycan biosynthesis. Immunity 12, 273-283.

Rammensee, H. G. (1995). Chemistry of peptides associated with MHC class I and class II molecules. Curr Opin Immunol 7, 85-96.

Rudd, C.E. (1999). Adaptors and molecular scaffolds in immune cell signaling. Cell 96, 5-8.

Rudolph, M. G., Luz, J. G., and Wilson, I. A. (2002). Structural and thermodynamic correlates of T cell signaling. Annu Rev Biophys Biomol Struct 31, 121-149.

Rudolph, M. G., and Wilson, I. A. (2002b). The specificity of TCR/pMHC interaction. Curr Opin Immunol 14, 52-65.

Sebzda, E., Wallace, V. A., Mayer, J., Yeung, R. S., Mak, T. W., and Ohashi, P. S. (1994). Positive and negative thymocyte selection induced by different concentrationsof a single peptide. Science 263, 1615-1618.

Speir, J. A., Garcia, K. C., Brunmark, A., Degano, M., Peterson, P. A., Teyton, L., and Wilson, I. A. (1998). Structural basis of 2C TCR allorecognition of H-2Ld peptide complexes. Immunity 8, 553-562.

Sprent, J., Cai, Z., Brunmark, A., Jackson, M. R., and Peterson, P. A. (1997). Constructing artificial antigen-presenting cells from Drosophila cells. Adv Exp Med Biol 417, 249-254.

Starr, T. K., Jameson, S. C., and Hogquist, K. A. (2003). Positive and negative selection of T cells. Annu Rev Immunol 21, 139-176.

Stotz, S. H., Bolliger, L., Carbone, F. R., and Palmer, E. (1999). T cell receptor (TCR) antagonism without a negative signal: evidence from T cell hybridomas expressing two independent TCRs. J Exp Med 189, 253-264.

Sun, Z. J., Kim, K. S., Wagner, G., and Reinherz, E. L. (2001). Mechanisms contributing to T cell receptor signaling and assembly revealed by the solution structure of an ectodomain fragment of the CD3 epsilon gamma heterodimer. Cell 105, 913-923.

Teng, M. K., Smolyar, A., Tse, A. G., Liu, J. H., Liu, J., Hussey, R. E., Nathenson, S. G., Chang, H. C., Reinherz, E. L., and Wang, J. H. (1998). Identification of a common docking topology with substantial variation among different TCR-peptide-MHC complexes. Curr Biol 8, 409-412.

Valitutti, S., Dessing, M., Aktories, K., Gallati, H., and Lanzavecchia, A. (1995a). Sustained signaling leading to T cell activation results from prolonged T cell receptor occupancy. Role of T cell actin cytoskeleton. J Exp Med 181, 577-584.

Valitutti, S., Muller, S., Cella, M., Padovan, E., and Lanzavecchia, A. (1995b). Serial triggering of many T-cell receptors by a few peptide-MHC complexes. Nature 375, 148-151.

van der Merwe, P.A. and Davis, S.J. (2003). Molecular interactions mediating T cell antigen recognition. Annu. Rev. Immunol. 21:659-84.

Van Kaer, L., Ashton-Rickardt, P. G., Ploegh, H. L., and Tonegawa, S. (1992). TAP1 mutant mice are deficient in antigen presentation, surface class I molecules, and CD4-8+ T cells. Cell 71, 1205-1214.

Watson, J. (1979). Continuous proliferation of murine antigen-specific helper T lymphocytes in culture. J Exp Med 150, 1510-1519.

Watson, J., Ralph, P., Sarkar, S., and Cohn, M. (1970). Leukemia viruses associated with mouse myeloma cells. Proc Natl Acad Sci U S A 66, 344-351.

Werlen, G., Hausmann, B., Naeher, D., and Palmer, E. (2003). Signaling life and death in the thymus: timing is everything. Science 299, 1859-1863.

Werlen, G., Hausmann, B., and Palmer, E. (2000). A motif in the alphabeta T-cell receptor controls positive selection by modulating ERK activity. Nature 406, 422-426.
Wheeler, C. J., von Hoegen, P., and Parnes, J. R. (1992). An immunological role for the CD8 beta-chain. Nature 357, 247-249.

Wu, L. C., Tuot, D. S., Lyons, D. S., Garcia, K. C., and Davis, M. M. (2002). Two-step binding mechanism for T-cell receptor recognition of peptide MHC. Nature 418, 552-556.

Yoon, S. T., Dianzani, U., Bottomly, K., and Janeway, C. A., Jr. (1994). Both high and low avidity antibodies to the T cell receptor can have agonist or antagonist activity. Immunity 1, 563-569.

6.Curriculum Vitae

Name: Naeher

First Name: Dieter

Date of Birth: 13.08.1973 in Basel (CH).

Citicienship: Basel; Switzerland.

Education:

1980 - 84	Primary School Kirchmatt Birsfelden (CH).
1984 - 89	Progymnasium Rheinpark Birsfelden (CH).
1989 - 92	Gymnasium Gründen Muttenz (CH).
1992	Matura.
1992 - 93	Cab driver, Mini 2000 AG, Basel.
1995	I. Pre-diploma Biologie II (molecular Biology).
1996	II. Pre-diploma Biologie II.
1997 - 98	Diploma work with Prof. M. Spiess, Dept. Biochemistry, Biocenter of the Uni. of Basel.
1998 - 99	Technical Lab Assistant with Prof. M. Spiess.
1999	Diploma in Biologie II (Main subject: Biochemistry).
1999	Summerstudentship with Prof. E. Palmer, Basel Institute for Immunology.
1999 - 2004	PhD Thesis with Prof. E. Palmer, Basel Institute for Immunology and Universitätsspital Basel.

Publications:

Teixeiro, E., Daniels, M. A., Hausmann, B., Schrum, A. G., Naeher, D., Luescher, I., Thome, M., Bragado, R., and Palmer, E. (2004). T cell division and death are segregated by mutation of TCRbeta chain constant domains. Immunity 21, 515-526.

Doucey, M. A., Legler, D. F., Faroudi, M., Boucheron, N., Baumgaertner, P., Naeher, D., Cebecauer, M., Hudrisier, D., Ruegg, C., Palmer, E., et al. (2003). The beta1 and beta3 integrins promote T cell receptor-mediated cytotoxic T lymphocyte activation. J Biol Chem 278, 26983-26991.

Werlen, G., Hausmann, B., Naeher, D., and Palmer, E. (2003). Signaling life and death in the thymus: timing is everything. Science 299, 1859-1863.

Naeher, D., Luescher, I. F., and Palmer, E. (2002). A role for the alpha-chain connecting peptide motif in mediating TCR-CD8 cooperation. J Immunol 169, 2964-2970.

Doucey, M. A., Goffin, L., Naeher, D., Michielin, O., Baumgartner, P., Guillaume, P., Palmer, E., and Luescher, I. F. (2003). CD3 delta establishes a functional link between the T cell receptor and CD8. J Biol Chem 278, 3257-3264.

Rosch, K., Naeher, D., Laird, V., Goder, V., and Spiess, M. (2000). The topogenic contribution of uncharged amino acids on signal sequence orientation in the endoplasmic reticulum. J Biol Chem 275, 14916-14922.

During the time of my PhD studies I have attended the lectures of the following professors:

Prof. Dr. Ed Palmer, Prof. Dr. Gennaro de Libero, Prof. Dr. Immanuel Lüscher, Prof. Dr Antonius Rolink, Prof. Dr. Fritz Melchers, Prof. Dr. Roland Gisler, Prof. Dr. Jean Pieters, Prof. Dr. Kurt Balmer-Hofer, Prof. Dr. Micheal Hall, Prof. Dr. Urs Jenal, Prof. Dr. Niklaus Weiss, Prof. Dr. Gerhard Christophori, PD Dr. Rolf Jessberger, PD Dr. Hans Reimer Rodewald and DP Dr. Natascha Kralli.